

3RD CBM - China Workshop

Dense matter EOS and neutron star structure

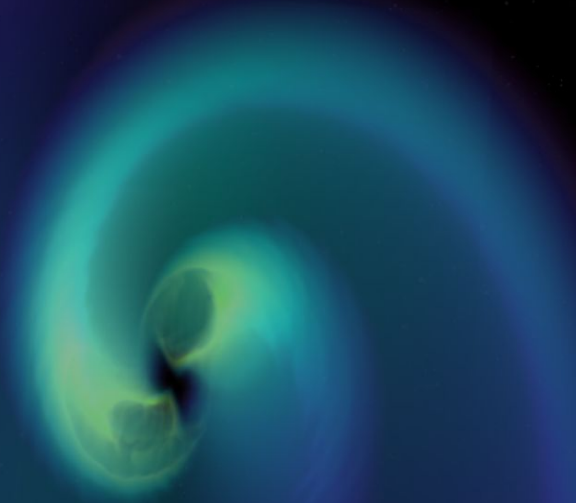
Ang Li

Department of Astronomy, Xiamen Univ.

liang@xmu.edu.cn

<http://astro.xmu.edu.cn/LiAng/>

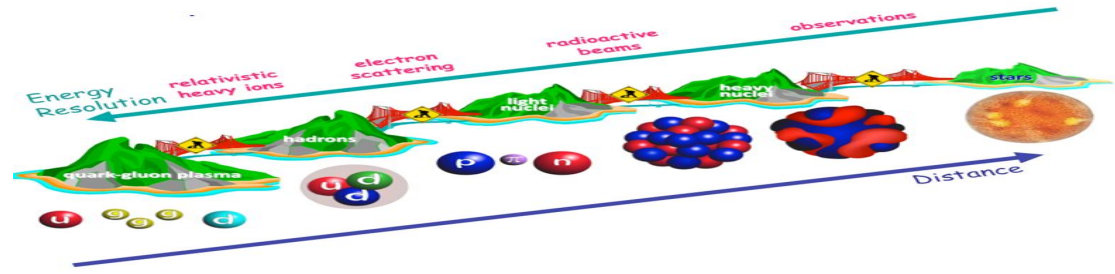
FIRST COSMIC EVENT OBSERVED IN GRAVITATIONAL WAVES AND LIGHT



In this talk

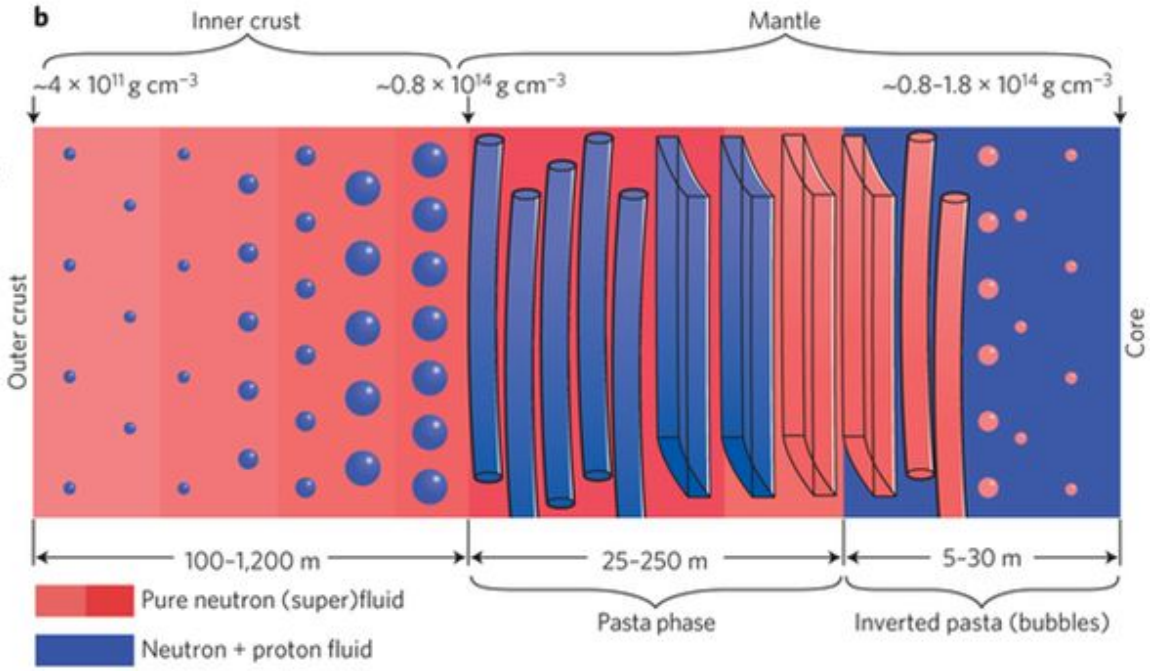
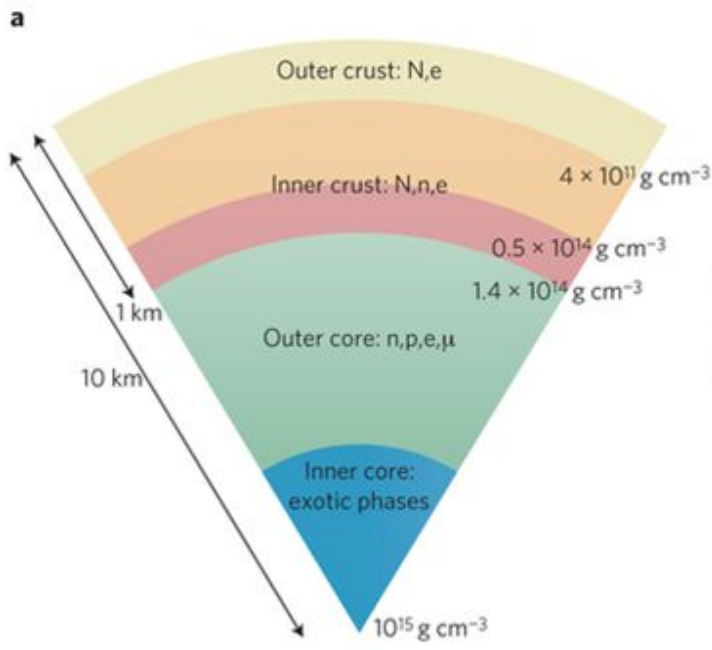
- Intro of NS
- NS EOS from GW170817
- New NS EOS “QMF18” proposed

► Neutron star

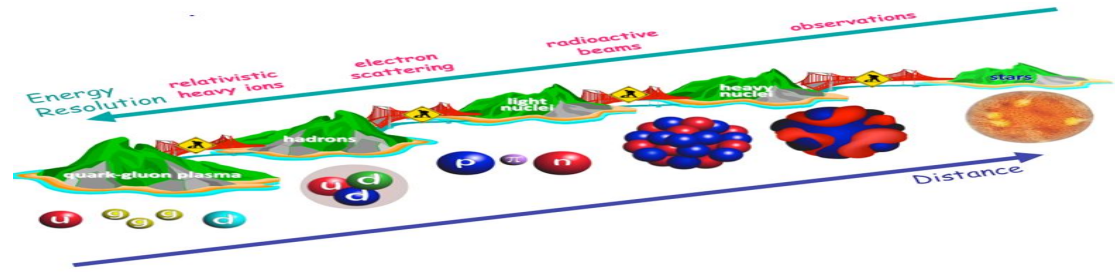


► QCD + weak-interaction equilibrium + EM radiation + GR effect

1. Nuclear force + many-body quantum equation
2. Effective theory from quark/hadron level

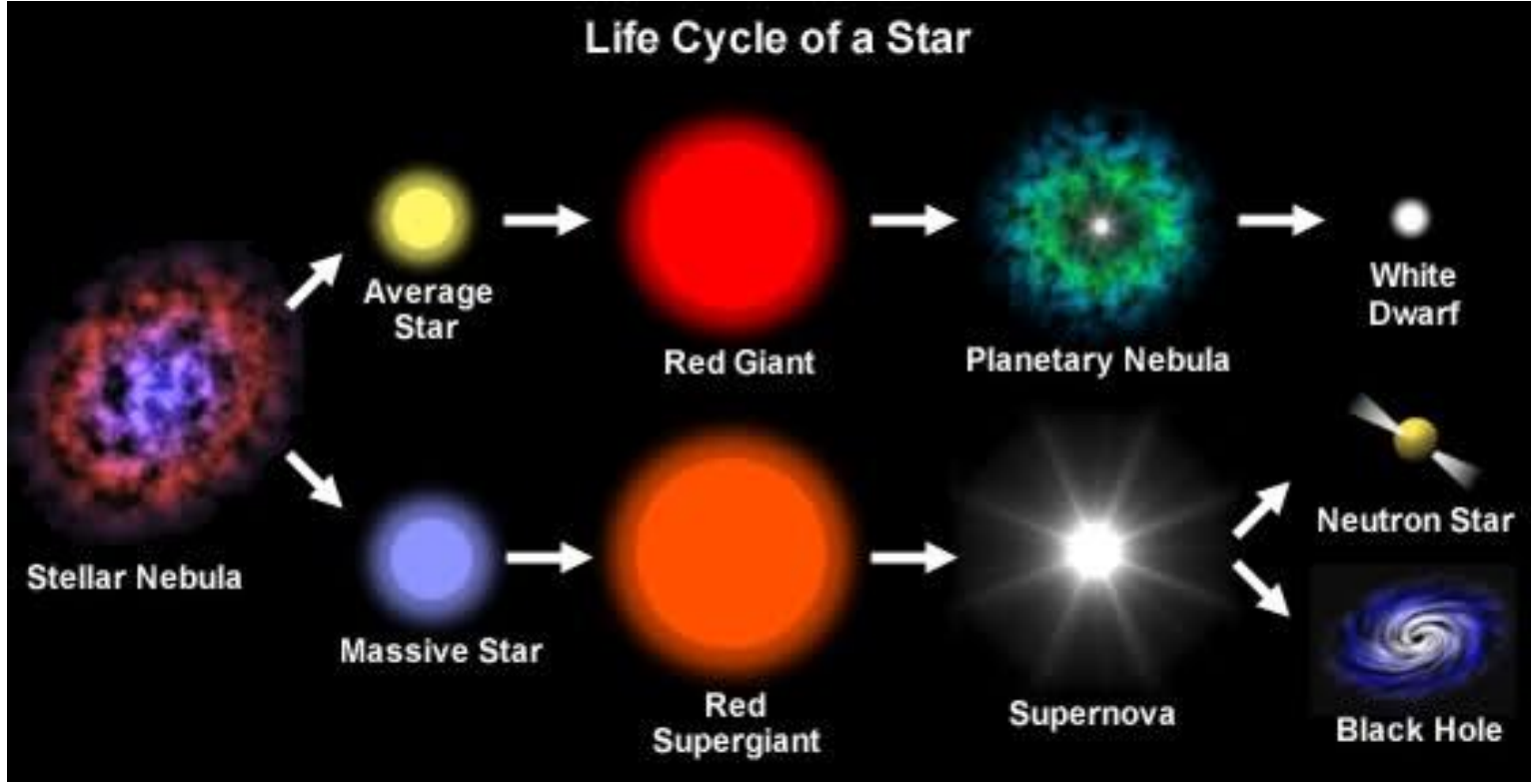


► Neutron star

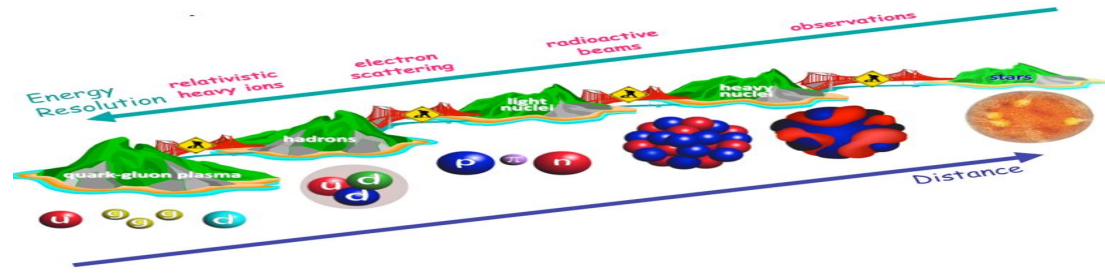


► QCD + weak-interaction equilibrium + EM radiation + GR effect

- 1. Nuclear force + many-body quantum equation
- 2. Effective theory from quark/hadron level



► Neutron star

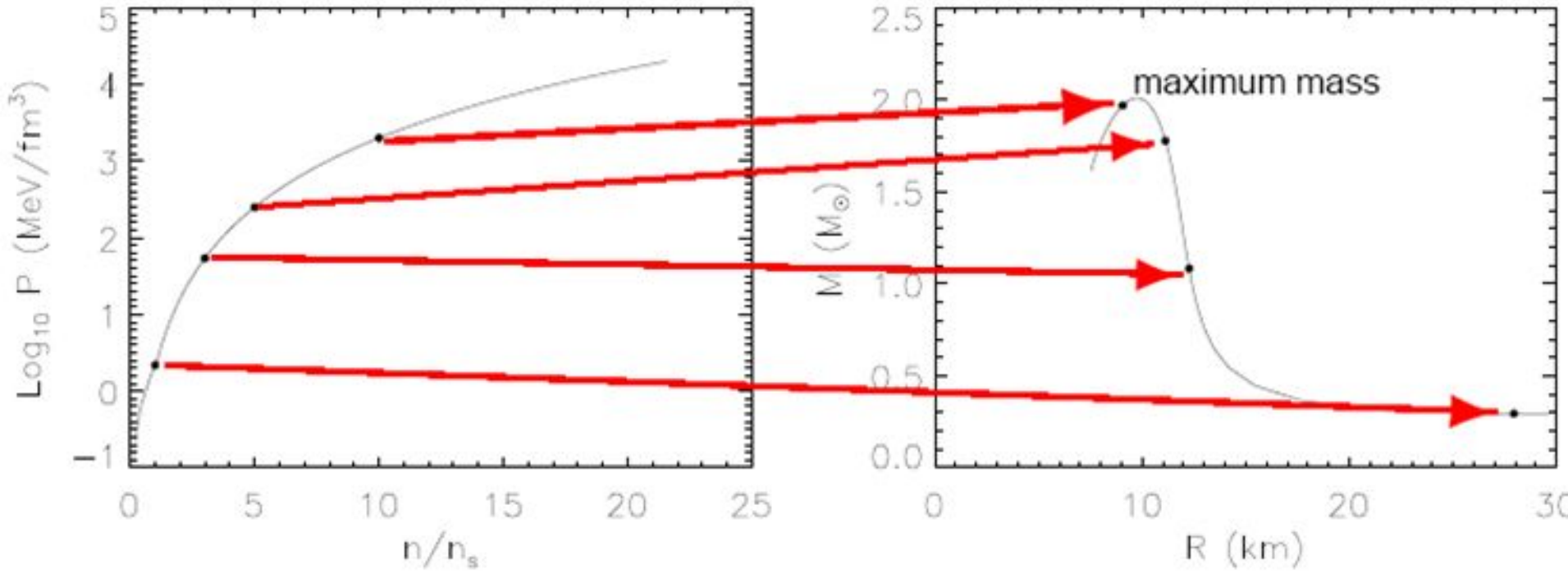


► QCD + weak-interaction equilibrium + EM radiation + GR effect

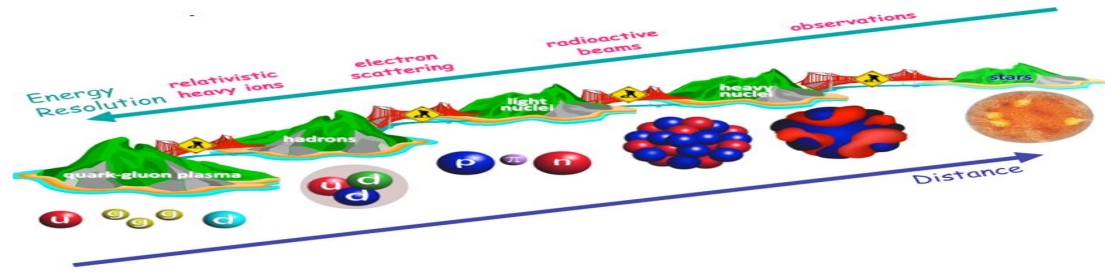
1. Nuclear force + many-body quantum equation
2. Effective theory from quark/hadron level

► $M(R)$ relation is unique to the underlying EOS

Courtesy: J. Lattimer



► Neutron star

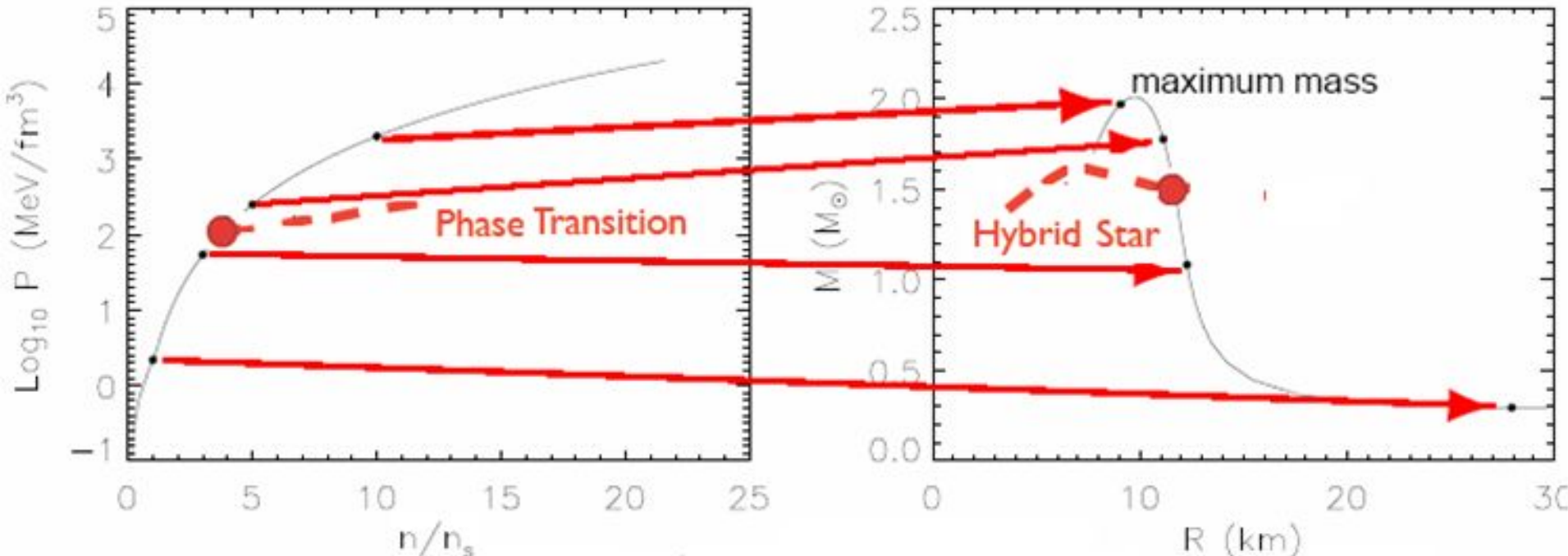


► QCD + weak-interaction equilibrium + EM radiation + GR effect

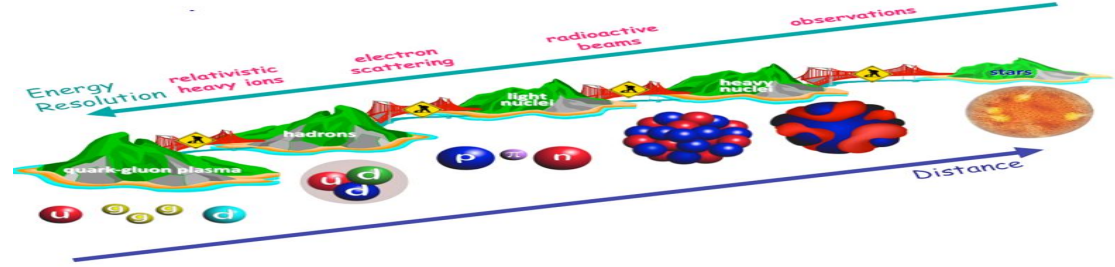
1. Nuclear force + many-body quantum equation
2. Effective theory from quark/hadron level

► $M(R)$ relation is unique to the underlying EOS

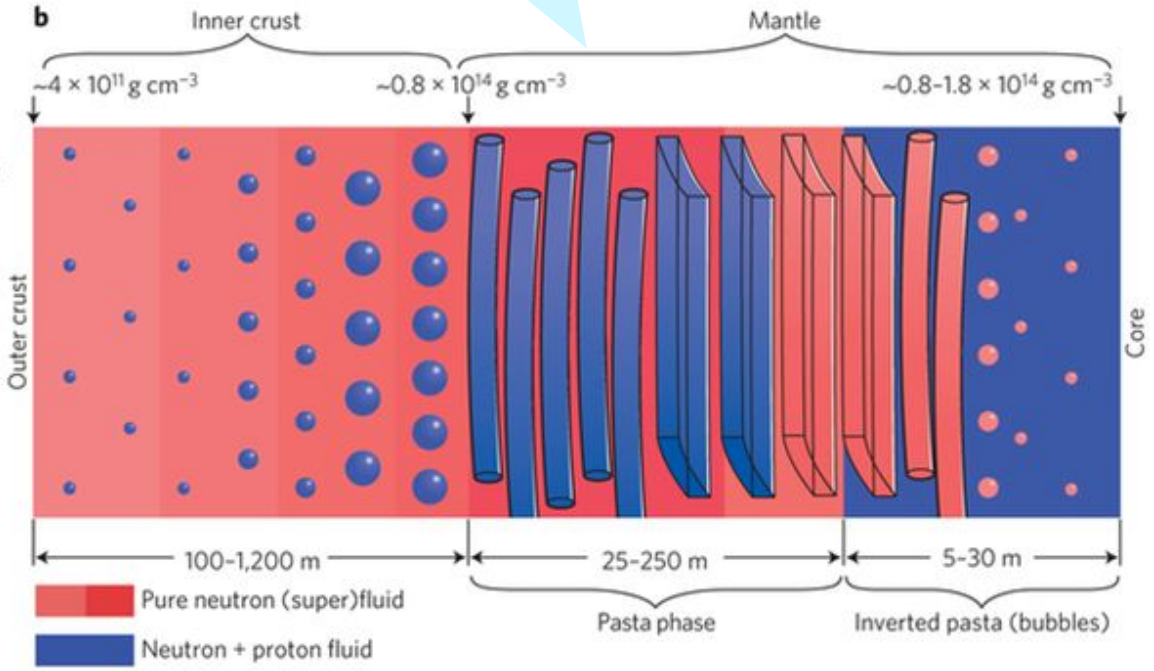
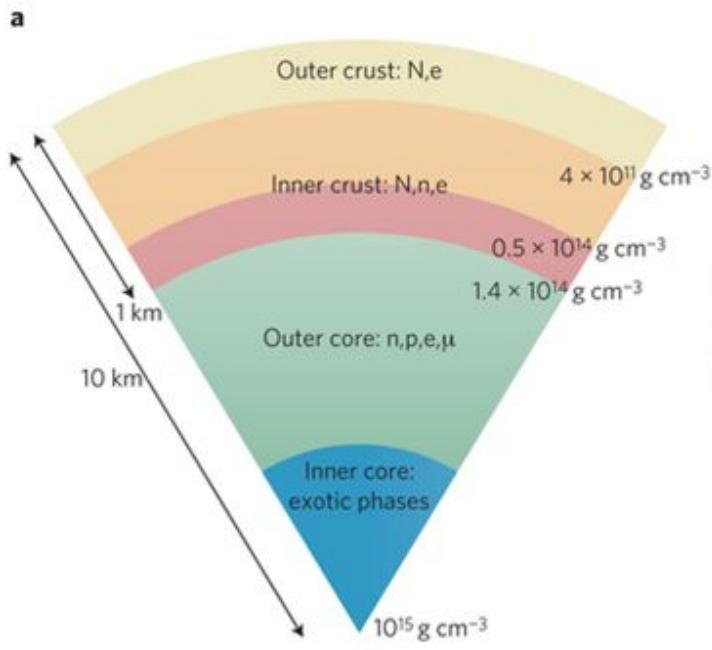
Courtesy: J. Lattimer



► Neutron star



- Gravity bound: Many layers; Crust in the surface constituted by normal nuclei
- Superfluid likely near the surface, from neutron drip density ($4 \times 10^{11} \text{ g/cm}^3$) to nuclear saturation density (10^{14} g/cm^3): Inner crust + Mantle/Pasta.



Neutron Star Crust

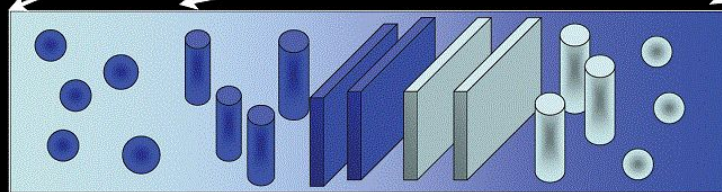
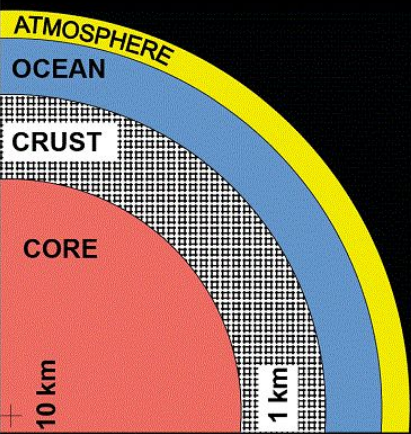
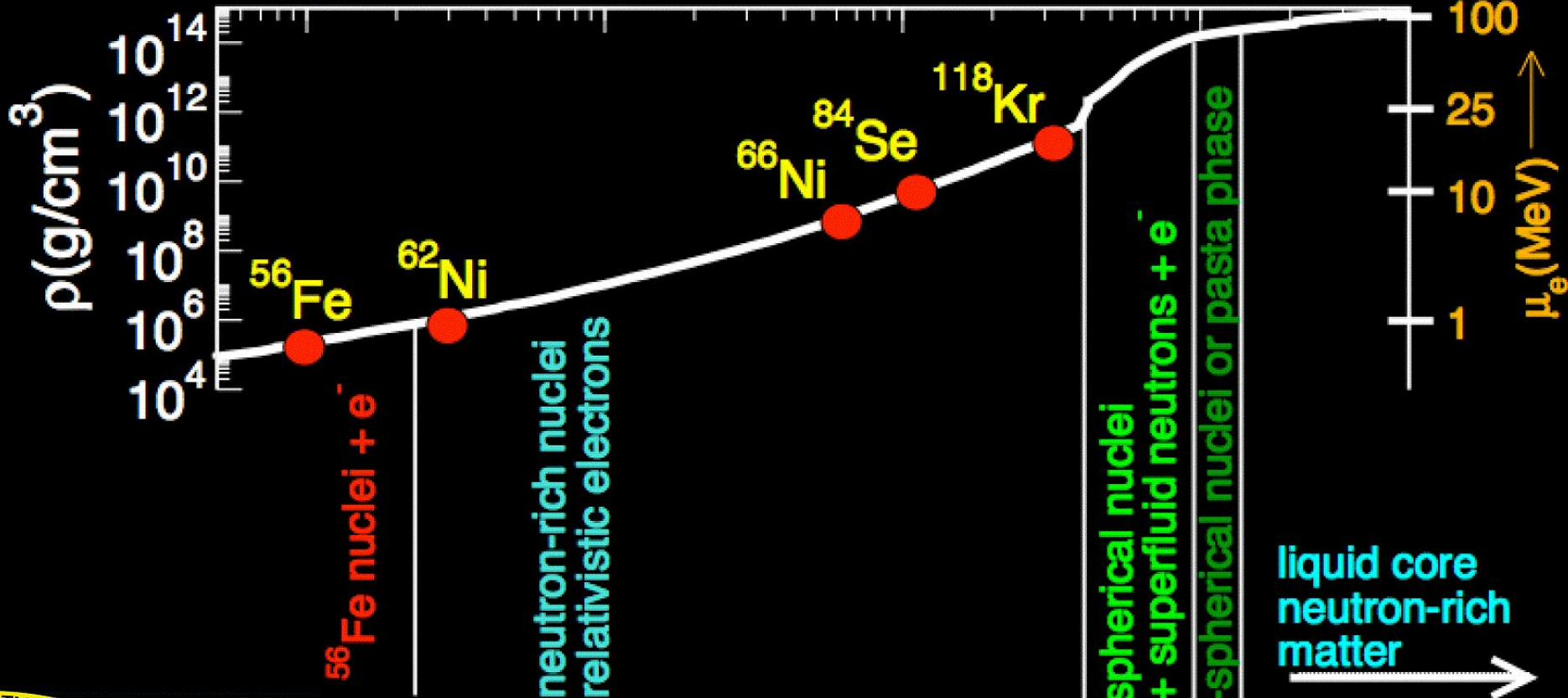
Depth (km)

0.001

0.01

0.1

1



► Outer crust

— From 1970s

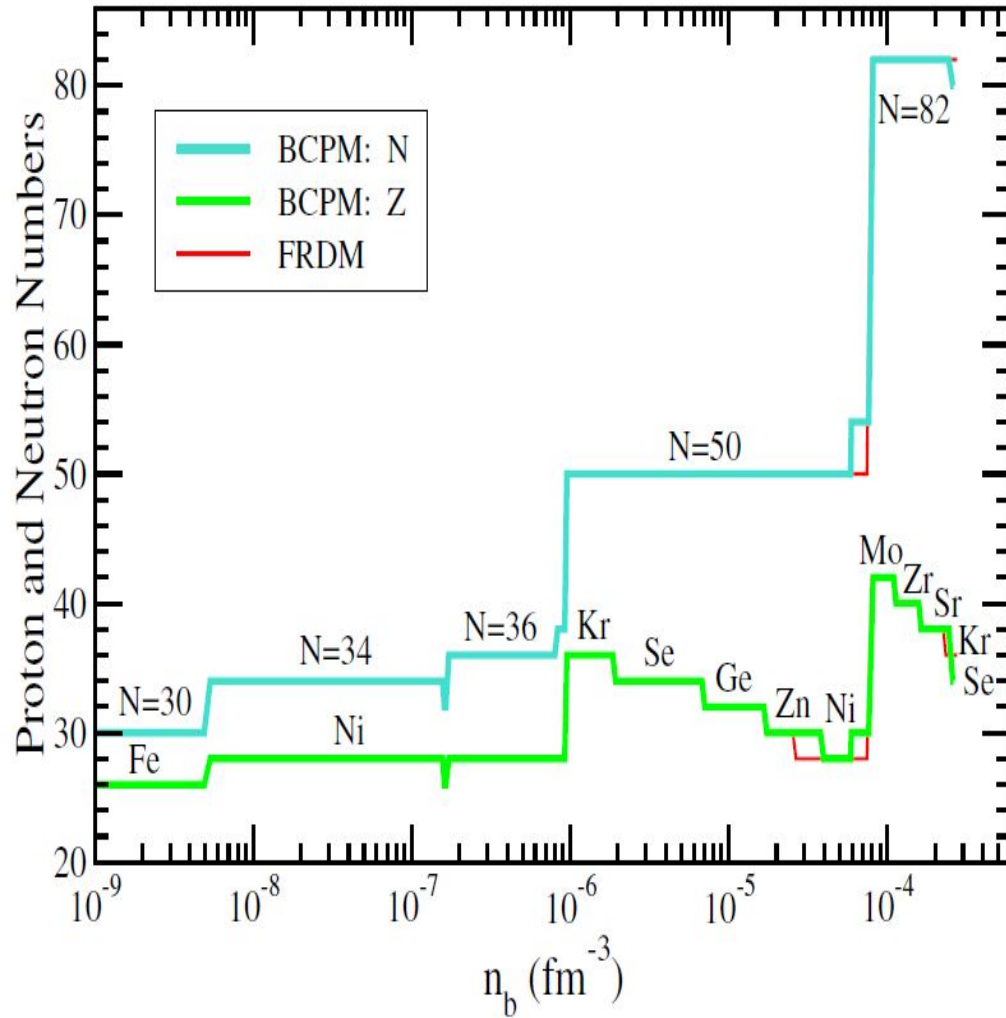


Fig. 1. Neutron (N) and proton (Z) numbers of the predicted nuclei in the outer crust of a neutron star using the experimental nuclear masses (Audi et al. 2012; Wolf et al. 2013) when available and the BCPM energy density functional or the FRDM mass formula (Möller et al. 1995) for the unmeasured masses.

$$E(A, Z, n_b) = E_N + E_{el} + E_I$$

$$E_N(A, Z) = M(A, Z) = (A - Z)m_n + Zm_p - B(A, Z).$$

$$E_{el} = \mathcal{E}_{el} V,$$

$$\mathcal{E}_{el} = \frac{k_{Fe}}{8\pi^2} (2k_{Fe}^2 + m_e^2) \sqrt{k_{Fe}^2 + m_e^2} - \frac{m_e^4}{8\pi^2} \ln \left[\left(k_{Fe} + \sqrt{k_{Fe}^2 + m_e^2} \right) / m_e \right],$$

$$E_I = -C_1 \frac{Z^2}{A^{1/3}} k_{Fb}$$

$$P = - \left(\frac{\partial E}{\partial V} \right)_{T,A,Z} = \mu_e n_e - \mathcal{E}_{el} - \frac{n_b}{3} C_1 \frac{Z^2}{A^{4/3}} k_{Fb}$$

$$\begin{aligned} \mu(A, Z, P) &= \frac{E(A, Z, n_b)}{A} + \frac{P}{n_b} \\ &= \frac{M(A, Z)}{A} + \frac{Z}{A} \mu_e - \frac{4}{3} C_1 \frac{Z^2}{A^{4/3}} k_{Fb}. \end{aligned} \quad (18)$$

For a fixed pressure, Eq. (18) is minimized with respect to the mass number A and the atomic charge Z of the nucleus in order to find the optimal configuration. The nuclear masses $M(A, Z)$

Table 4. Composition and equation of state of the outer crust.

n_b (fm^{-3})	Z	A	ϵ (g cm^{-3})	P (erg cm^{-3})	Γ
6.2203E-12	26	56	1.0317E+04	9.5393E+18	1.797
6.3129E-11	26	56	1.0471E+05	5.3379E+20	1.688
6.3046E-10	26	56	1.0457E+06	2.3241E+22	1.586
4.9516E-09	26	56	8.2138E+06	5.4155E+23	1.470
6.3067E-09	28	62	1.0462E+07	7.3908E+23	1.459
2.5110E-08	28	62	4.1659E+07	5.3113E+24	1.400
7.9402E-08	28	62	1.3176E+08	2.6112E+25	1.369
1.5828E-07	28	62	2.6269E+08	6.6859E+25	1.358
1.6400E-07	26	58	2.7220E+08	6.9610E+25	1.357
1.7778E-07	28	64	2.9508E+08	7.4978E+25	1.356
3.1622E-07	28	64	5.2496E+08	1.6340E+26	1.350
5.0116E-07	28	64	8.3212E+08	3.0390E+26	1.345
7.9431E-07	28	64	1.3191E+09	5.6433E+26	1.343
8.5093E-07	28	66	1.4132E+09	5.9393E+26	1.342
9.2239E-07	28	66	1.5319E+09	6.6181E+26	1.342
9.9998E-07	36	86	1.6609E+09	7.1858E+26	1.341
1.2587E-06	36	86	2.0908E+09	9.7829E+26	1.340
1.5845E-06	36	86	2.6324E+09	1.3318E+27	1.340
1.8587E-06	36	86	3.0881E+09	1.6492E+27	1.339
1.9952E-06	34	84	3.3151E+09	1.7369E+27	1.339
3.1620E-06	34	84	5.2552E+09	3.2161E+27	1.338
5.0116E-06	34	84	8.3320E+09	5.9526E+27	1.337
6.7858E-06	34	84	1.1285E+10	8.9241E+27	1.336
7.5849E-06	32	82	1.2615E+10	9.8815E+27	1.336
9.9996E-06	32	82	1.6635E+10	1.4293E+28	1.335
1.2589E-05	32	82	2.0947E+10	1.9437E+28	1.335
1.6595E-05	32	82	2.7622E+10	2.8107E+28	1.335
1.9053E-05	30	80	3.1718E+10	3.2111E+28	1.335
2.5118E-05	30	80	4.1828E+10	4.6433E+28	1.334
3.1621E-05	30	80	5.2673E+10	6.3132E+28	1.334
3.7973E-05	30	80	6.3269E+10	8.0596E+28	1.334
4.1685E-05	28	78	6.9462E+10	8.6285E+28	1.334
5.8754E-05	28	78	9.7955E+10	1.3639E+29	1.334
6.3093E-05	30	84	1.0520E+11	1.4867E+29	1.334
7.6207E-05	30	84	1.2711E+11	1.9125E+29	1.334
8.4137E-05	42	124	1.4035E+11	2.0101E+29	1.334
1.0964E-04	42	124	1.8299E+11	2.8616E+29	1.334
1.2022E-04	40	122	2.0067E+11	3.1040E+29	1.334
1.4125E-04	40	122	2.3584E+11	3.8485E+29	1.334
1.5667E-04	40	122	2.6163E+11	4.4187E+29	1.334
1.6982E-04	38	120	2.8364E+11	4.7062E+29	1.334
2.0416E-04	38	120	3.4112E+11	6.0164E+29	1.334
2.4265E-04	38	120	4.0556E+11	7.5746E+29	1.334
2.6155E-04	34	114	4.3721E+11	7.7582E+29	1.334

— From 1970s

► Outer crust

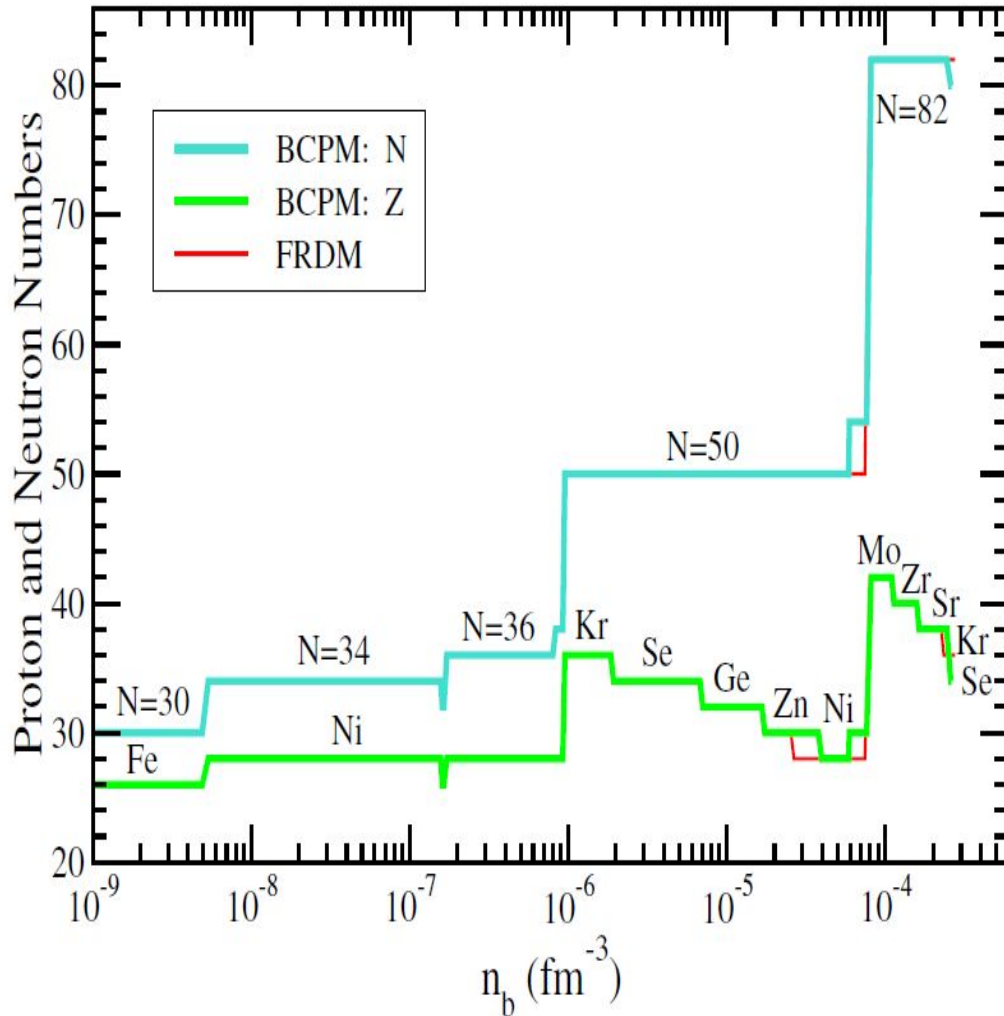


Fig. 1. Neutron (N) and proton (Z) numbers of the predicted nuclei in the outer crust of a neutron star using the experimental nuclear masses (Audi et al. 2012; Wolf et al. 2013) when available and the BCPM energy density functional or the FRDM mass formula (Möller et al. 1995) for the unmeasured masses.

Courtesy: S. Reddy

Neutron Star Crust

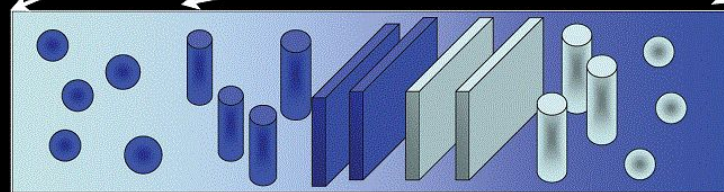
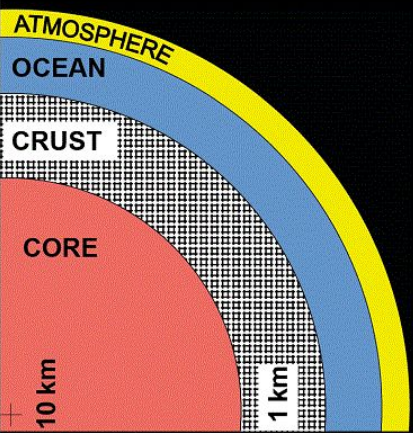
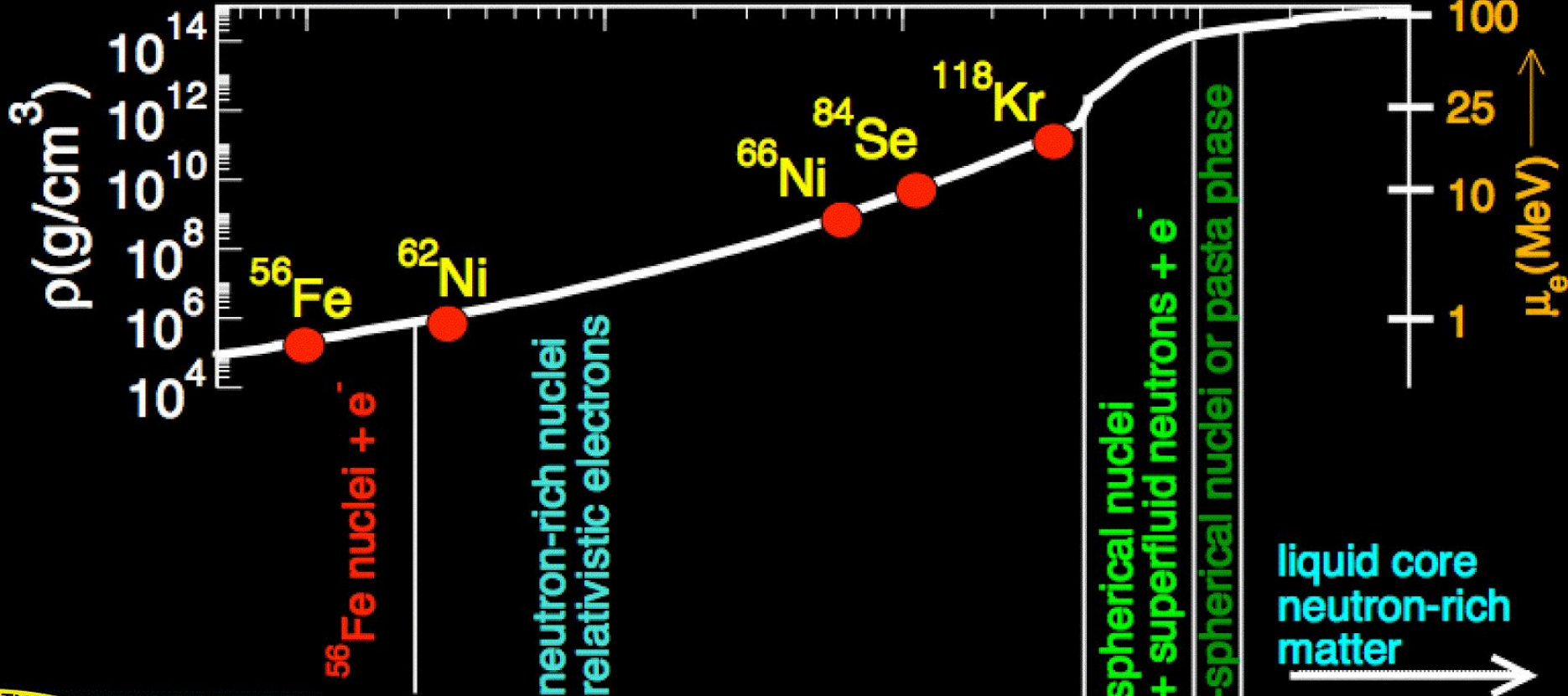
Depth (km)

0.001

0.01

0.1

1



► Inner crust

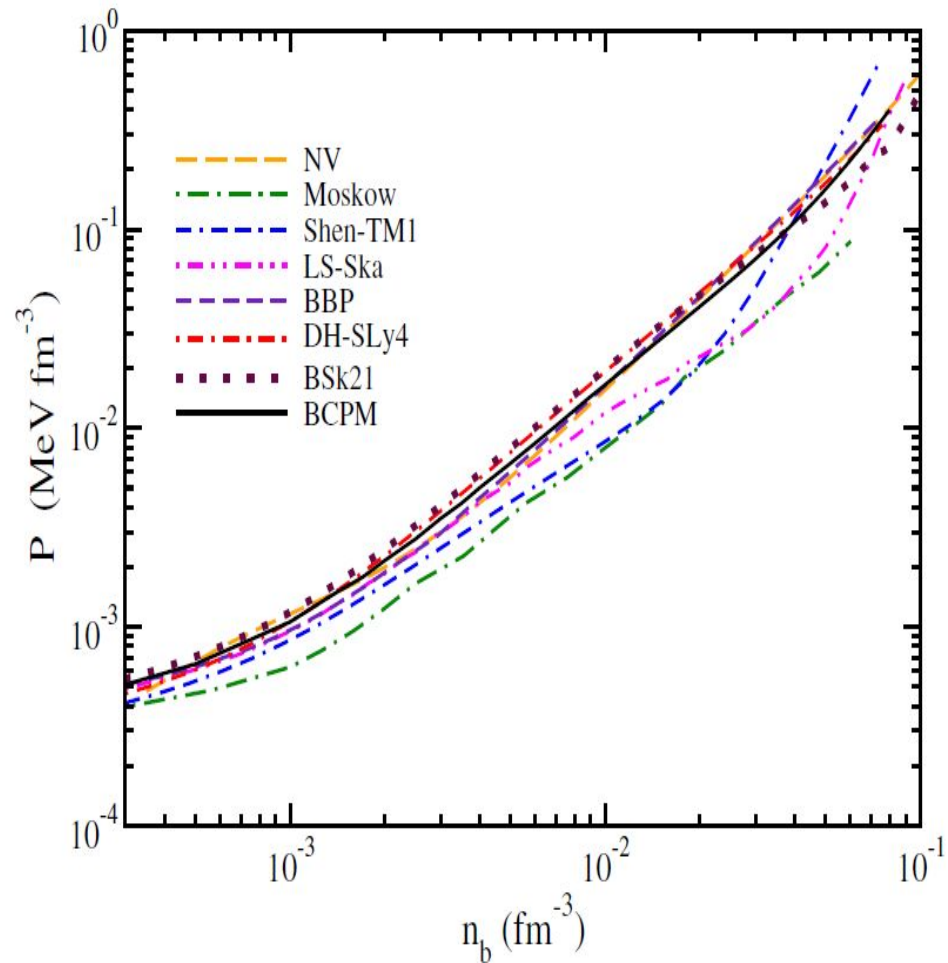
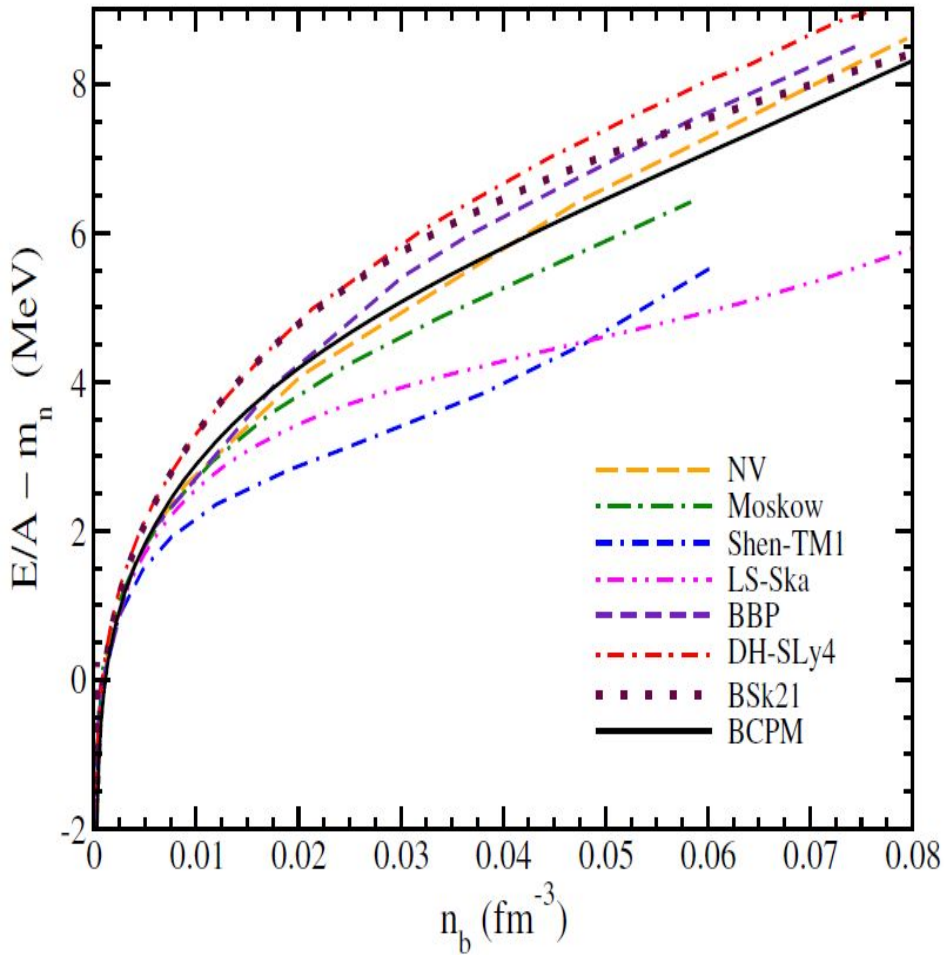
In the domain from ρ_{drip} to ρ_{nuc} , matter is composed of nuclei, electrons, and free neutrons. The nuclei disappear at the upper end of this density range because their binding energy decreases with increasing density. We can understand this in part since the strong attractive “tensor” force between two unlike nucleons in the 3S_1 state, which is crucial in binding the deuteron (cf. Section 8.3), does not act between neutrons because of the Pauli principle. In fact, a system of pure neutrons is unbound at any density. So, as the density increases and the nuclei become more neutron rich, their stability decreases until a critical value of neutron number is reached, at which point the nuclei dissolve, essentially by merging together.

——From 1970s

At the bottom layers of the inner crust the equilibrium nuclear shape may change from sphere, to cylinder, slab, tube (cylindrical hole), and bubble (spherical hole) before going into uniform matter. These shapes are generically known as “nuclear pasta”.

or “mantle” (Gusakov et al. 2004)

► Inner crust



- Compressible Liquid Drop Model (CLDM)
- Thomas-Fermi (TF) scheme

► Inner crust [Liquid Drop](#)

They write the total energy density as

$$\begin{aligned}\varepsilon &= \varepsilon(A, Z, n_N, n_n, V_N) \\ &= n_N(W_N + W_L) + \varepsilon_n(n_n)(1 - V_N n_N) + \varepsilon_e(n_e)\end{aligned}$$

charge neutrality

$$n_e = Zn_N$$

baryon density

$$n = An_N + (1 - V_N n_N)n_n$$

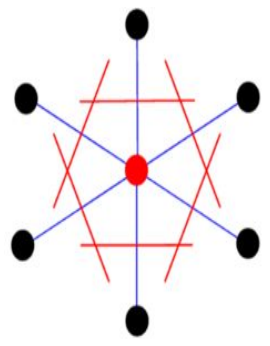
$$n_n = \frac{N_n}{V_n}$$

Here n_N is the number density of nuclei, n_n the number density of neutrons outside of nuclei (“neutron gas”), and the new feature is the dependence on V_N , the volume of a nucleus. The quantity V_N decreases in response to the outside pressure of the neutron gas and so must be treated as a variable. The quantity W_N is the energy of a nucleus, including the rest mass of the nucleus, and depends on A , Z , n_n , and V_N . The lattice energy is denoted by W_L , while ε_n and ε_e are the energy densities of the neutron gas and electron gas respectively. Note that $V_N n_N$ is the fraction of volume occupied by nuclei, and $1 - V_N n_N$ the fraction occupied by the neutron gas.

Equilibrium is determined by minimizing ε at fixed n .

► Inner crust

Thomas-Fermi (TF)



WS cell:
 The smallest (primitive) cell which displays the full symmetry of the lattice.

The total energy of an ensemble of $A-Z$ neutrons, Z protons, and Z electrons in a spherical Wigner-Seitz (WS) cell of volume $V_c = 4\pi R_c^3/3$ can be expressed as

$$E = E(A, Z, R_c) = \int_{V_c} \left[\mathcal{H}(n_n, n_p) + m_n n_n + m_p n_p + \mathcal{E}_{el}(n_e) + \mathcal{E}_{coul}(n_p, n_e) + \mathcal{E}_{ex}(n_p, n_e) \right] d\mathbf{r}. \quad (19)$$

The term $\mathcal{H}(n_n, n_p)$ is the contribution of the nuclear energy density, without the nucleon rest masses. In our approach it reads

$$\mathcal{H}(n_n, n_p) = \frac{3}{5} \frac{(3\pi^2)^{2/3}}{2m_n} n_n^{5/3}(\mathbf{r}) + \frac{3}{5} \frac{(3\pi^2)^{2/3}}{2m_p} n_p^{5/3}(\mathbf{r}) + \mathcal{V}(n_n(\mathbf{r}), n_p(\mathbf{r})), \quad (20)$$

where the neutron and proton kinetic energy densities are written in the TF approximation and $\mathcal{V}(n_n, n_p)$ is the interacting part

term $\mathcal{E}_{el}(n_e)$ in Eq. (19) is the relativistic energy density due to the motion of the electrons, including their rest mass.

we computed \mathcal{E}_{el} using the energy density of a uniform relativistic Fermi gas.

$$\mathcal{E}_{coul}(n_p, n_e) = \frac{1}{2} (n_p(\mathbf{r}) - n_e) (V_p(\mathbf{r}) - V_e(\mathbf{r}))$$

$$\mathcal{E}_{ex}(n_p, n_e) = -\frac{3}{4} \left(\frac{3}{\pi} \right)^{1/3} e^2 (n_p^{4/3}(\mathbf{r}) + n_e^{4/3})$$

Taking functional derivatives of Eq. (19) with respect to the particle densities and including the conditions of charge neutrality and constant average baryon density with suitable Lagrange multipliers, leads to the variational equations

plus the β -equilibrium condition

$$\mu_e = \mu_n - \mu_p,$$

Table 7. Composition of state of the inner crust.

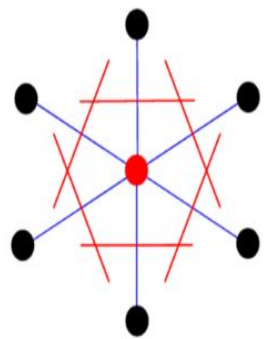
n_b (fm^{-3})	ϵ (g cm^{-3})	P (erg cm^{-3})	Γ
0.0003	5.0138E+11	8.2141E+29	0.443
0.0005	8.3646E+11	1.0417E+30	0.560
0.00075	1.2555E+12	1.3844E+30	0.747
0.0010	1.6746E+12	1.6984E+30	0.874
0.0014	2.3456E+12	2.3837E+30	1.004
0.0017	2.8488E+12	2.8551E+30	1.070
0.0020	3.3522E+12	3.4653E+30	1.121
0.0025	4.1915E+12	4.4319E+30	1.183
0.0030	5.0310E+12	5.6159E+30	1.226
0.0035	5.8706E+12	6.7099E+30	1.257
0.0040	6.7106E+12	8.0318E+30	1.280
0.0050	8.3909E+12	1.0646E+31	1.307
0.0060	1.0072E+13	1.3476E+31	1.319
0.0075	1.2594E+13	1.8085E+31	1.322
0.0088	1.4781E+13	2.2469E+31	1.318
0.0100	1.6801E+13	2.6490E+31	1.312
0.0120	2.0168E+13	3.3595E+31	1.303
0.0135	2.2694E+13	3.9198E+31	1.299
0.0150	2.5221E+13	4.5016E+31	1.297
0.0170	2.8591E+13	5.2957E+31	1.300
0.0180	3.0276E+13	5.7163E+31	1.303
0.0200	3.3648E+13	6.5647E+31	1.314
0.0225	3.7864E+13	7.6683E+31	1.334
0.0250	4.2081E+13	8.8299E+31	1.360
0.0275	4.6299E+13	1.0060E+32	1.392
0.0300	5.0519E+13	1.1361E+32	1.427
0.0325	5.4740E+13	1.2746E+32	1.466
0.0350	5.8962E+13	1.4221E+32	1.507
0.0375	6.3186E+13	1.5794E+32	1.550
0.0400	6.7411E+13	1.7473E+32	1.594
0.0425	7.1637E+13	1.9266E+32	1.638
0.0450	7.5864E+13	2.1181E+32	1.681
0.0475	8.0092E+13	2.3227E+32	1.725
0.0500	8.4322E+13	2.5411E+32	1.767
0.0520	8.7706E+13	2.7258E+32	1.800
0.0540	9.1092E+13	2.9200E+32	1.832
0.0560	9.4478E+13	3.1239E+32	1.864
0.0580	9.7865E+13	3.3370E+32	1.893
0.0600	1.0125E+14	3.5604E+32	1.922
0.0620	1.0464E+14	3.7946E+32	1.950
0.0640	1.0803E+14	4.0390E+32	1.976
0.0650	1.0973E+14	4.1651E+32	1.988
0.0660	1.1142E+14	4.2941E+32	2.000
0.0680	1.1481E+14	4.5601E+32	2.023
0.0700	1.1821E+14	4.8370E+32	2.045
0.0720	1.2160E+14	5.1245E+32	2.065
0.0740	1.2499E+14	5.4230E+32	2.083
0.0750	1.2669E+14	5.5763E+32	2.091
0.0760	1.2839E+14	5.7321E+32	2.100
0.0770	1.3008E+14	5.8903E+32	2.107
0.0780	1.3178E+14	6.052E+32	2.114
0.0790	1.3348E+14	6.217E+32	2.121
0.0800	1.3518E+14	6.354E+32	2.127

Table 6. Composition of the inner crust.

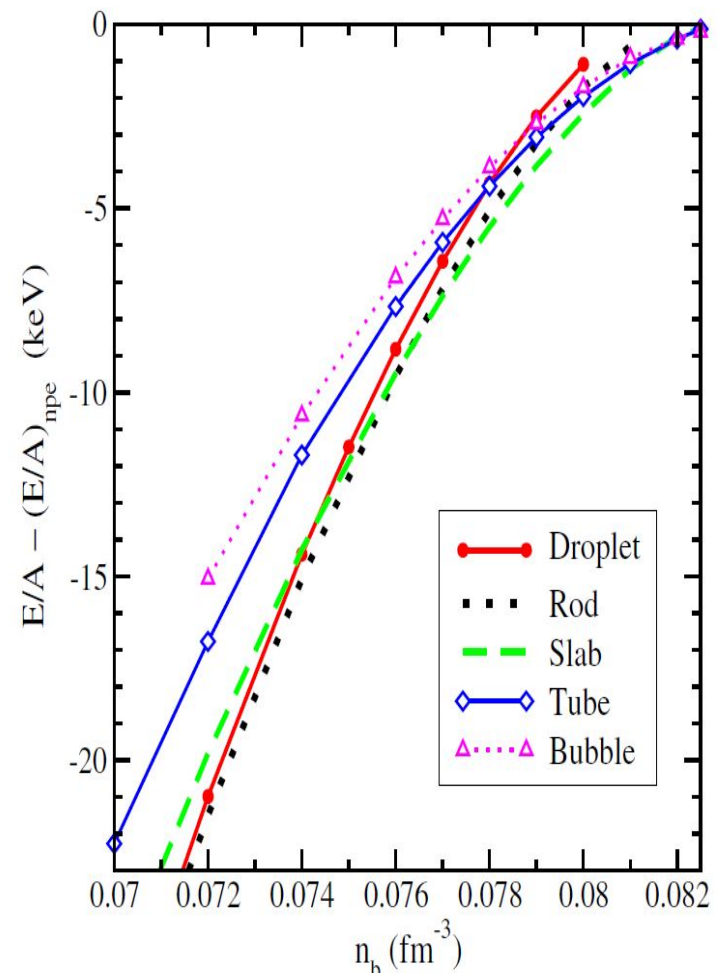
n_b (fm^{-3})	Z	A	R_c (fm)
0.0003	34.934	112.991	44.8000
0.0005	34.237	153.293	41.8300
0.00075	33.479	213.369	40.8000
0.0010	36.012	264.978	39.8450
0.0014	34.265	333.809	38.4675
0.0017	36.291	376.721	37.5400
0.0020	35.091	414.026	36.6975
0.0025	36.104	466.725	35.4550
0.0030	34.519	511.212	34.3925
0.0035	35.645	550.067	33.4775
0.0040	34.549	585.320	32.6900
0.0050	34.990	648.872	31.4075
0.0060	35.472	707.137	30.4150
0.0075	35.711	787.198	29.2625
0.0088	35.252	848.825	28.4500
0.0100	36.094	898.261	27.7825
0.0120	36.181	963.496	26.7625
0.0135	35.863	999.069	26.0450
0.0150	35.339	1025.682	25.3675
0.0170	34.982	1051.388	24.5325
0.0180	34.461	1061.641	24.1475
0.0200	34.036	1078.235	23.4350
0.0225	33.477	1094.430	22.6450
0.0250	32.910	1104.446	21.9300
0.0275	32.204	1104.566	21.2450
0.0300	31.290	1092.541	20.5625
0.0325	30.203	1069.599	19.8800
0.0350	29.036	1039.295	19.2100
0.0375	27.959	1008.341	18.5850
0.0400	27.152	984.099	18.0425
0.0425	26.665	968.891	17.5900
0.0450	26.549	965.017	17.2350
0.0475	26.701	968.928	16.9500
0.0500	26.955	974.581	16.6950
0.0520	27.096	975.352	16.4825
0.0540	27.065	968.814	16.2400
0.0560	26.808	953.172	15.9575
0.0580	26.322	928.561	15.6350
0.0600	25.650	897.063	15.2825
0.0620	25.080	869.075	14.9575
0.0640	24.833	852.005	14.7025
0.0650	24.750	844.737	14.5850
0.0660	24.672	837.603	14.4700
0.0680	24.613	826.389	14.2625
0.0700	24.674	818.891	14.0825
0.0720	24.875	815.658	13.9325
0.0740	25.249	817.728	13.8175
0.0750	25.502	820.707	13.7725
0.0760	25.810	825.326	13.7375
0.0770	26.190	832.083	13.7150
0.0780	26.615	840.127	13.7000
0.0790	27.111	850.432	13.6975
0.0800	27.677	863.085	13.7075

Thomas-Fermi (TF)

Inner crust



WS cell:
The smallest (primitive) cell which displays the full symmetry of the lattice.



► QCD + weak-interaction equilibrium + EM radiation + GR effect

1. Nuclear force + many-body quantum equation

2. Effective theory from quark/hadron level

Green's Function Monte Carlo

Chiral Perturbation Theory (ChPT)

Variational Many-Body (VMB)

V_{lowk} + Renormalization Group

Brueckner-Hartree-Fock (BHF)

Dirac-Brueckner-Hartree-Fock (DBHF)

Quark mean-field (QMF)

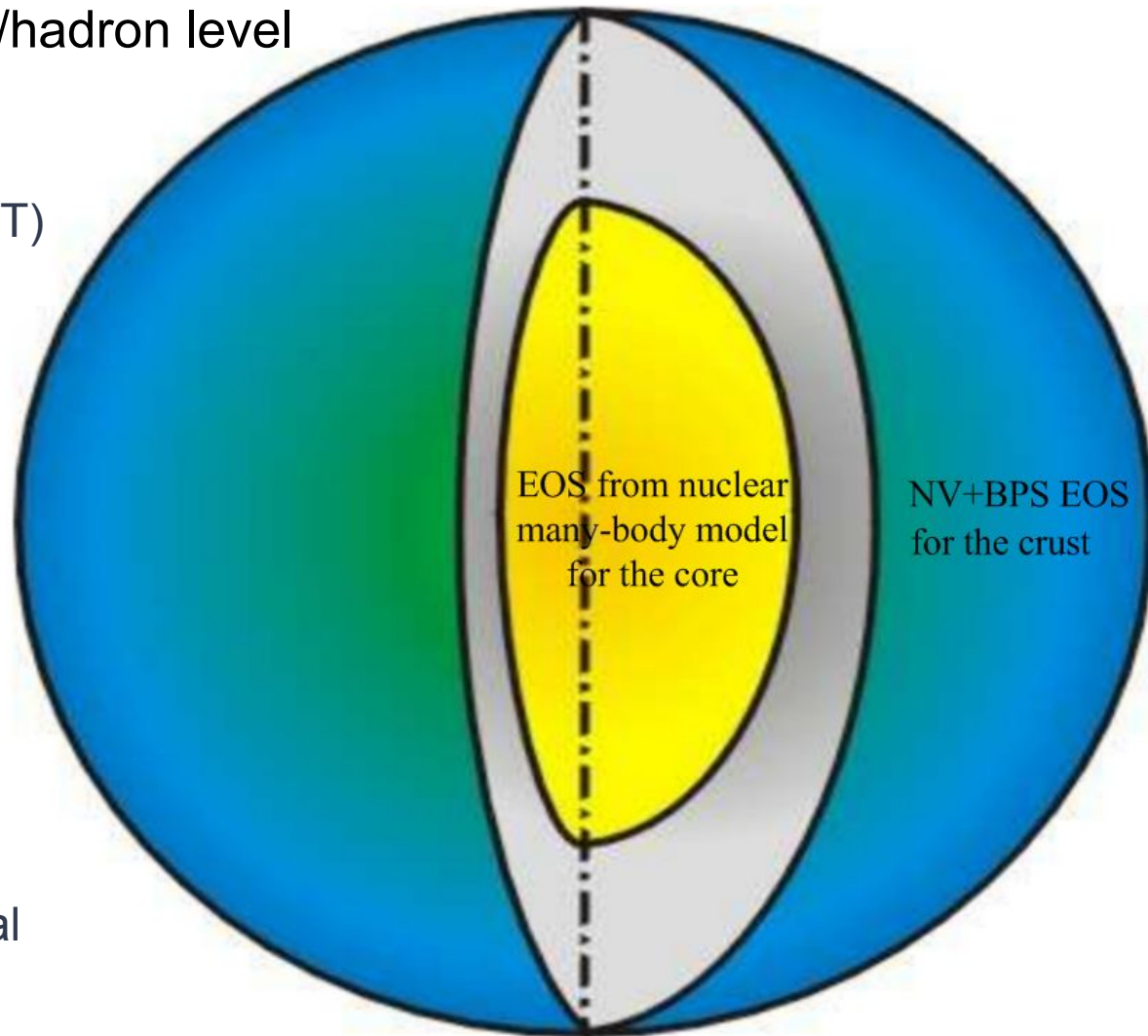
Quark Meson Coupling (QMC)

Relativistic mean-field (RMF)

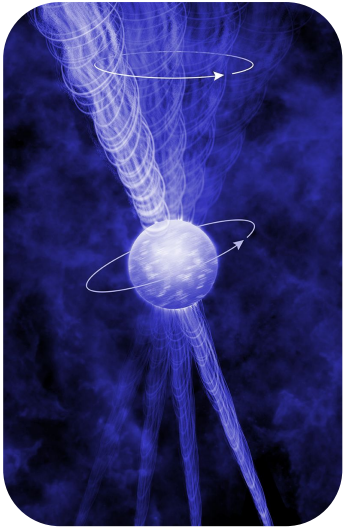
Skyrme energy density functional

...

N.B. From NS model to its astro. correspondence: Thermal; Neutrino; Rotation; Magnetic field, etc



► Rotation



- **NS/QS structures are unique to the underlying EoS.**

❑ Static (TOV)

$$\frac{dP(r)}{dr} = -\frac{GM(r)\varepsilon(r)}{r^2} \frac{\left[1 + \frac{P(r)}{\varepsilon(r)}\right] \left[1 + \frac{4\pi r^3 P(r)}{M(r)}\right]}{1 - \frac{2GM(r)}{r}}, \quad (1)$$

$$\frac{dM(r)}{dr} = 4\pi r^2 \varepsilon(r), \quad (2)$$

❑ Slow rotation $\Omega \ll \Omega_{\max} \approx \sqrt{GM/R^3}$

Spherical-symmetry metric + Axis-symmetry perturbation

**Vela pulsar @ AL, Dong, Wang, Xu, 2016
ApJS 1512.00340**

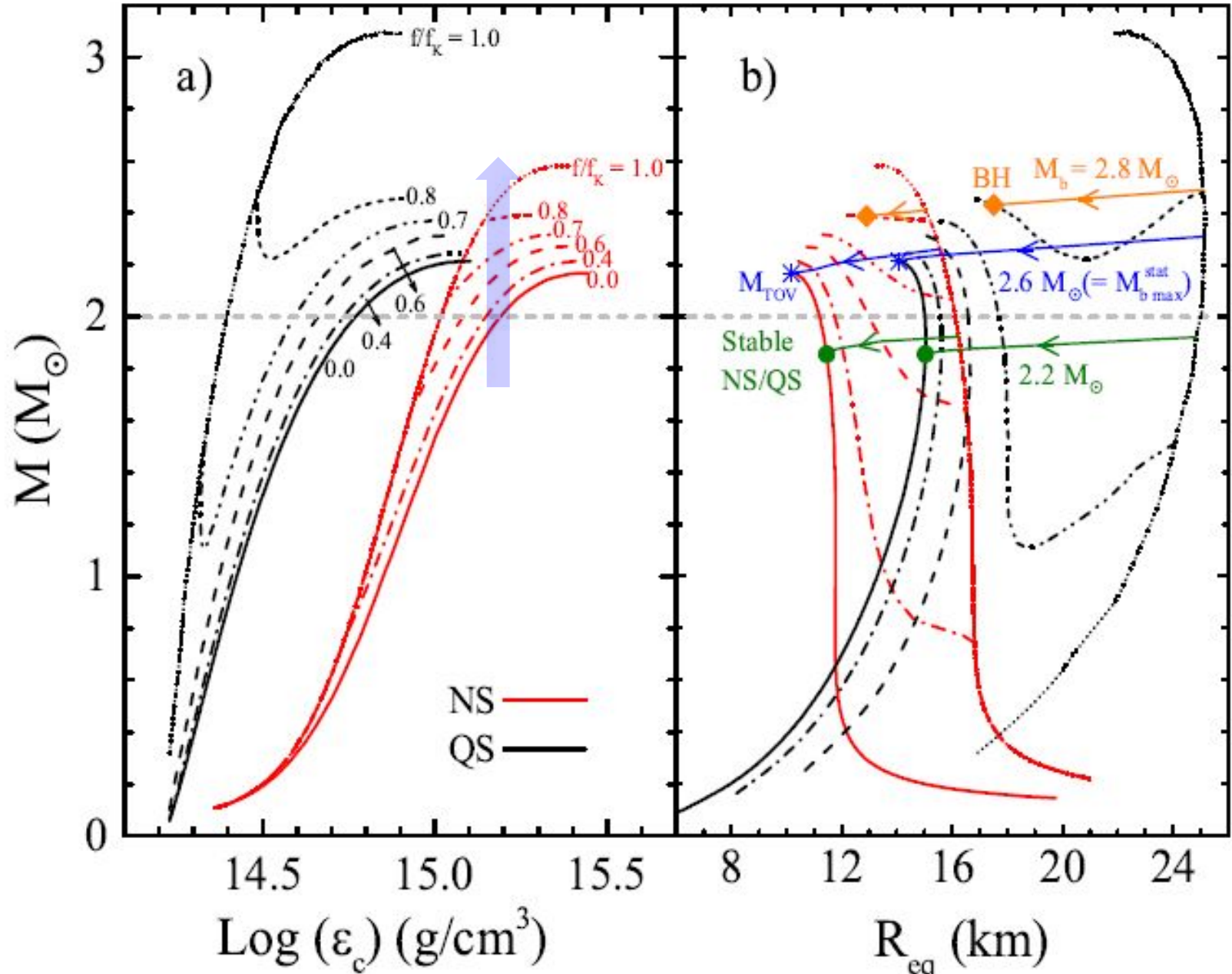
❑ Fast rotation

**Relativistic stars in general relativity from *rns* code
(www/gravity.phys.uwm.edu/rns),**

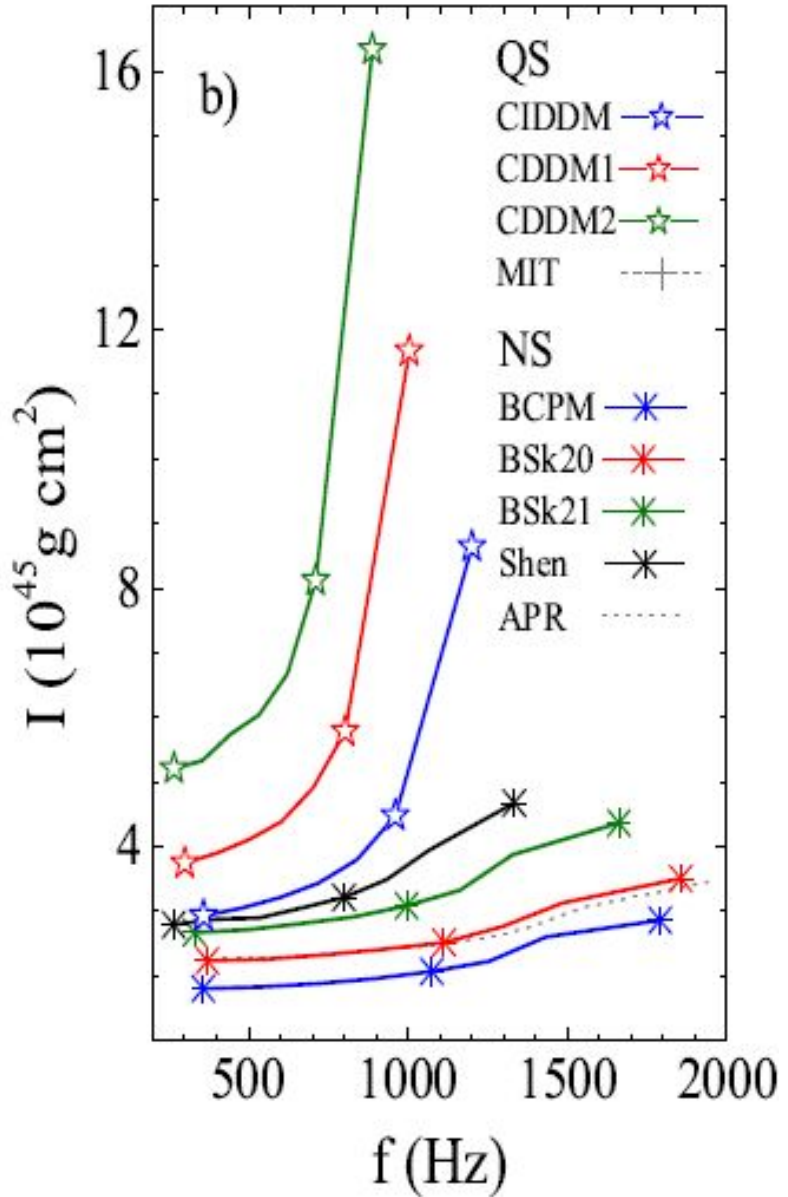
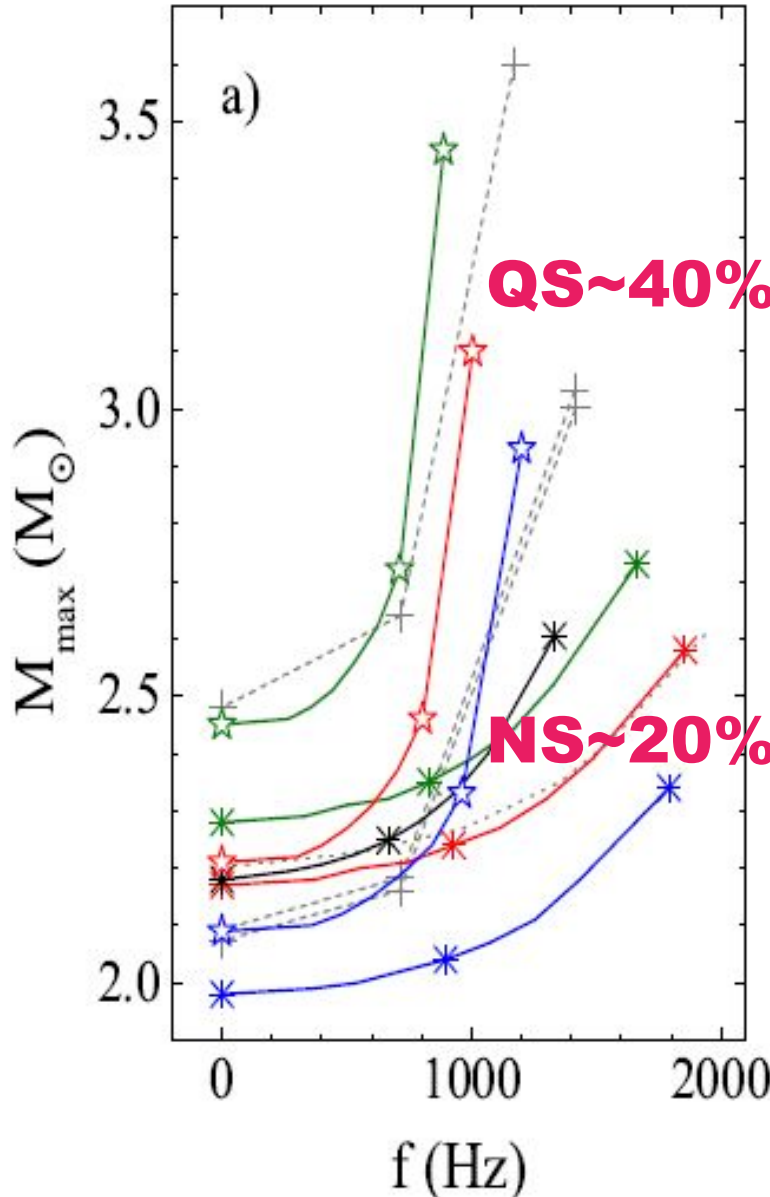
Komatsu H, Eriguchi Y and Hachisu I 1989 *Mon. Not. R. Astron. Soc.* **237** 355
 Cook G B, Shapiro S L and Teukolsky S A 1994 *ApJ* **422** 227
 Stergioulas N and Friedman J L 1995 *ApJ* **444** 306

**AL, Zhang, Zhang, Gao, Qi, Liu,
2016 PRD, 1606.02934**

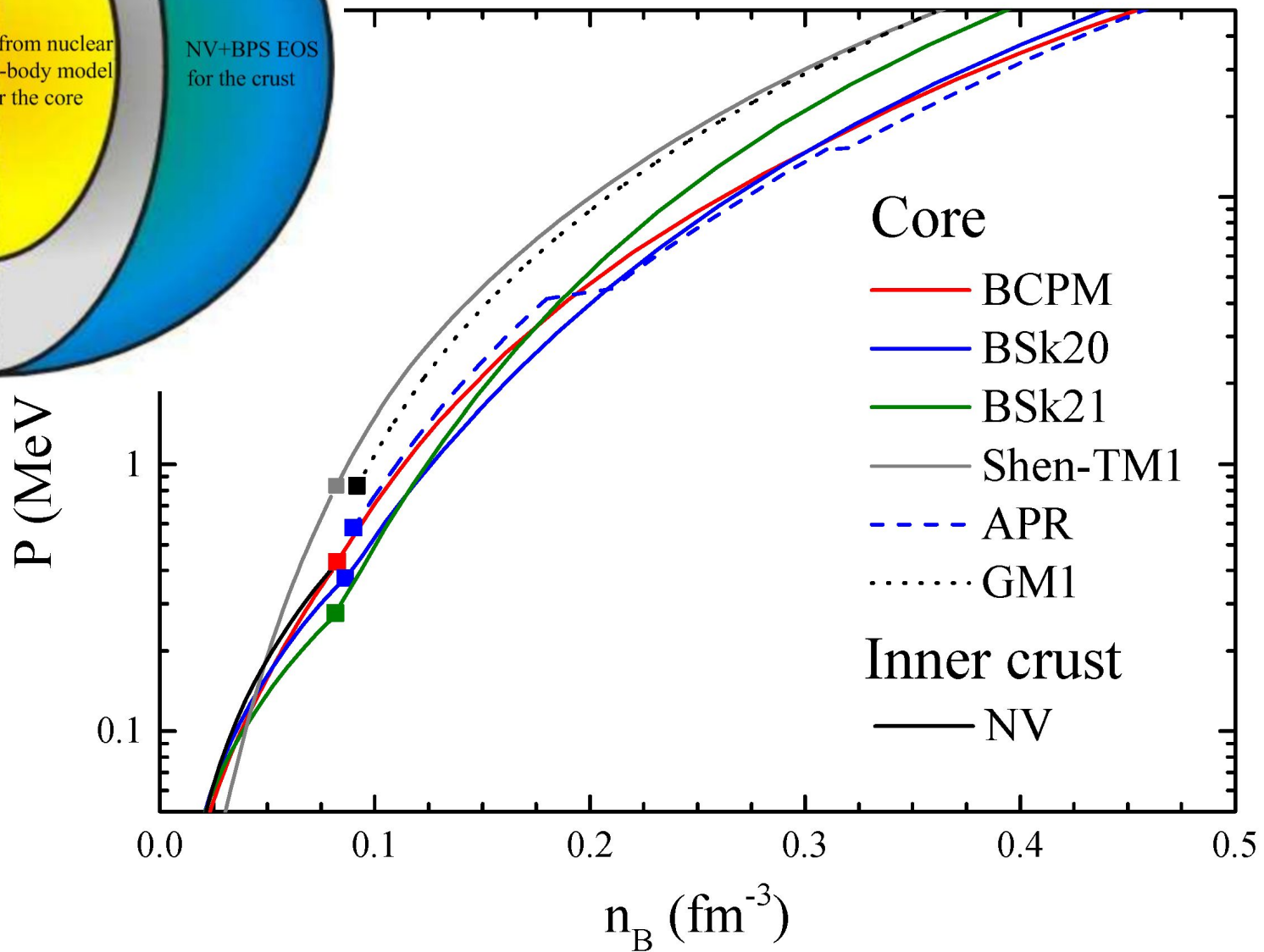
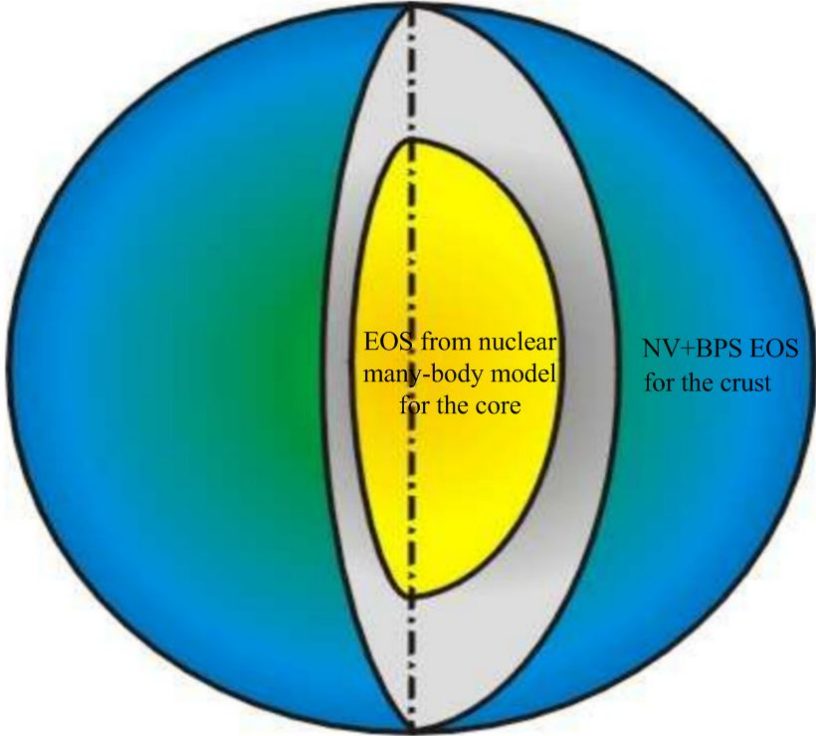
► Mass vs. density & frequency



► Mass and Moment of inertia vs. frequency



AL, Zhang, Qi, Burgio,
1610.0877



► Unified NS EoS

All EoS segments using **same** nuclear interaction.

eg., BCPM, BSk21 & others (Potekhin et al. 2013, Sharma et al. 2015, Fortin et al. 2016, etc)

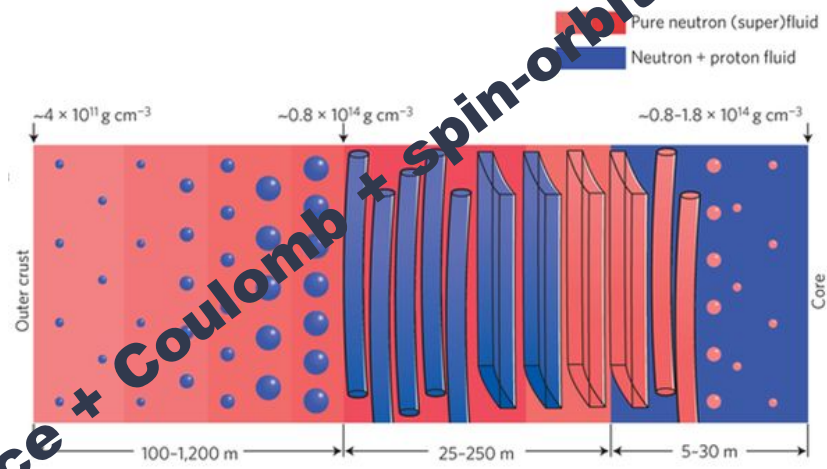
► Consistent core-crust transition properties.

Core:

- Green's Function Monte Carlo
- Chiral Perturbation Theory (ChPT)
- Variational Many-Body (VMB)
- V_{lowk} + Renormalization Group
- Brueckner-Hartree-Fock (BHF)
- Dirac-Brueckner-Hartree-Fock (DBHF)
- Quark mean-field (QMF)
- Quark Meson Coupling (QMC)
- Relativistic mean-field (RMF)
- Skyrme energy density functional

Inner crust:

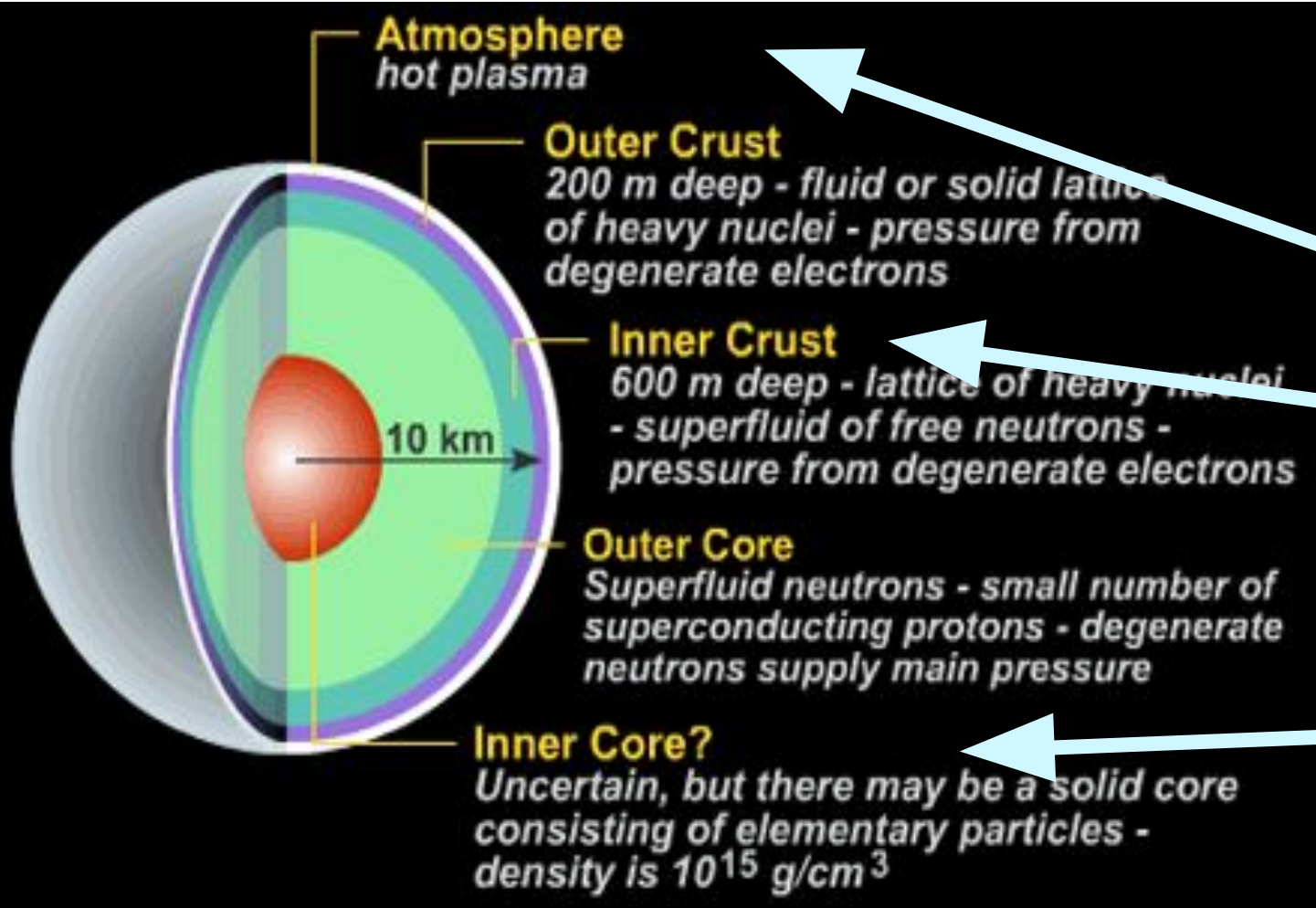
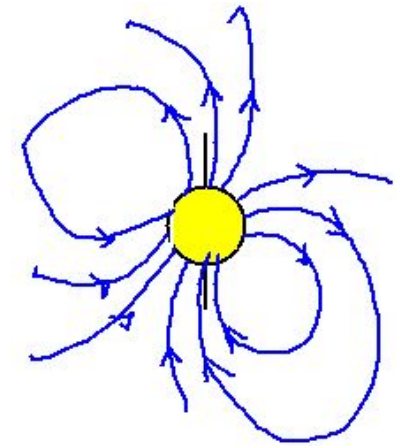
- Compressible Liquid Drop (CLDM)
- Thomas-Fermi (TF) approximation



Infinite uniform nuclear matter:
Bulk

+ surface + Coulomb + spin-orbit + pairing

► Astrophysical observables
(NICER, Athena, eXTP, FAST, SKA, LIGO/VIRGO)



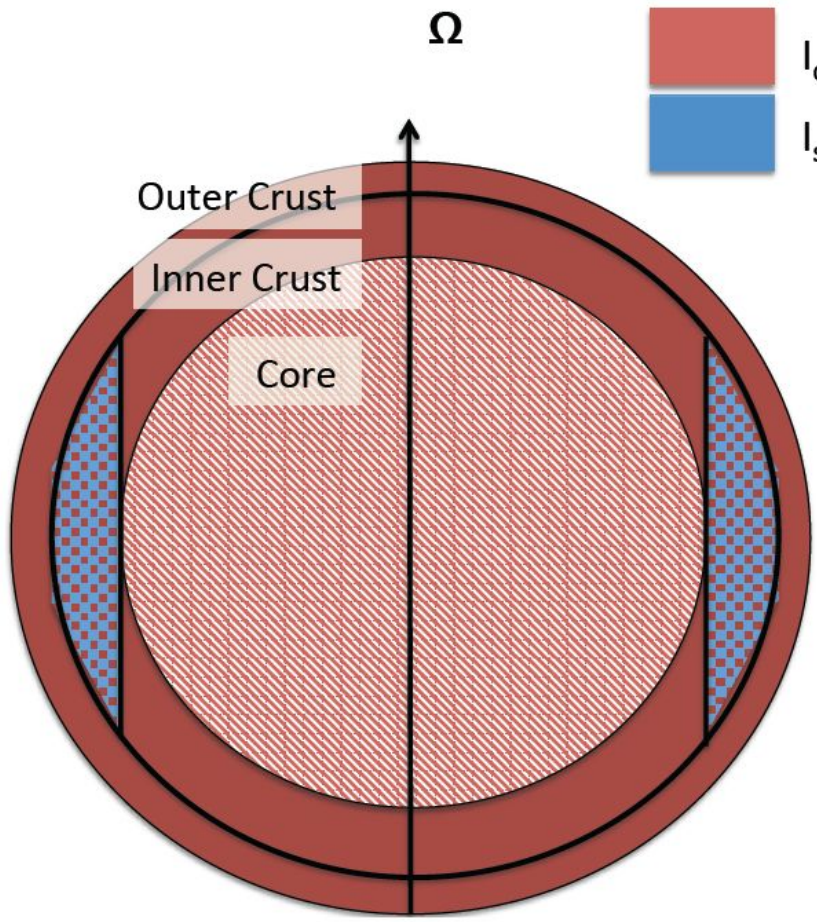
Hot X-ray

Glitch

(e.g., AL et al. 2016 ApJS)

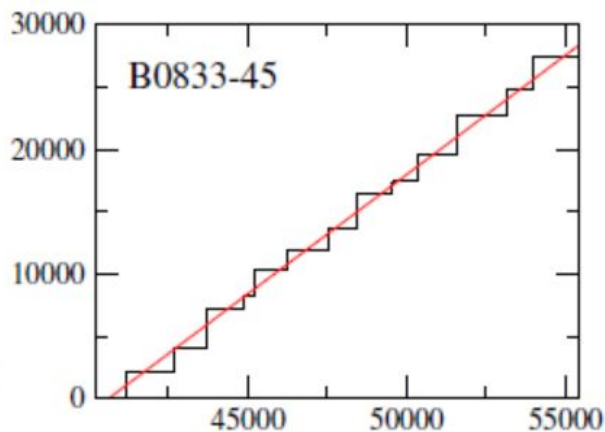
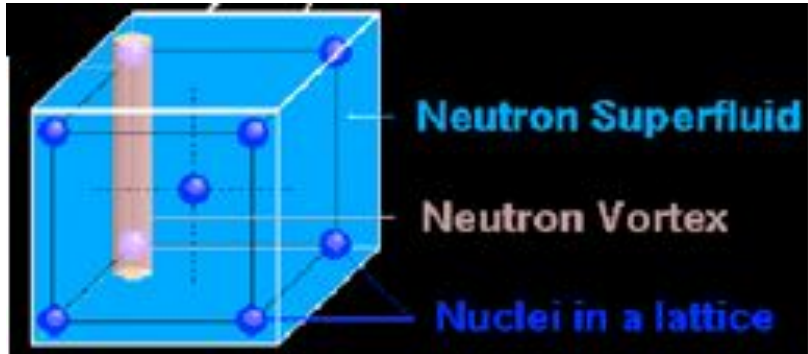
Mass/Radius

► **Glitch: Superfluid/two-component model**



I_c **Charged component**
 I_s **Superfluid component**

Decouple/Recouple/Decouple/Recouple...
 Unpin/Pin/Unpin/Pin...



The accumulated $\sum_i \Delta\Omega_p^i / \Omega_p$ ($\times 10^{-9}$) as a function of the modified Julian date

Assuming the star is rotating uniformly with a stellar frequency Ω far smaller than the Kepler frequency at the equator ($\Omega \ll \Omega_{max} \approx \sqrt{GM/R^3}$), the moment of inertia of a star with a radius R and an angular frequency Ω can be calculated in the slow-rotation approximation based on the above spherical-symmetry metric combined with an axis-symmetry perturbation (Hartle & Thorne 1968):

$$I = \frac{8\pi}{3} \int_0^R r^4 e^{-\nu(r)} \frac{\bar{\omega}(r)}{\Omega} \frac{(\varepsilon(r) + P(r))}{\sqrt{1 - 2GM(r)/r}} dr, \quad (3)$$

where $\nu(r)$ is a radially-dependent metric function given by

P = 89.33 milliseconds
for Vela.

$$\nu(r) = \frac{1}{2} \ln \left(1 - \frac{2GM}{R} \right) - G \int_r^R \frac{(M(x) + 4\pi x^3 P(x))}{x^2 (1 - 2GM(x)/x)} dx, \quad (4)$$

and $\bar{\omega}$ is the frame dragging angular velocity given by

$$\frac{1}{r^3} \frac{d}{dr} \left(r^4 j(r) \frac{d\bar{\omega}(r)}{dr} \right) + 4 \frac{dj(r)}{dr} \bar{\omega}(r) = 0, \quad (5)$$

where

$$I_c = \frac{8\pi}{3} \int_{R_c}^R r^4 e^{-\nu(r)} \frac{\bar{\omega}(r)}{\Omega} \frac{(\varepsilon(r) + P(r))}{\sqrt{1 - 2GM(r)/r}} dr$$

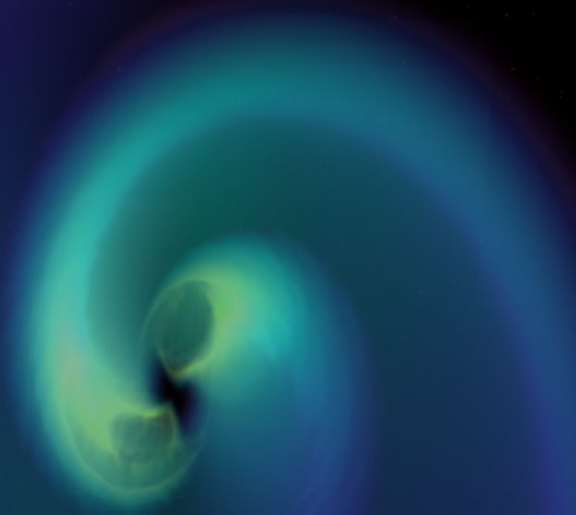
$$j(r) = e^{-\nu(r)-\lambda(r)} = \sqrt{1 - 2GM(r)/r} e^{-\nu(r)},$$

“Glitch crisis”

AL et al. 2016 ApJS

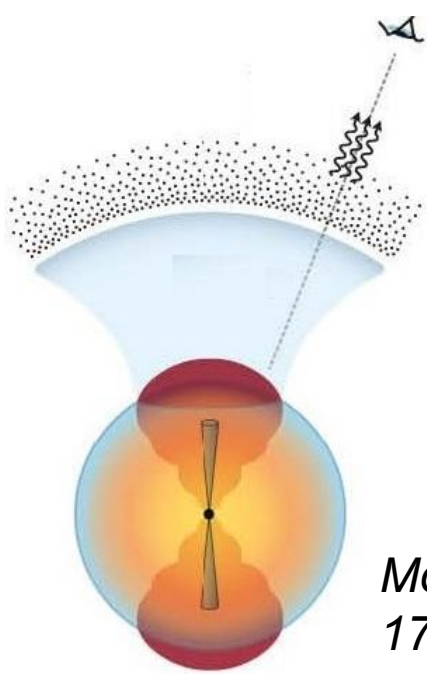
for $r \leq R$.

FIRST COSMIC EVENT OBSERVED IN GRAVITATIONAL WAVES AND LIGHT



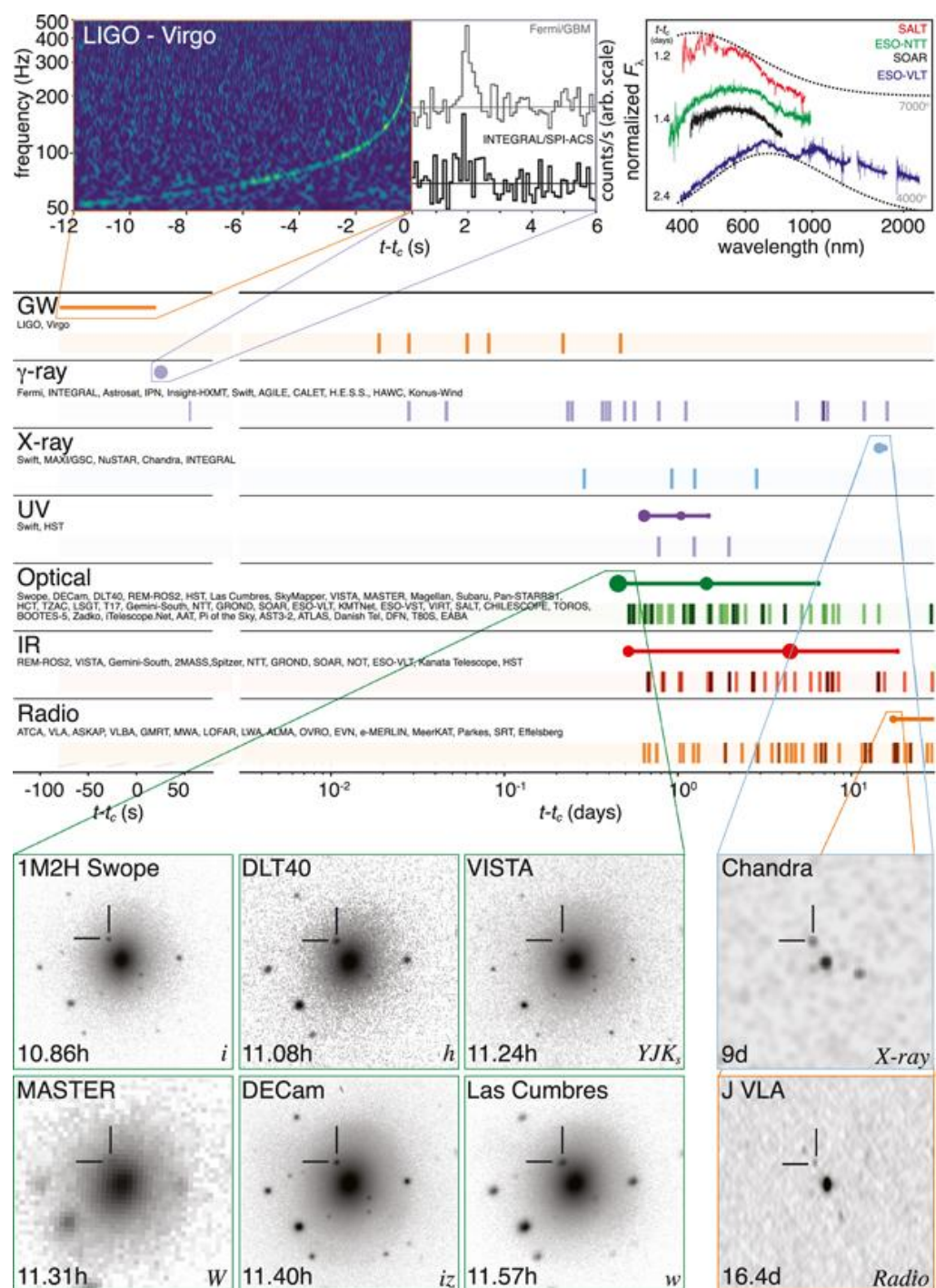
In this talk

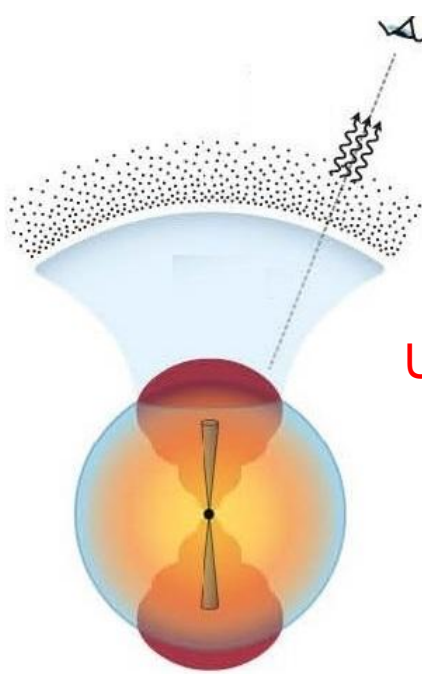
- Intro of NS
- NS EOS from GW170817
- New NS EOS “QMF18” proposed



Mooley et al.,
1711.11573

- ▶ GW
- ▶ Neutrino: none
- ▶ γ -ray: 1.7 s
- ▶ X-ray: 9 days
- ▶ UV/Optical/IR: 2 days
- ▶ Radio: 16 days





Uncertain:

- EOS
- Ejecta mass
- Mass ratio
- Jet structure
- ...

Long-lived NS as remnant?

1. Spin period
2. Magnetic field
3. Ellipticity
4. ...

S.-K. Ai, H. Gao, Z.-G. Dai, X.-F. Wu, A. Li and B. Zhang, **1802.00571**
 #The allowed parameter space of a long-lived neutron star as the merger remnant of GW170817

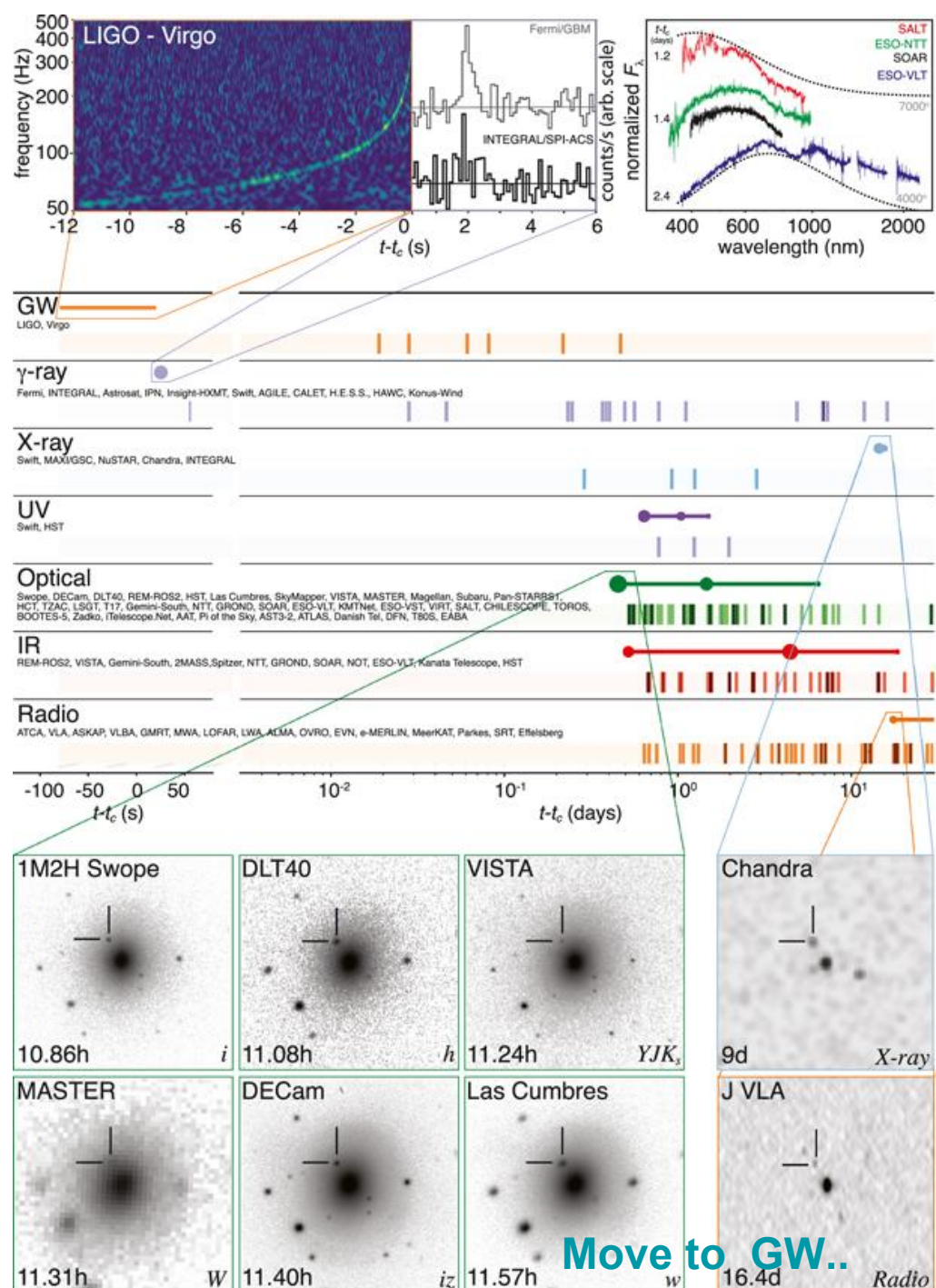


TABLE I. Source properties for GW170817: we give ranges encompassing the 90% credible intervals for different assumptions of the waveform model to bound systematic uncertainty. The mass values are quoted in the frame of the source, accounting for uncertainty in the source redshift.

	Low-spin priors ($ \chi \leq 0.05$)	High-spin priors ($ \chi \leq 0.89$)
Primary mass m_1	1.36–1.60 M_\odot	1.36–2.26 M_\odot
Secondary mass m_2	1.17–1.36 M_\odot	0.86–1.36 M_\odot
Chirp mass \mathcal{M}	1.188 $^{+0.004}_{-0.002}$ M_\odot	1.188 $^{+0.004}_{-0.002}$ M_\odot
Mass ratio m_2/m_1	0.7–1.0	0.4–1.0
Total mass m_{tot}	2.74 $^{+0.04}_{-0.01}$ M_\odot	2.82 $^{+0.47}_{-0.09}$ M_\odot
Radiated energy E_{rad}	$> 0.025 M_\odot c^2$	$> 0.025 M_\odot c^2$
Luminosity distance D_L	40 $^{+8}_{-14}$ Mpc	40 $^{+8}_{-14}$ Mpc
Viewing angle Θ	$\leq 55^\circ$	$\leq 56^\circ$
Using NGC 4993 location	$\leq 28^\circ$	$\leq 28^\circ$
Combined dimensionless tidal deformability $\tilde{\Lambda}$	≤ 800	≤ 700
Dimensionless tidal deformability $\Lambda(1.4M_\odot)$	≤ 800	≤ 1400

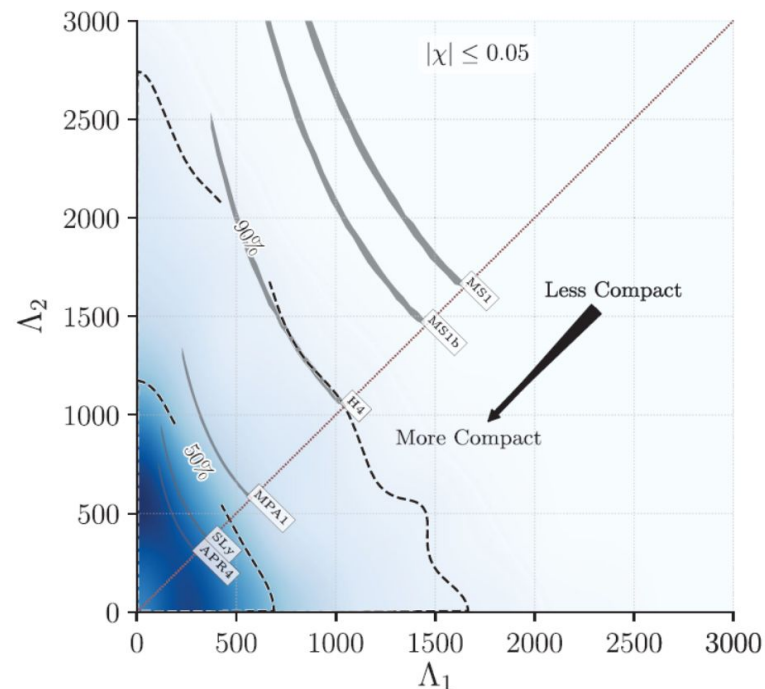
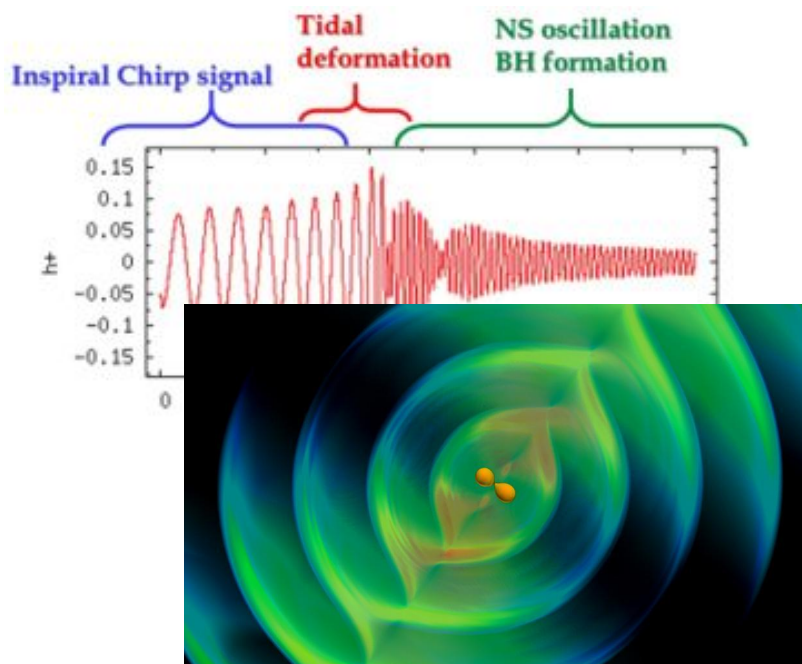
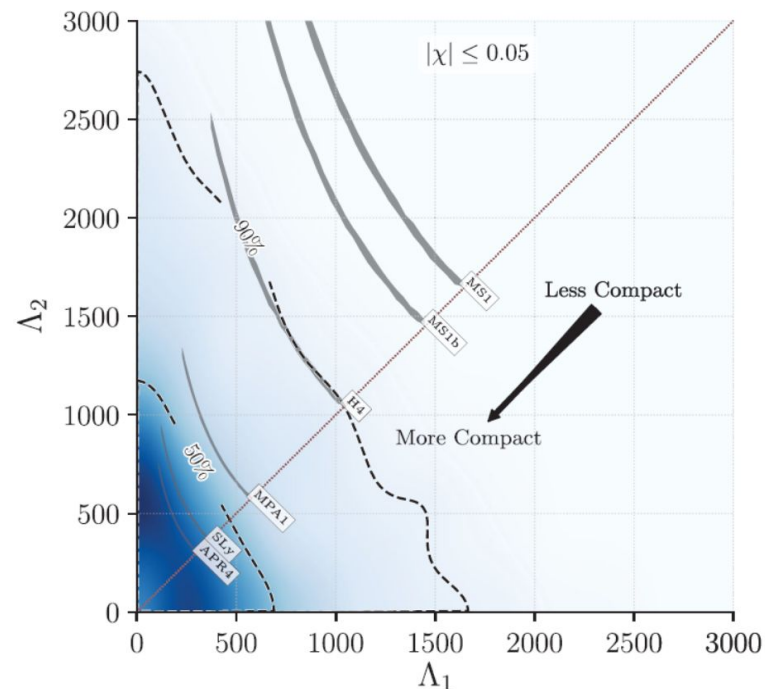
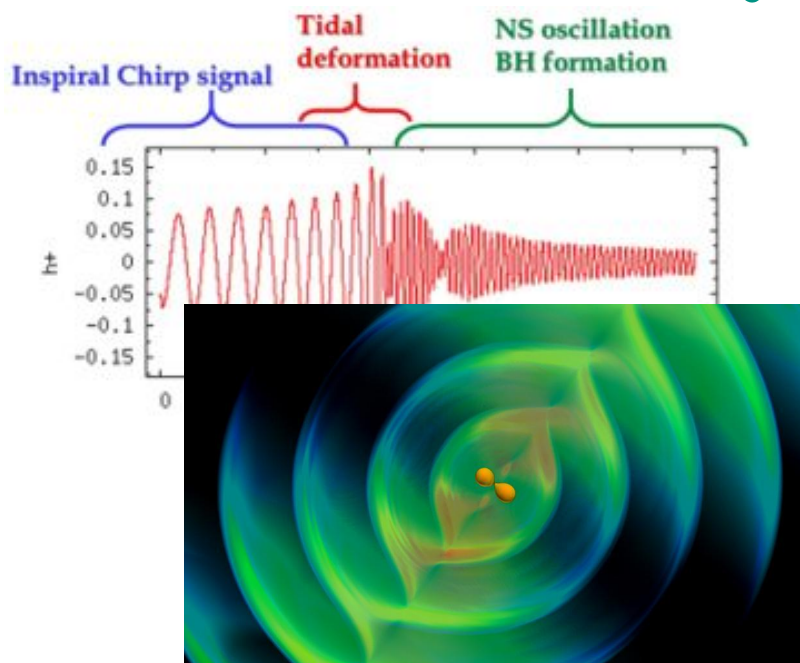


TABLE I. Source properties for GW170817: we give ranges encompassing the 90% credible intervals for different assumptions of the waveform model to bound systematic uncertainty. The mass values are quoted in the frame of the source, accounting for uncertainty in the source redshift.

	Low-spin priors ($ \chi \leq 0.05$)	High-spin priors ($ \chi \leq 0.89$)
Primary mass m_1	1.36–1.60 M_\odot	1.36–2.26 M_\odot
Secondary mass m_2	1.17–1.36 M_\odot	0.86–1.36 M_\odot
Chirp mass \mathcal{M}	1.188 $^{+0.004}_{-0.002}$ M_\odot	1.188 $^{+0.004}_{-0.002}$ M_\odot
Mass ratio m_2/m_1	0.7–1.0	0.4–1.0
Total mass m_{tot}	2.74 $^{+0.04}_{-0.03}$ M_\odot	2.82 $^{+0.47}_{-0.09}$ M_\odot
Radiated energy E_{rad}	$> 0.025 M_\odot c^2$	$> 0.025 M_\odot c^2$
Luminosity distance D_L	40 $^{+8}_{-11}$ Mpc	40 $^{+8}_{-14}$ Mpc
Viewing angle Θ	$\leq 55^\circ$	$\leq 56^\circ$
Using NGC 4993 location	$\leq 28^\circ$	$\leq 28^\circ$
Combined dimensionless tidal deformability $\tilde{\Lambda}$	≤ 800	≤ 700
Dimensionless tidal deformability $\Lambda(1.4M_\odot)$	≤ 800	≤ 1400

More reasonable
considering magnetic braking
during the binary evolution



► From EoS to Λ

The tidal Love numbers k_2 is obtained from the ratio of the induced quadrupole moment Q_{ij} to the applied tidal field E_{ij} (Damour & Nagar 2009; Damour et al. 1992; Hinderer 2008): $Q_{ij} = -k_2 \frac{2R^5}{3G} E_{ij}$, where R is the NS radius. k_2 depends on the compactness M/R and the quantity y_R . y_R is determined by solving the following differential equation for y ,

$$r \frac{dy(r)}{dr} + y(r)^2 + y(r)F(r) + r^2 Q(r) = 0, \quad (14)$$

where $F(r)$ and $Q(r)$ are functionals of $\mathcal{E}(r)$, $P(r)$ and $M(r)$:

$$F(r) = \frac{r - 4\pi r^3 [\mathcal{E}(r) - P(r)]}{r - 2M(r)}, \quad (15)$$

$$Q(r) = \frac{4\pi r \left(5\mathcal{E}(r) + 9P(r) + \frac{\mathcal{E}(r)+P(r)}{\partial P/\partial \mathcal{E}} - \frac{6}{4\pi r^2} \right)}{r - 2M(r)} - 4 \left[\frac{M(r) + 4\pi r^3 P(r)}{r^2(1 - 2M(r)/r)} \right]^2. \quad (16)$$

$$\begin{aligned} k_2 &= \frac{1}{20} \left(\frac{2M}{R} \right)^5 \left(1 - \frac{2M}{R} \right)^2 \left[2 - y_R + (y_R - 1) \frac{2M}{R} \right] \\ &\times \left\{ \frac{2M}{R} \left(6 - 3y_R + \frac{3M}{R} (5y_R - 8) + \frac{1}{4} \left(\frac{2M}{R} \right)^2 \right. \right. \\ &\times \left. \left[26 - 22y_R + \left(\frac{2M}{R} \right) (3y_R - 2) + \left(\frac{2M}{R} \right)^2 (1 + y_R) \right] \right\} \\ &+ 3 \left(1 - \frac{2M}{R} \right)^2 \left[2 - y_R + (y_R - 1) \frac{2M}{R} \right] \\ &\times \ln \left(1 - \frac{2M}{R} \right) \Big\}^{-1}. \end{aligned} \quad (17)$$

Zhu, Zhou & AL
1802.05510

One can then compute the dimensionless tidal deformability Λ , which is related to the compactness M/R and the Love number k_2 through $\Lambda = \frac{2}{3} k_2 (M/R)^{-5}$.

▶ $\Lambda_{1.4} \lesssim 800$ for low-spin spior

▶ NS EOS

#Gravitational-wave constraints on the neutron-star-matter Equation of State
Annala et al., **1711.02644, PRL**

#GW170817: Joint Constraint on the Neutron Star Equation of State from
Multimessenger Observations
Radice et al., **1711.03647, ApJL**

#Neutron skins and neutron stars in the multi-messenger era
Fattoyev, et al., **1711.06615, PRL**

#Imprints of the nuclear symmetry energy on the tidal deformability of neutron stars
Krastev & Li, **1801.04620**

▶ QS EOS

#Constraints on interquark interaction parameters with GW170817 in a binary strange
star scenario
Zhou, Zhou & **AL, 1711.04312, PRD**

▶ $\Lambda_{1.4} \lesssim 800$ for low-spin spior

▶ CET + pQCD ($\gtrsim 2.6$ GeV)

▶ $\pm 24\%$ uncertainty @ $1.1n_0$

Soft/hard hadronic component

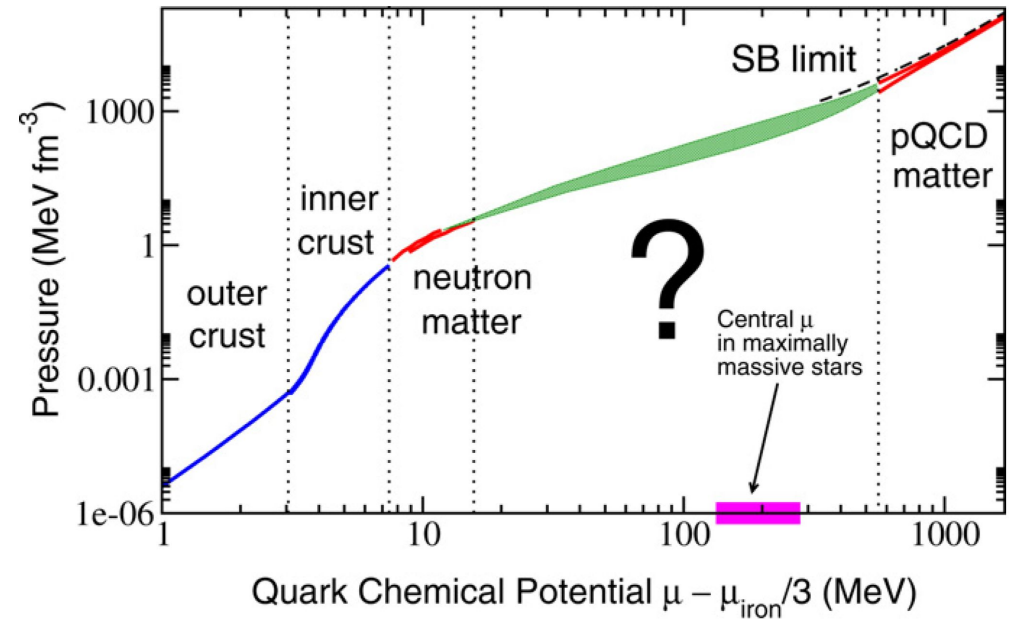
($0.6-1.1n_0$; Hebeler et al. 2013):

$\Lambda_{1.4} = (120/161, 1353/1504)$

▶ $M_{\text{TOV}} \gtrsim 2.0$: $R_{1.4} > 9.9$ km

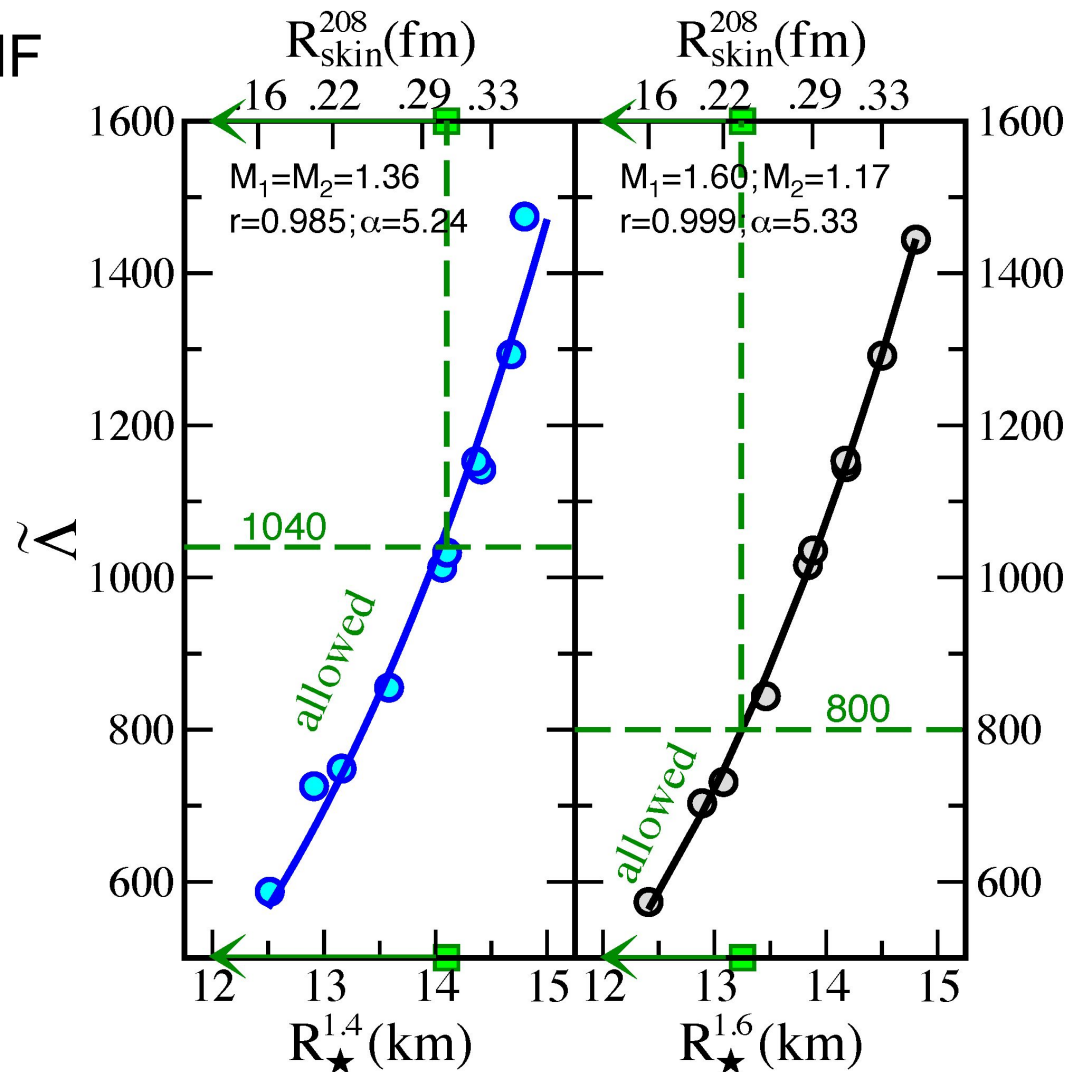
$\Lambda_{1.4} \lesssim 800$: $R_{1.4} < 13.6$ km

Annala et al., 1711.02644, PRL



3-tropes	All EoSs	$2M_{\odot}$	$\Lambda < 800$
γ_1	0.2-8.5	0.7-8.5	0.7-6.6
$M_{\text{max}} [M_{\odot}]$	<0.5-3.0	2.0-3.0	2.0-2.7
$R(1.4M_{\odot})$ [km]	7.1-14.6	10.7-14.6	10.7-13.6
4-tropes	All EoSs	$2M_{\odot}$	$\Lambda < 800$
γ_1	0.05-8.5	0.6-8.5	0.6-6.7
$M_{\text{max}} [M_{\odot}]$	<0.5-3.2	2.0-3.2	2.0-3.0
$R(1.4M_{\odot})$ [km]	6.6-14.6	9.9-14.6	9.9-13.6

- ▶ $\Lambda_{1.4} \lesssim 800$ for low-spin spior
 - ▶ 10 representative EOSs of RMF models;
 - ▶ $\Lambda_{1.4} \lesssim 800$: $R_{1.6} \leq 13.25\text{km}$
 $R_{\text{skin}}^{208} \leq 0.25\text{fm}$
 - ▶ PREX experiment:
 (Abrahamyan, et al. 2012;
 Horowitz et al., 2012)
- $$R_{\text{skin}}^{208} = 0.33^{+0.16}_{-0.18}\text{fm}$$
- ▶ Stiff low + Soft high:
 phase transition in the
 neutron-star interior?!
- (Hyperon puzzle/**dilemma**,
 Delta(1232)/hyperon/Kaon/quark
complication)



Strange Quark Star

Neutron Star

- Surface**
- Degenerate electron layer

- Core**
- Electrons
 - u,d,s quarks (color-superconducting)

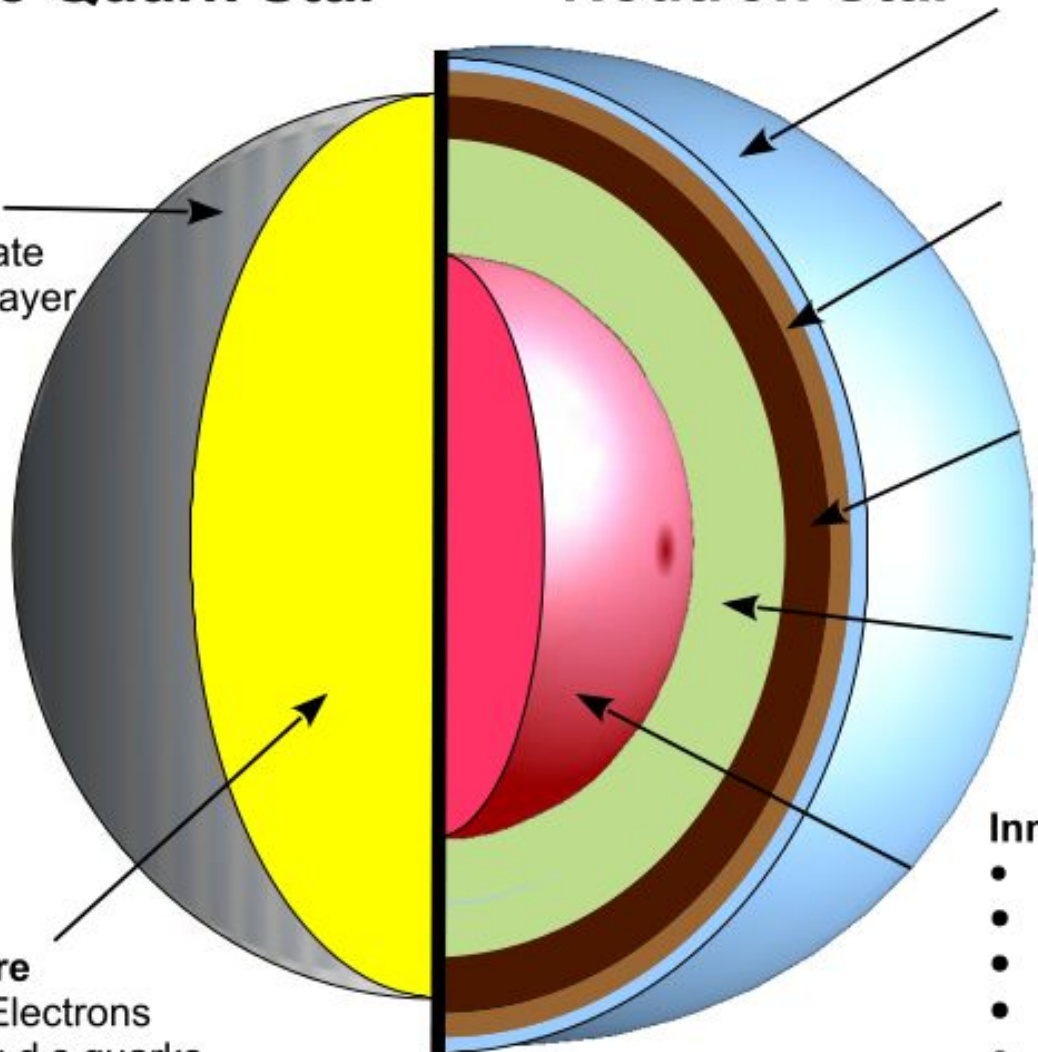
- Surface**
- Hydrogen/Helium plasma
 - Iron nuclei

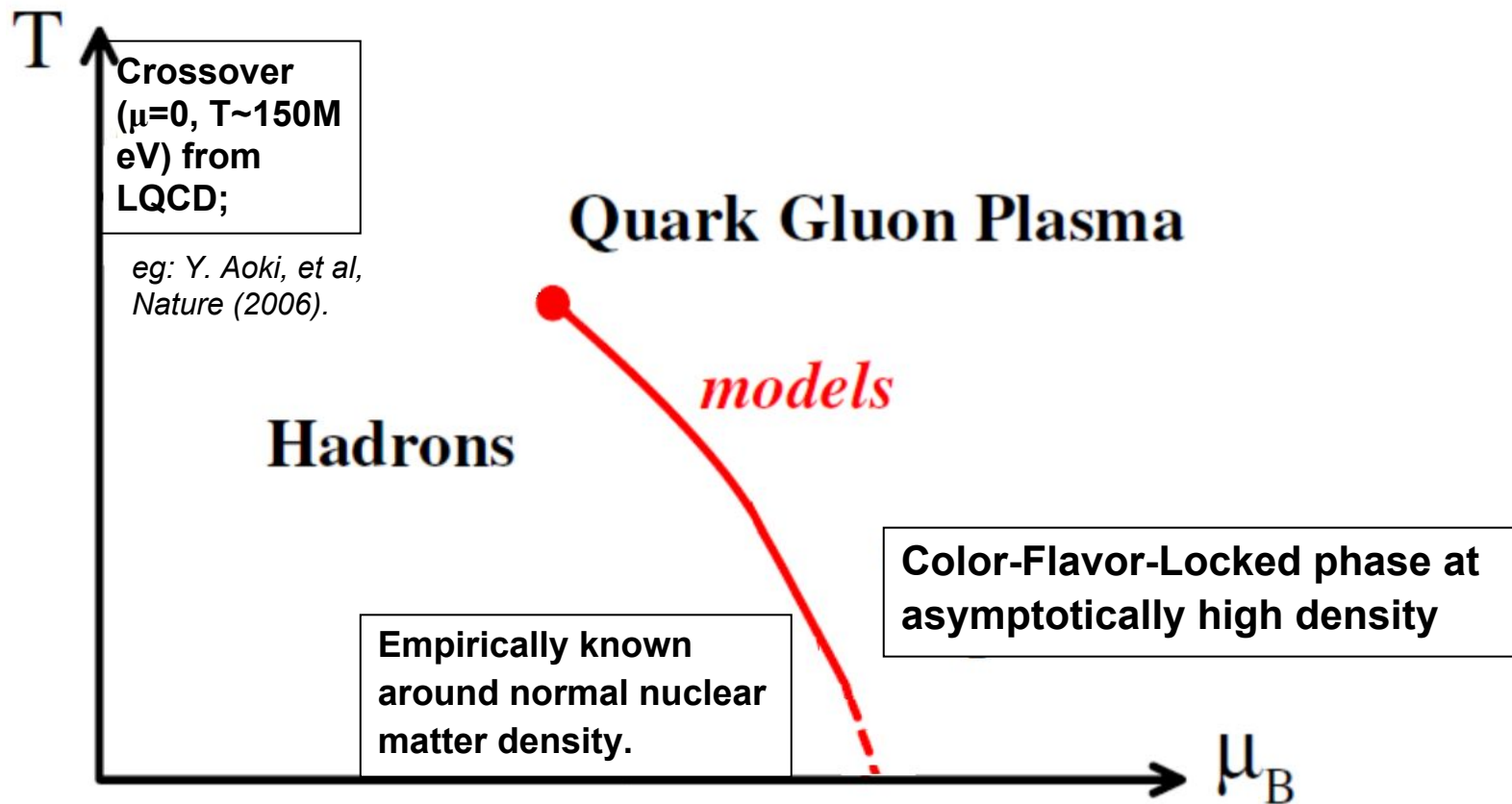
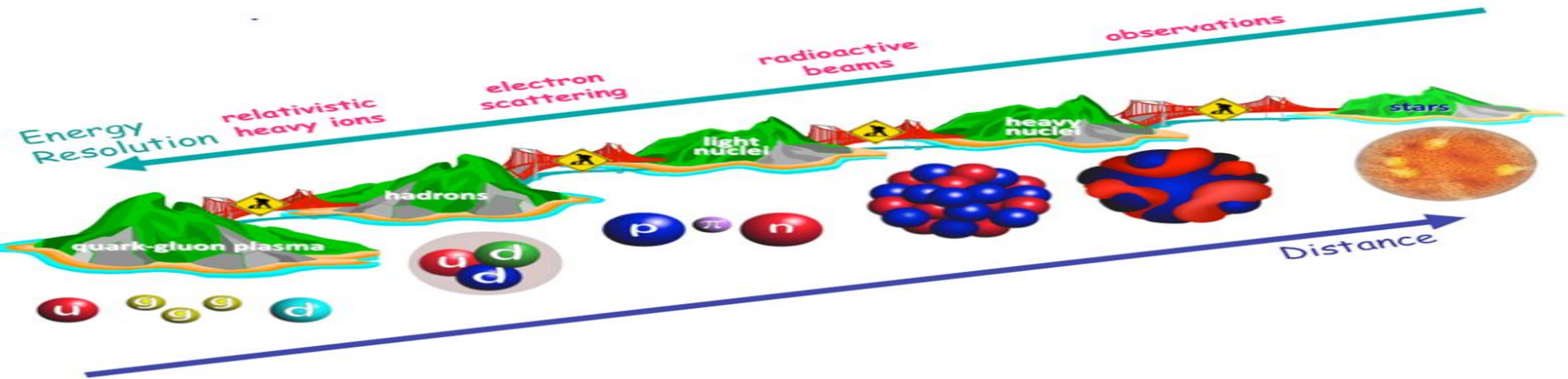
- Outer Crust**
- Ions
 - Electron gas

- Inner Crust**
- Heavy ions
 - Relativistic electron gas
 - Superfluid neutrons

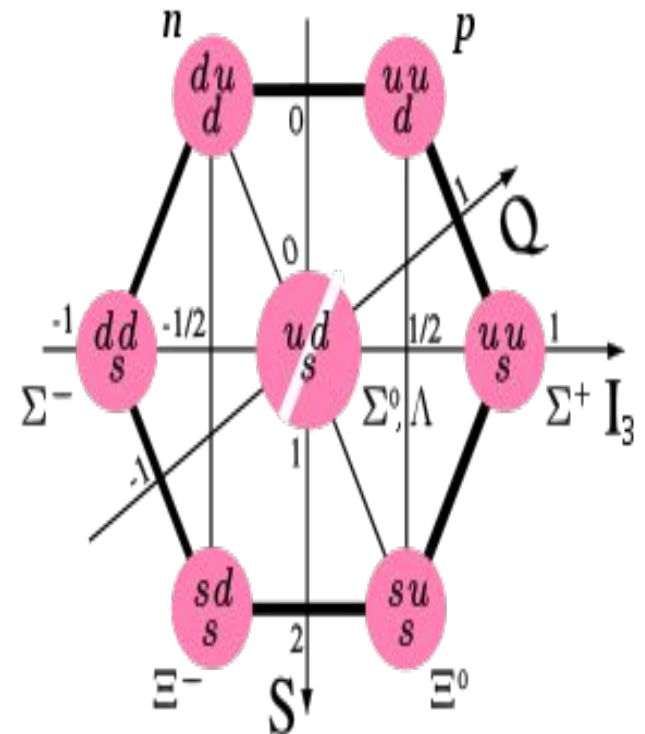
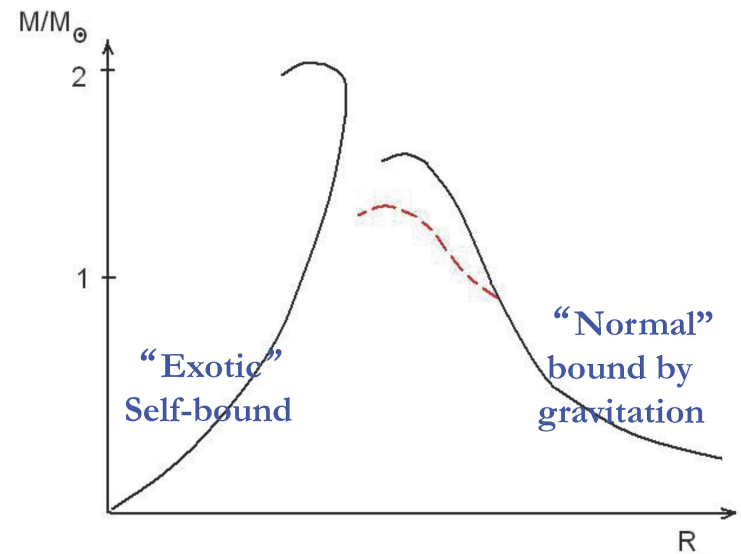
- Outer Core**
- Neutrons, protons
 - Electrons, muons

- Inner Core**
- Neutrons
 - Superconducting protons
 - Electrons, muons
 - Hyperons (Σ , Λ , Ξ)
 - Deltas (Δ)
 - Boson (π , K) condensates
 - Deconfined (u,d,s) quarks/color-superconducting quark matter





- ▶ Two-branch picture?
- ▶ Any strangeness phase transition leads to softer EOS (lower M_{TOV}) (Hyperon puzzle) (e.g., **AL** et al. 2006, 2010, 2013, 2016);
- ▶ Nucleonic EOS sufficiently stiff, or only weak soften (late appearance) of Delta(1232)/hyperon/Kaon/quark (e.g., **AL** et al. 2015);
- ▶ Universal baryonic repulsive three-body force, or stiff quark core;
- ▶ Study of hyperon interaction (NY,YY,NNY,NYY,YYY) through hyperonnuclei/scattering experiments VERY IMPORTANT (e.g., **AL** et al. 2007, 2013; Hu, **AL** et al. 2014).



► Hyperon interaction (NY,YY,NNY,NYY,YYY) through hyperon nuclei/scattering experiments are VERY IMPORTANT 1/2

- **Microscopic** scheme, e.g., BHF;
- Nijmegen soft-core NY potentials (NSC89/ESC08...) model, fitted to the available experimental NY scattering data;
- Presently, 4233 NN data, 52 NY data, weak $\Lambda\Lambda$ attraction (Nagara event, Takahashi et al., PRL 2001)

With these potentials, the various G -matrices are evaluated by solving numerically the Bethe-Goldstone equation, which can be written in operator form as

$$G_{ab}[W] = V_{ab} + \sum_c \sum_{p,p'} V_{ac} |pp'\rangle \frac{Q_c}{W - E_c + i\varepsilon} \langle pp'| G_{cb}[W], \quad (6)$$

where the indices a, b, c indicate pairs of baryons, and the Pauli operator Q_c and energy E_c characterize the propagation of intermediate baryon pairs. The pair energy in a given channel $c = (B_1 B_2)$ is

$$E_{(B_1 B_2)} = T_{B_1}(k_{B_1}) + T_{B_2}(k_{B_2}) + U_{B_1}(k_{B_1}) + U_{B_2}(k_{B_2}), \quad (7)$$

with $T_B(k) = m_B + k^2/2m_B$, where the various s.p. potentials are given by

$$U_B(k) = \sum_{B'=n,p,\Lambda,\Sigma^-} U_B^{(B')}(k) \quad (8)$$

and are determined self-consistently from the G -matrices,

$$U_B^{(B')}(k) = \sum_{k' < k_F^{(B')}} \text{Re} \langle kk'| G_{(BB')(BB')} [E_{(BB')}(k, k')] |kk'\rangle_A. \quad (9)$$

The coupled eqs. (6)–(9) define the BHF scheme with the

e.g., Burgio, Schulze, **AL**, 1101.0726
PRC 2011

► Hyperon interaction (NY,YY,NNY,NYY,YYY) through hyperonnuclei/scattering experiments are VERY IMPORTANT 2/2

- Phenomenological scheme, e.g., RMF/QMF;
- Meson coupling constant ($\sigma\omega\rho\dots$)

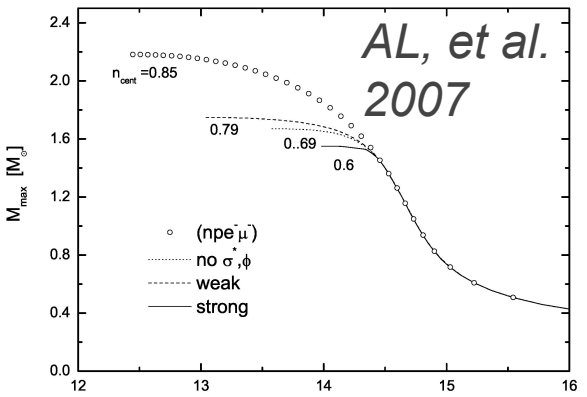
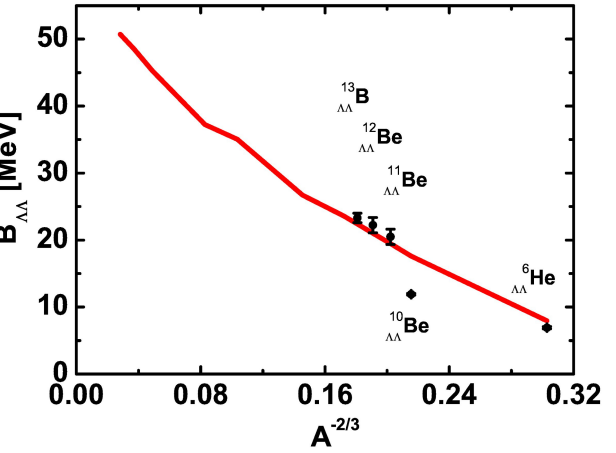
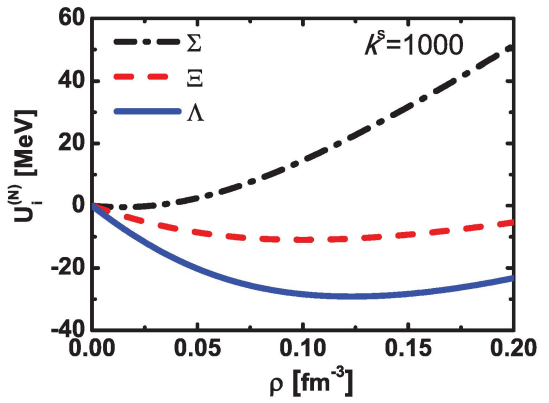
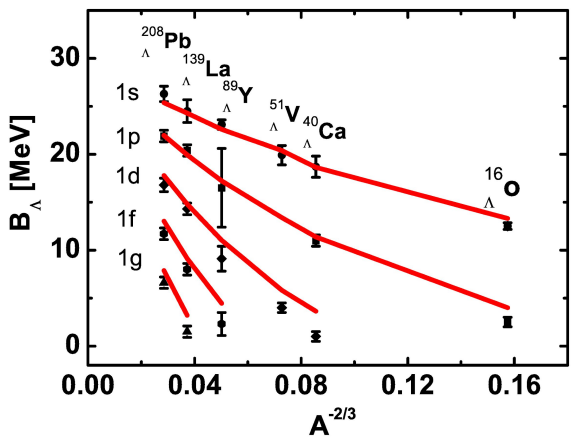
$$\mathcal{L} = \bar{\psi} \left[i\gamma_\mu \partial^\mu - M_N^* - g_\omega \omega \gamma^0 - g_\rho \rho \tau_3 \gamma^0 - e \frac{(1 + \tau_3)}{2} A \gamma^0 \right] \psi$$

$$+ \bar{\psi}_\Lambda \left[i\gamma_\mu \partial^\mu - M_\Lambda^* - g_\omega^\Lambda \omega \gamma^0 \right] \psi_\Lambda$$

$$- \frac{1}{2} (\nabla \sigma)^2 - \frac{1}{2} m_\sigma^2 \sigma^2 - \frac{1}{4} g_3 \sigma^4$$

$$+ \frac{1}{2} (\nabla \omega)^2 + \frac{1}{2} m_\omega^2 \omega^2 + \frac{1}{4} c_3 \omega^4$$

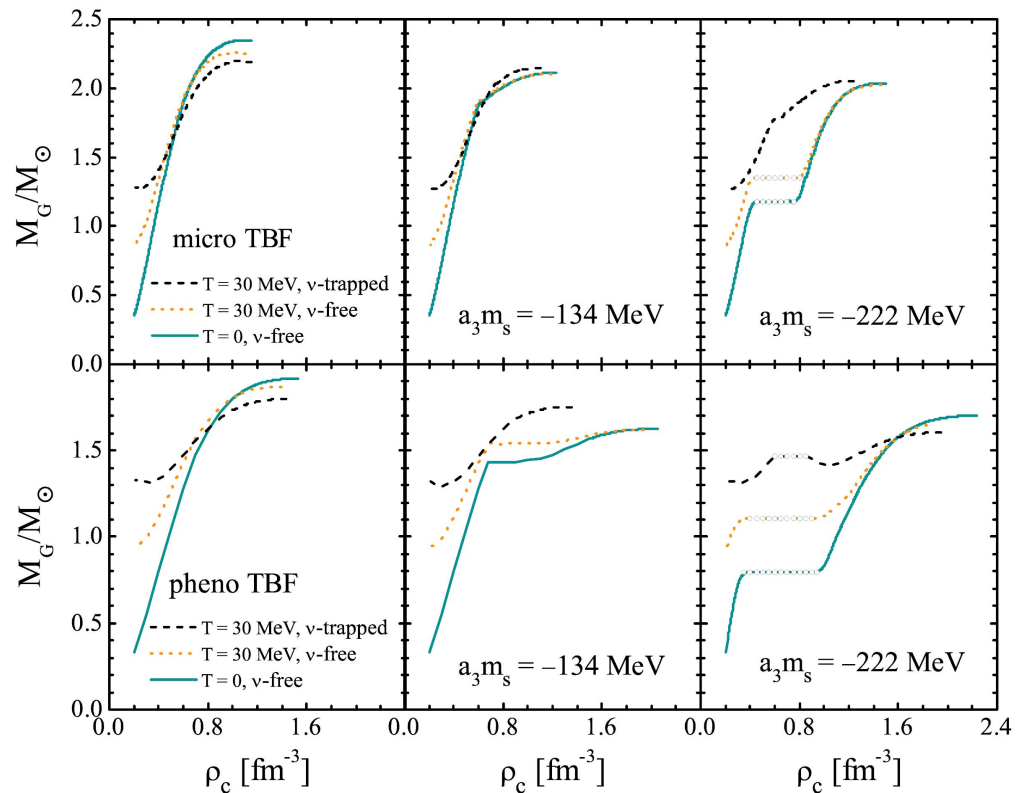
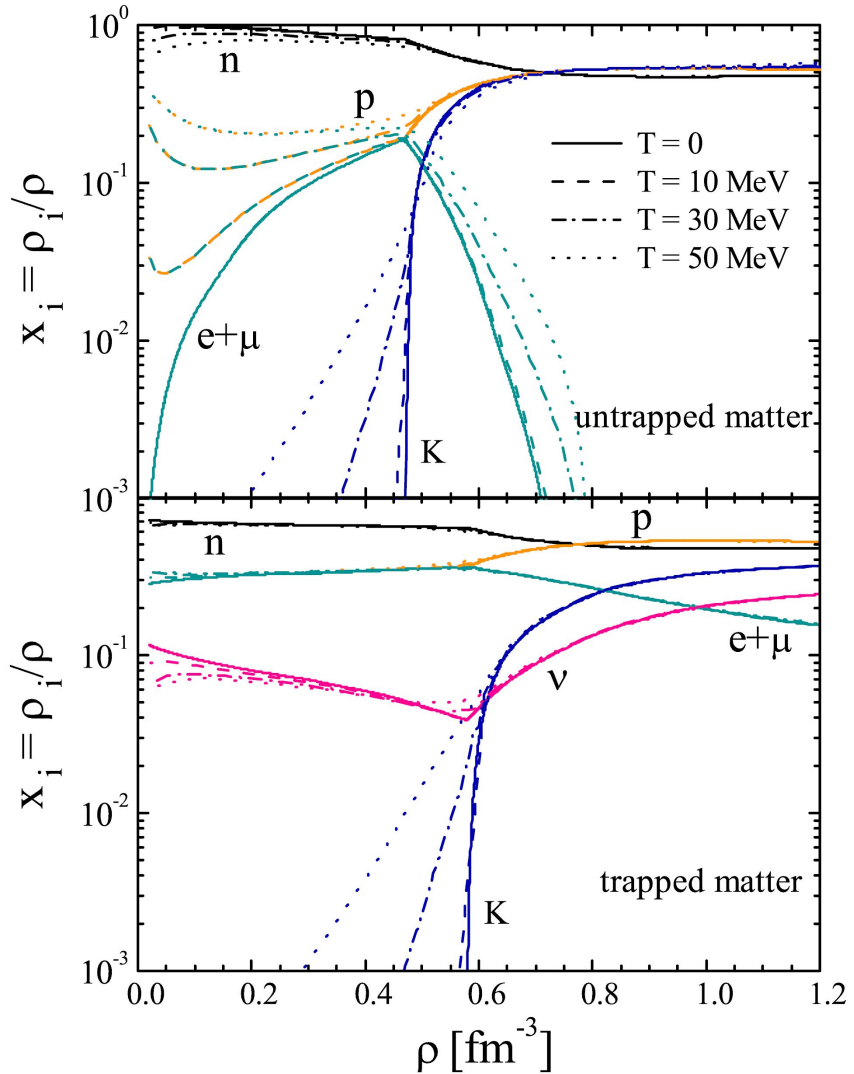
$$+ \frac{1}{2} (\nabla \rho)^2 + \frac{1}{2} m_\rho^2 \rho^2 + \frac{1}{2} (\nabla A)^2$$



e.g., Hu, AL, Shen & Toki, 1310.3602 PTEP 2014

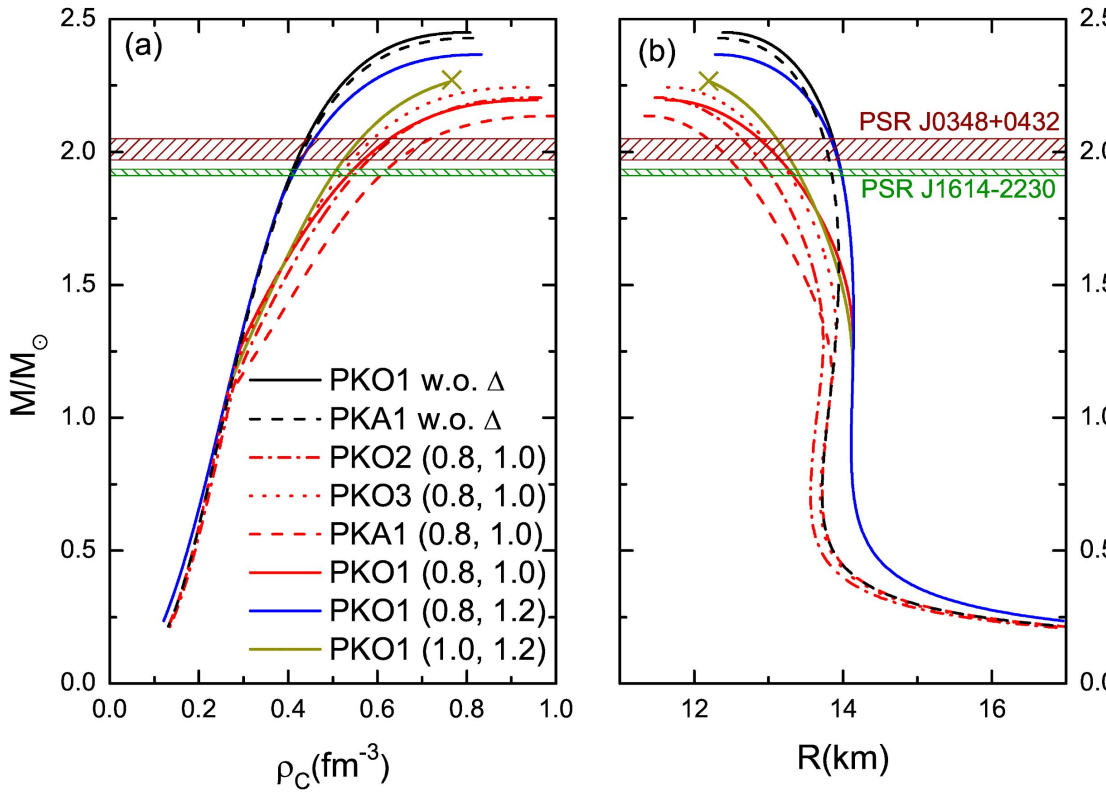
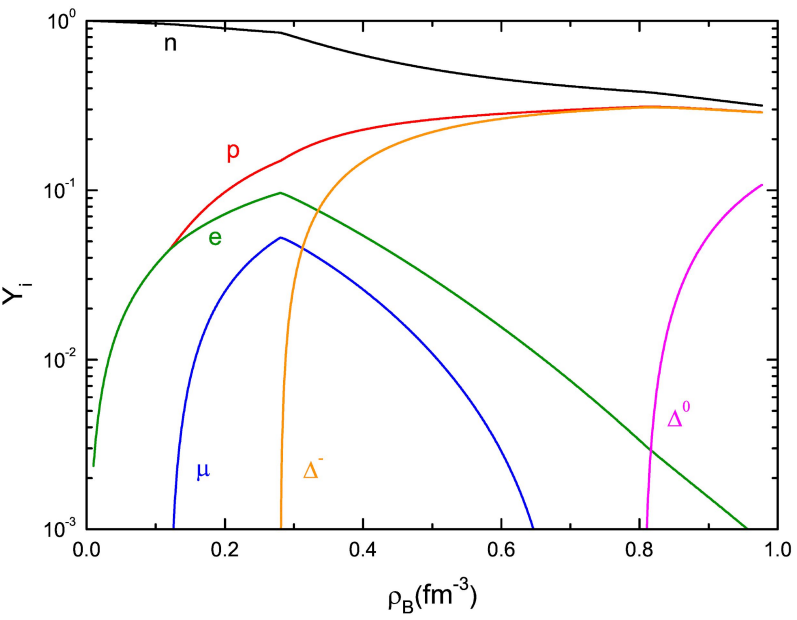
► Weak soften (late appearance) of Delta(1232)/hyperon/Kaon/quark;

e.g., AL, et al. PRC 2006, 2010

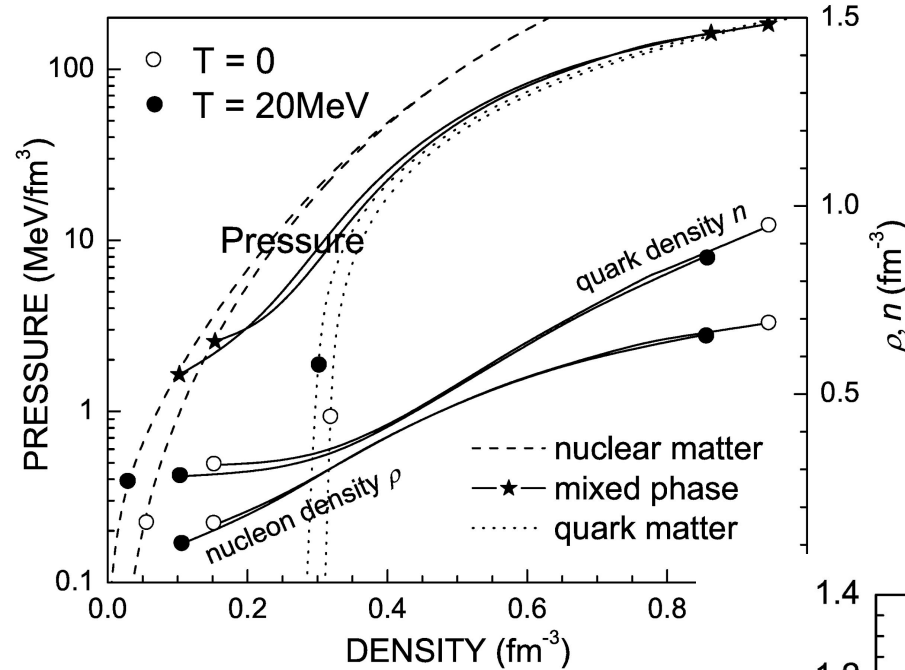


► Weak soften (late appearance) of Delta(1232)/hyperon/Kaon/quark;

e.g., Zhu, AL, Hu, Sagawa PRC 2016

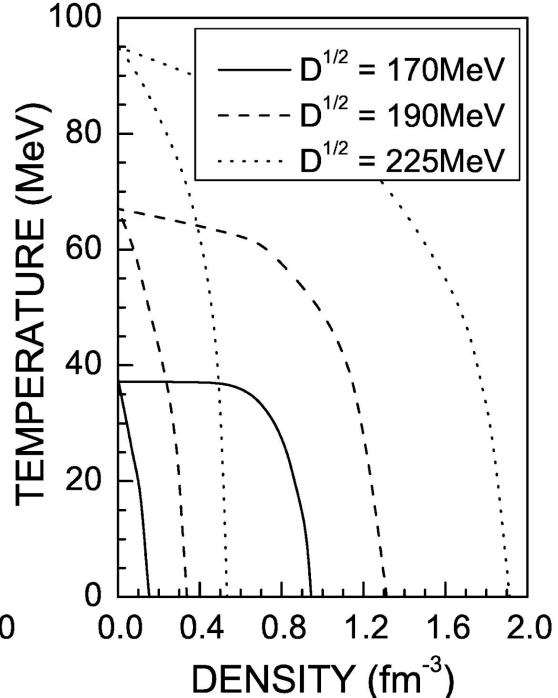
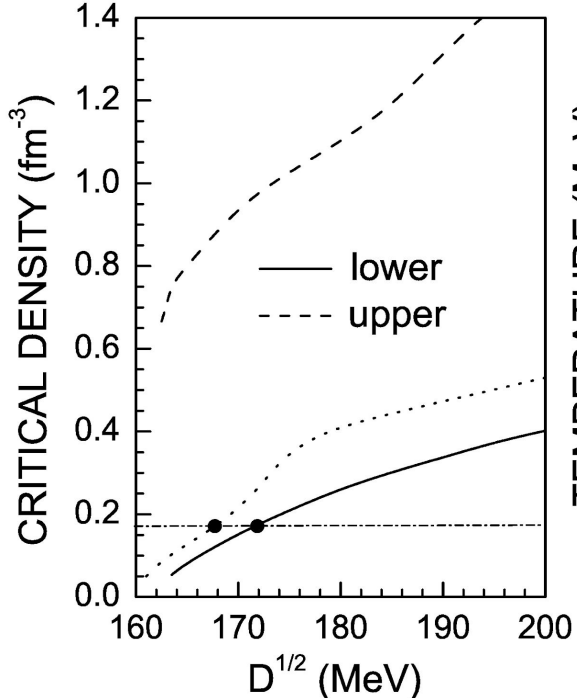
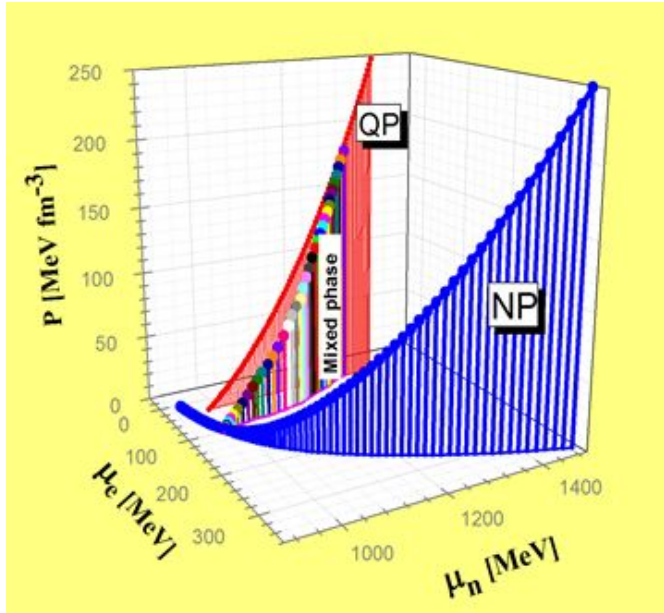


Hadron-quark deconfinement

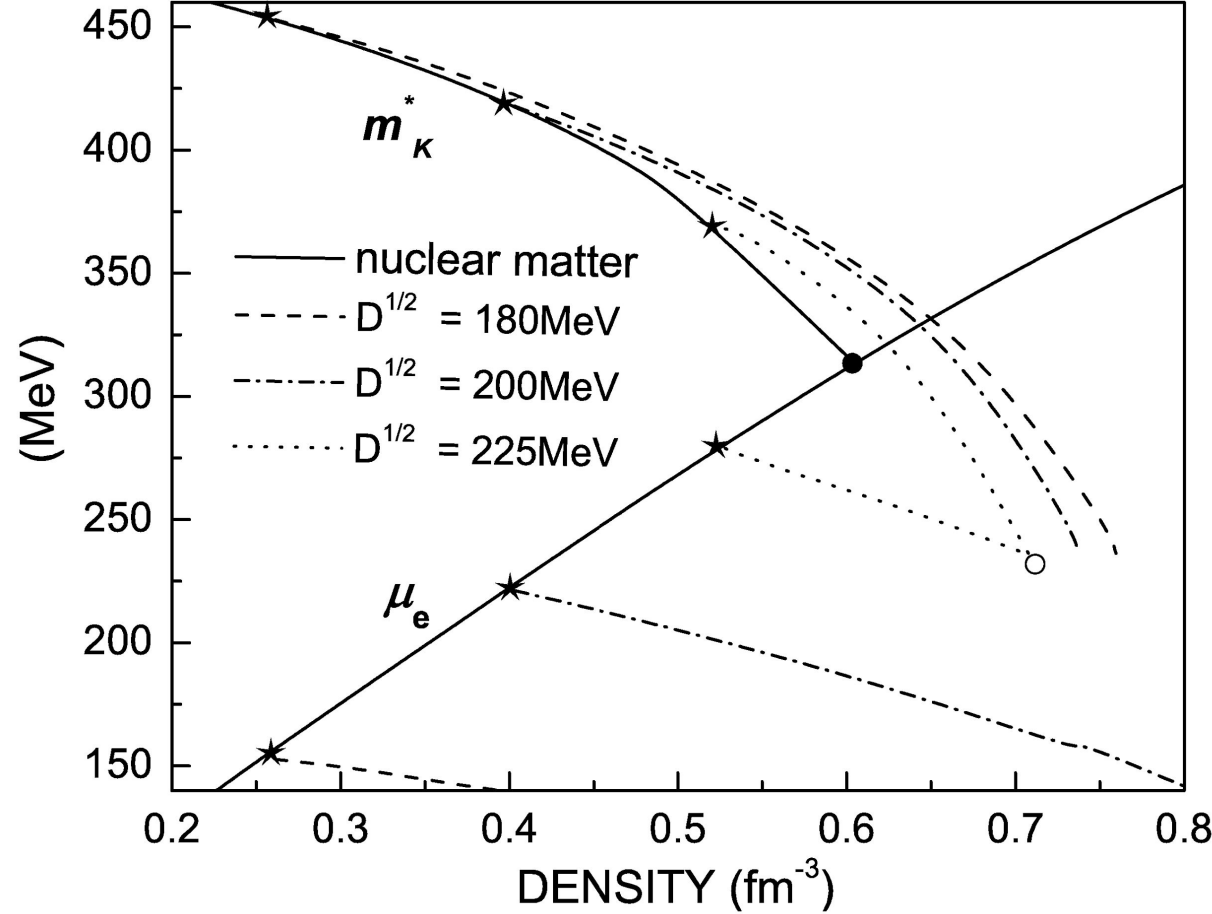
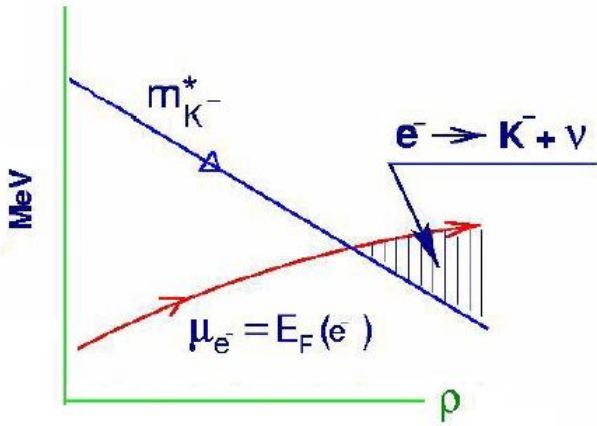


- ▶ Low density: Pure nuclear matter;
- ▶ Middle: Hadron-quark mixed phase;
- ▶ High density: Pure quark matter.

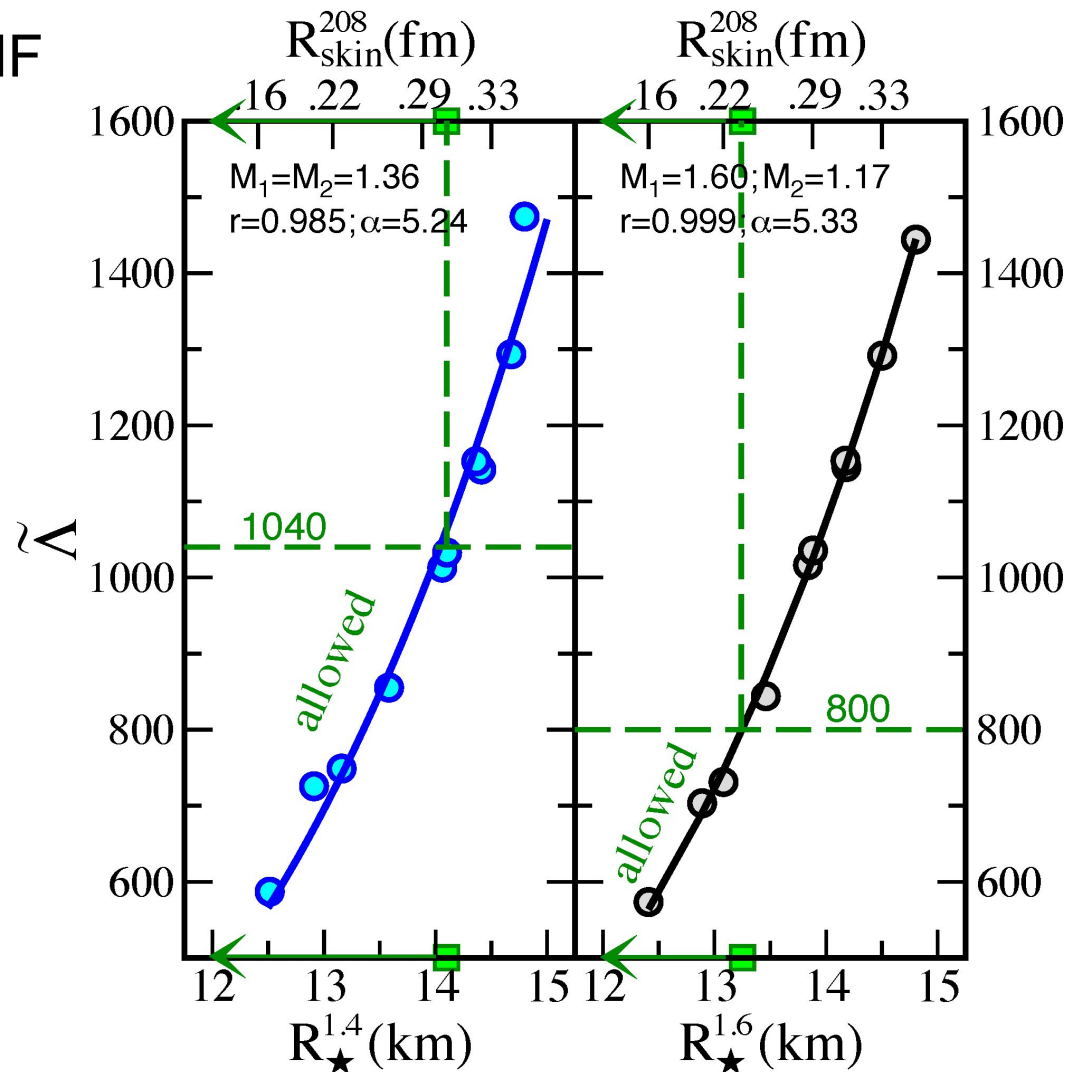
AL, et al. PRC 2015



► Competitive among different strangeness phase transition
 eg., free quarks vs. Kaons



- ▶ $\Lambda_{1.4} \lesssim 800$ for low-spin spior
 - ▶ 10 representative EOSs of RMF models;
 - ▶ $\Lambda_{1.4} \lesssim 800$: $R_{1.6} \leq 13.25\text{km}$
 $R_{\text{skin}}^{208} \leq 0.25\text{fm}$
 - ▶ PREX experiment:
 (Abrahamyan, et al. 2012;
 Horowitz et al., 2012)
- $$R_{\text{skin}}^{208} = 0.33^{+0.16}_{-0.18}\text{fm}$$
- ▶ Stiff low + Soft high:
 phase transition in the
 neutron-star interior?!
- (Hyperon puzzle/**dilemma**,
 Delta(1232)/hyperon/Kaon/quark
excitement)



► $\Lambda_{1.4} \lesssim 800$ for low-spin spior + EM

► GR hydrodynamics

code WhiskyTHC;

► Assumption:

UV/Optical/IR from

kilonova;

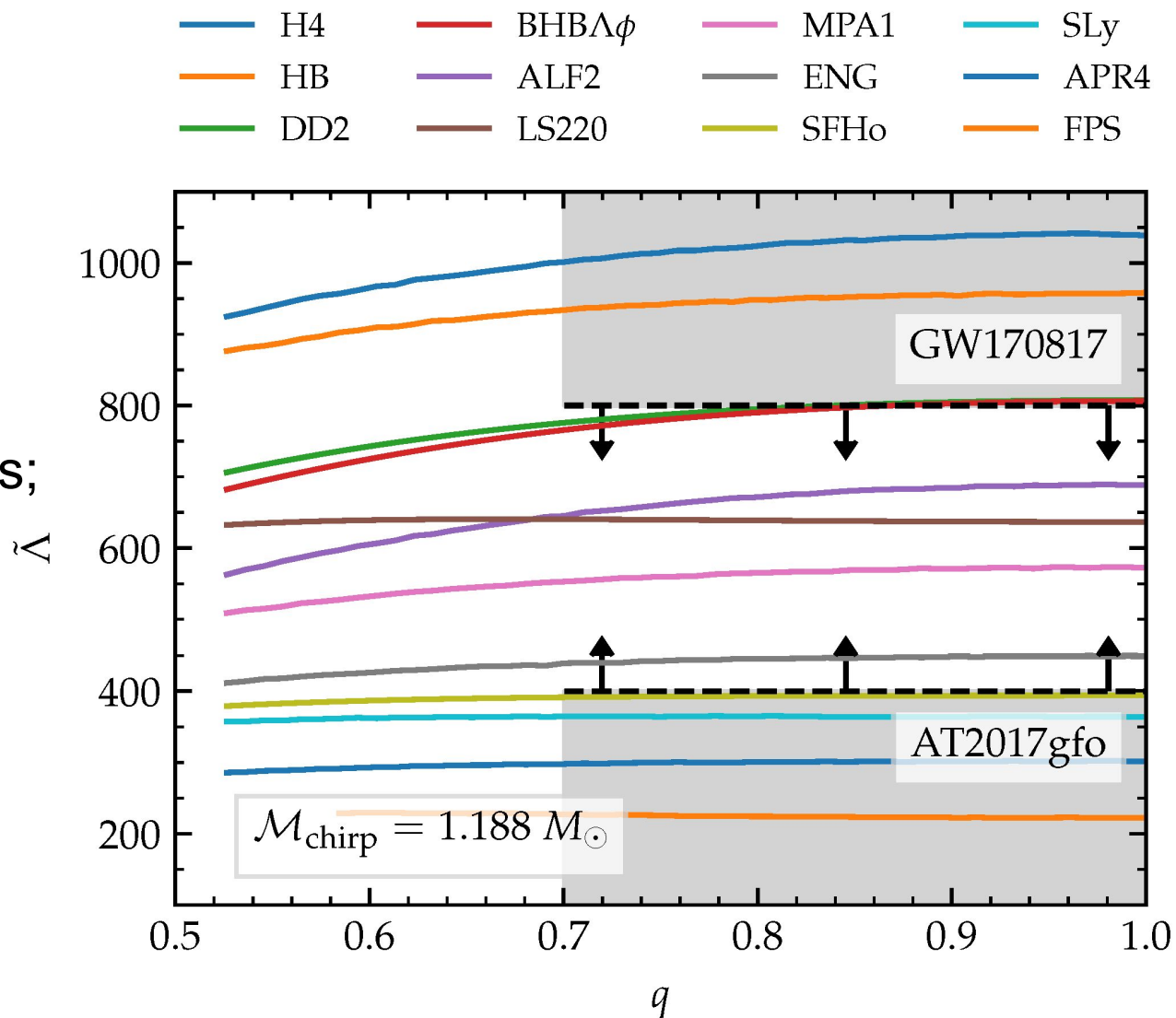
► 29 merger simulations;

► 12 NS EOSs;

► Rule out extremely

stiff NS EOS.

Radice et al., [1711.03647](#),
ApJL



▶ $\Lambda_{1.4} \lesssim 800$ for low-spin spior + EM

▶ GR hydrodynamics
code WhiskyTHC;

▶ Assumption:

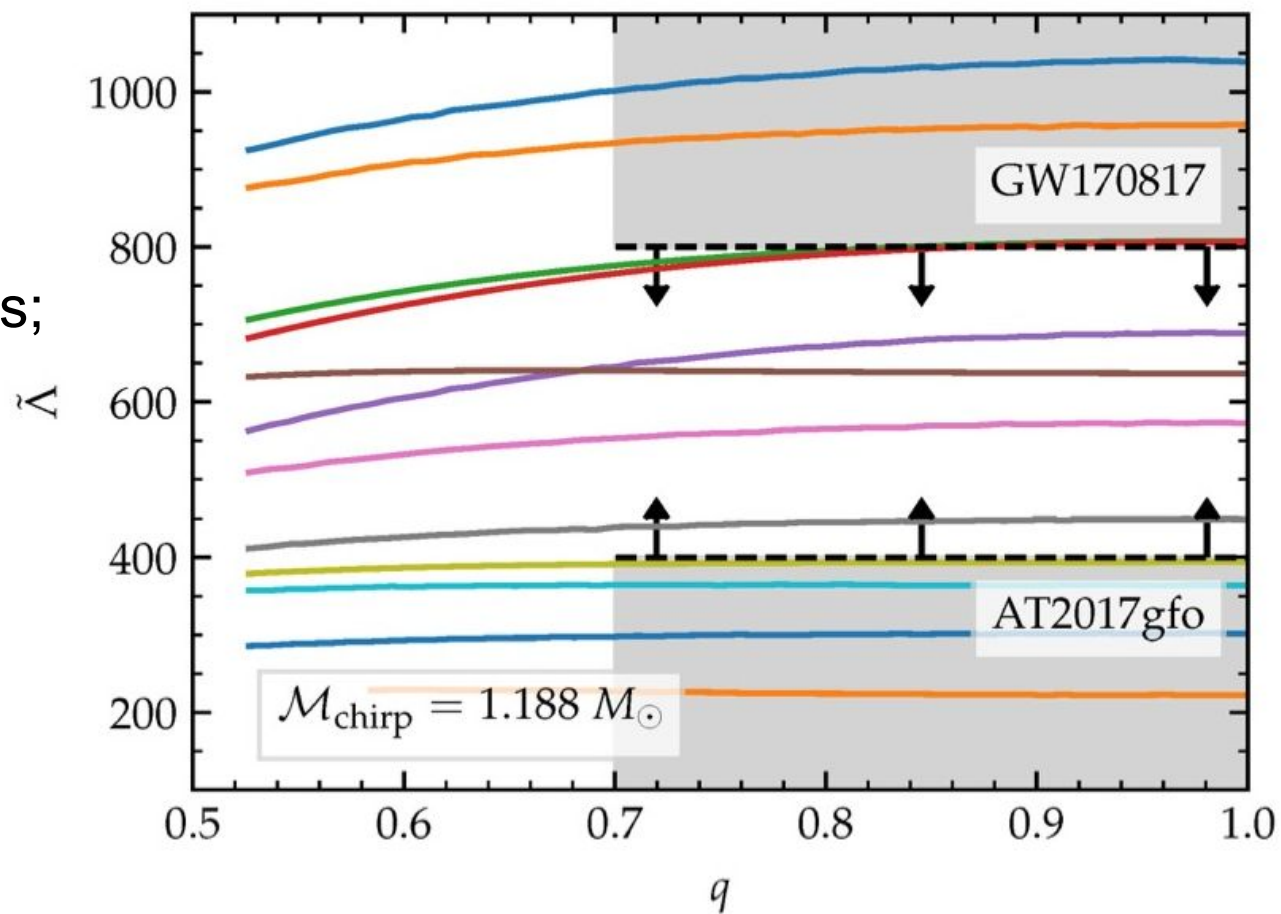
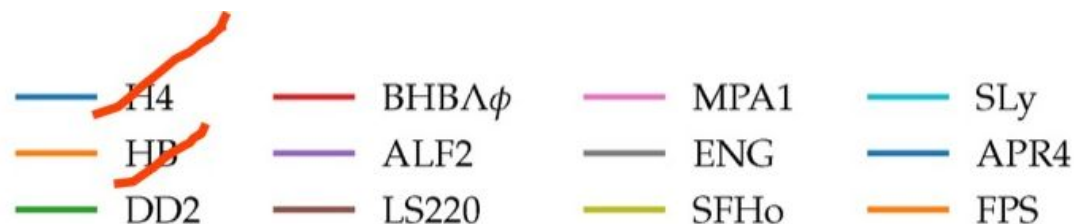
UV/Optical/IR from
kilonova;

▶ 29 merger simulations;

▶ 12 NS EOSs;

▶ **Rule out** extremely
stiff NS EOS.

Radice et al., [1711.03647](#),
ApJL

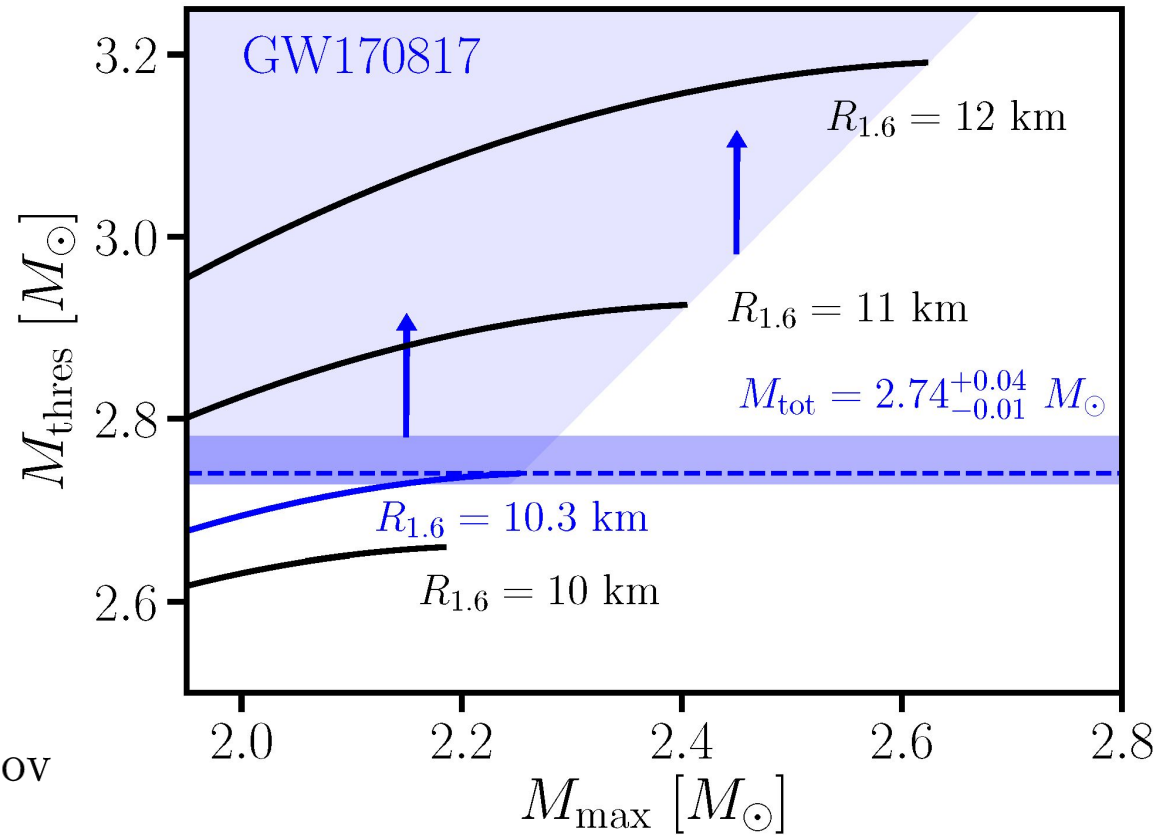


- ▶ EM
- ▶ 3D relativistic smoothed particle hydrodynamics (SPH) code;
- ▶ Assuming no prompt collapse;
- ▶ Large ejecta masses;
- ▶ A previous fitted formula for threshold binary mass:

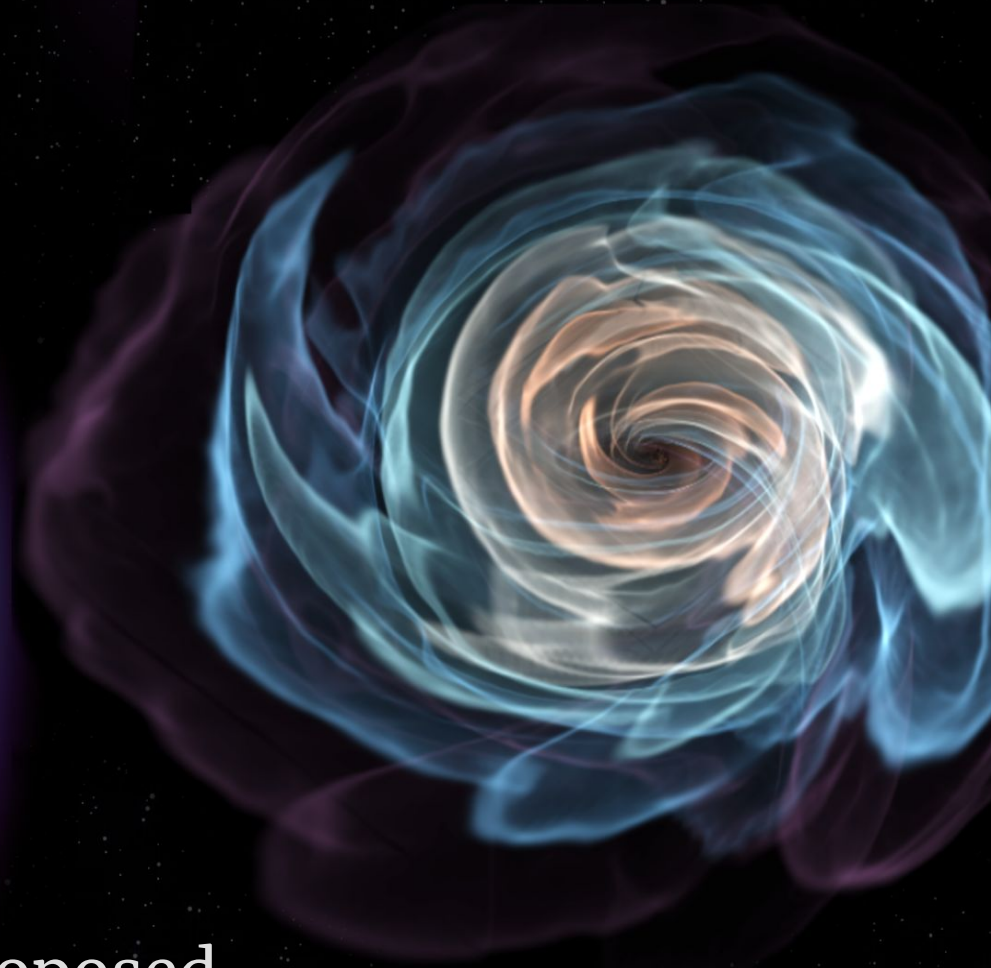
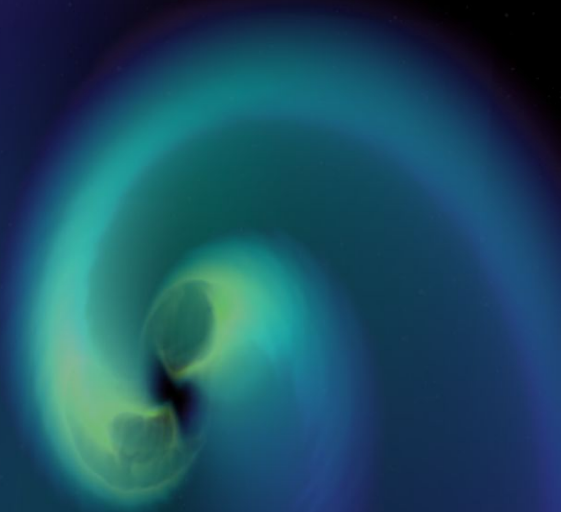
$$M_{\text{thres}} = \left(-3.606 \frac{M_{\text{TOV}}}{R_{1.6}} + 2.38\right) \times M_{\text{TOV}}$$

- ▶ Conclusion:

$$R_{1.6} \geq 10.68^{+0.15}_{-0.04} \text{ km}$$



FIRST COSMIC EVENT OBSERVED IN GRAVITATIONAL WAVES AND LIGHT



In this talk

- Intro of NS
- NS EOS from GW170817
- New NS EOS “QMF18” proposed

#Neutron star equation of state from the quark level in the light of

GW170817

*Zhu, Zhou & **AL** 1802.05510*

**Finite nuclei
experiments**

**Heavy ion flow
experiments**

**Observed properties of nuclear matter
at saturation and beyond**

Nuclear many-body theory

Supernovae

**Proto-neutron
stars**

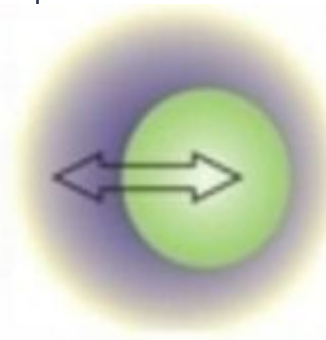
**Neutron
stars**

**Binary
Mergers**

etc

Finite nuclei experiments

Heavy ion flow experiments



Observed properties of nuclear matter at saturation and beyond

Nuclear many-body theory

Supernovae

Proto-neutron stars

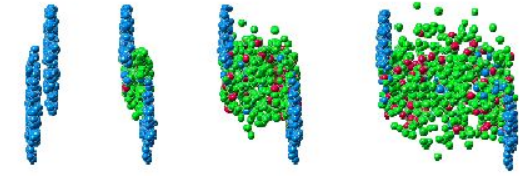
Neutron stars

Binary Mergers

etc

**Finite nuclei
experiments**

**Heavy ion flow
experiments**



**Observed properties of nuclear matter
at saturation and beyond**

Nuclear many-body theory

Supernovae

**Proto-neutron
stars**

**Neutron
stars**

**Binary
Mergers**

etc

**Finite nuclei
experiments**

**Heavy ion flow
experiments**

**Observed properties of nuclear matter
at saturation and beyond**

Nuclear many-body theory

Supernovae

**Proto-neutron
stars**

**Neutron
stars**

**Binary
Mergers**

etc

Finite nuclei experiments

Heavy ion flow experiments

Observed properties of nuclear matter

ρ_0	E/A	K	E_{sym}	L	M_N^*/M_N
[fm ⁻³]	[MeV]	[MeV]	[MeV]	[MeV]	/
0.16	-16	240	31	20/40/60/80	0.77

Nuclear many-body theory

Supernovae

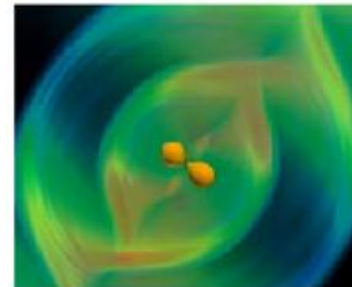
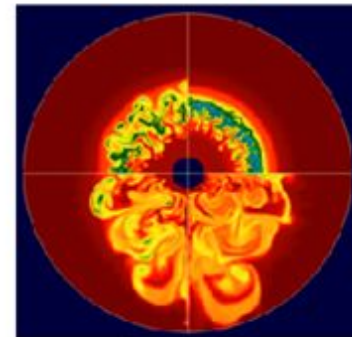
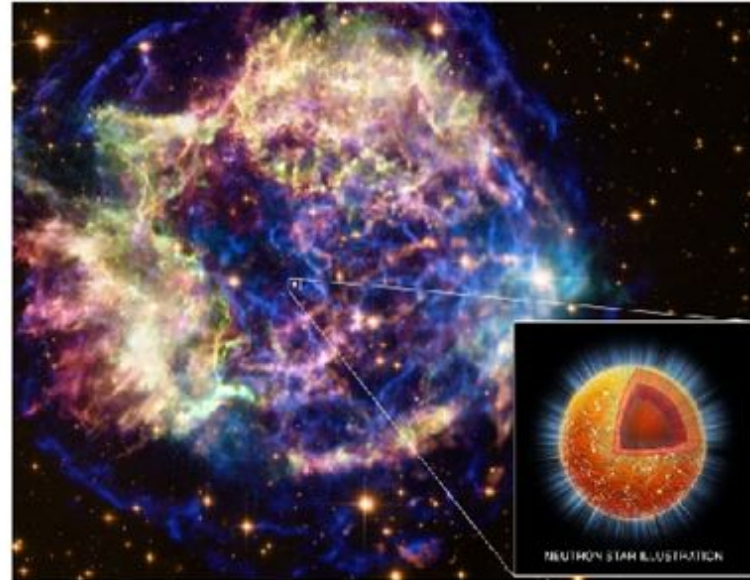
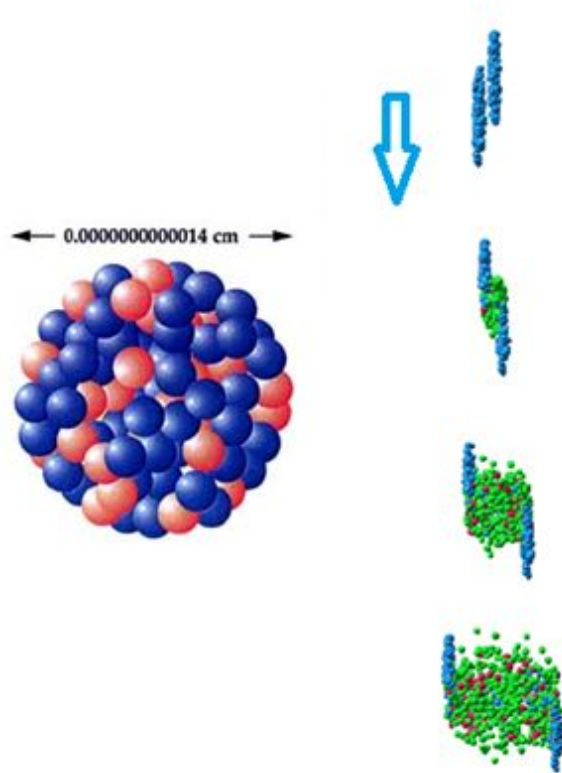
Proto-neutron stars

Neutron stars

Binary Mergers

etc

- ❑ Isobaric analog states (**IAS**) and from IAS and neutron skins (**IAS+skin**) (*Danielewicz & Lee 2014*);
- ❑ Electric dipole polarizability in ^{208}Pb (α_D) (*Zhang & Chen 2015*).



- Collective flow in **HIC** (*Danielewicz et al. 2002*);
- Transport in **HIC** (*Tsang et al. 2009*)
- ★ PSR J1614-2230 (*Demorest et al. 2010; Fonseca et al. 2016*);
- ★ PSR J0348+0432 (*Antoniadis et al. 2013*).

► NS EOS model from the quark level within QMF ($m_q \sim 300\text{MeV}$)

Step 1: Single nucleon

$$[\gamma^0(\epsilon_q - g_{\omega q}\omega - \tau_{3q}g_{\rho q}\rho) - \vec{\gamma} \cdot \vec{p} - (m_q - g_{\sigma q}\sigma) - U(r)]\psi_q(\vec{r}) = 0$$

$$U(r) = \frac{1}{2}(1 + \gamma^0)(ar^2 + V_0) \quad \begin{array}{l} V_0 = -62.257187 \text{ MeV} \\ a = 0.534296 \text{ fm}^{-3} \end{array} \left\{ \begin{array}{l} M_N = 939 \text{ MeV} \\ r_N = 0.87 \text{ fm.} \end{array} \right.$$

Step 2: Nucleon many-body system

$$\begin{aligned} \mathcal{L} = & \bar{\psi} (i\gamma_\mu \partial^\mu - M_N^* - g_{\omega N}\omega\gamma^0 - g_{\rho N}\rho\tau_3\gamma^0) \psi - \frac{1}{2}(\nabla\sigma)^2 - \frac{1}{2}m_\sigma^2\sigma^2 - \frac{1}{3}g_2\sigma^3 - \frac{1}{4}g_3\sigma^4 \\ & + \frac{1}{2}(\nabla\rho)^2 + \frac{1}{2}m_\rho^2\rho^2 + \frac{1}{2}(\nabla\omega)^2 + \frac{1}{2}m_\omega^2\omega^2 + \frac{1}{2}g_{\rho N}^2\rho^2\Lambda_v g_{\omega N}^2\omega^2, \end{aligned}$$

► $K=240 \pm 20$

(Colo et al. 2014)

$E_{\text{sym}} = 31.6 \pm 2.66$

$L = 58.9 \pm 16$

(Li & Han 2013)

$L \gtrsim 20$ (Centelles et al.

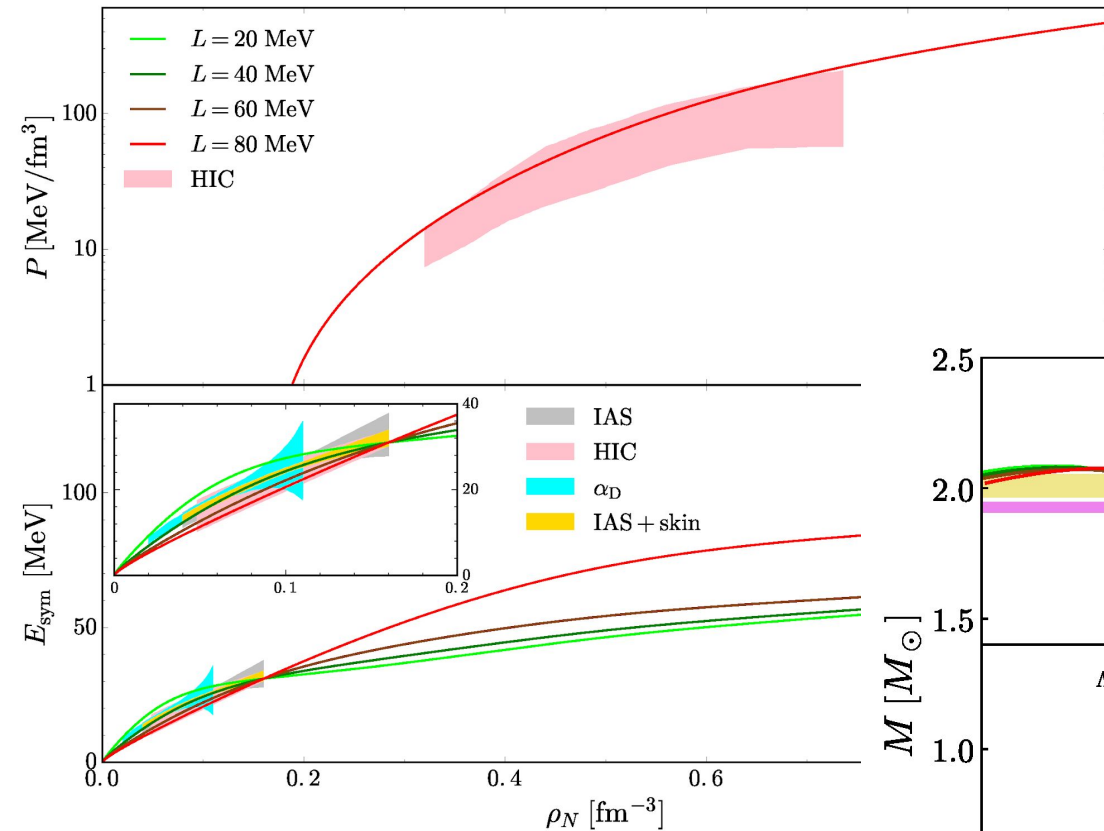
2009)

$L \lesssim 170$ (Cozma 2013)

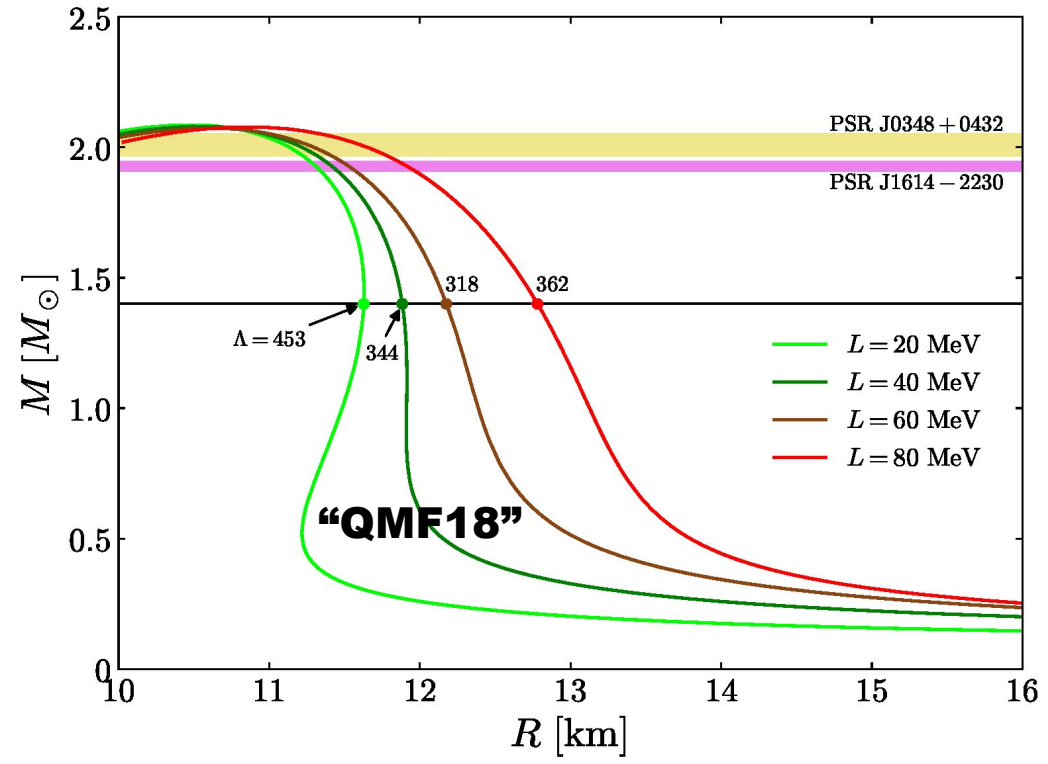
L [MeV]	$g_{\sigma q}$	$g_{\omega q}$	$g_{\rho q}$	g_2 [fm^{-1}]	g_3	Λ_v
20	3.8620366	2.9174838	6.9588083	14.6179599	-66.3442468	1.1080665
40	3.8620366	2.9174838	5.4129448	14.6179599	-66.3442468	0.7693664
60	3.8620366	2.9174838	4.5830609	14.6179599	-66.3442468	0.4306662
80	3.8620366	2.9174838	4.0459574	14.6179599	-66.3442468	0.0919661

ρ_0	E/A	K	E_{sym}	L	M_N^*/M_N
[fm^{-3}]	[MeV]	[MeV]	[MeV]	[MeV]	/
0.16	-16	240	31	20/40/60/80	0.77

- Ignore strangeness for the moment ($n_{pe\mu}$)
- EOS uncertain most in asymmetric part: good L -vs- R correlation, how about L -vs- Λ ?



Zhu, Zhou & AL
1802.05510



► “QMF18” from the quark level

► GR: $R > 2GM/c^2$

► $P < \infty$: $R > (9/4)GM/c^2$

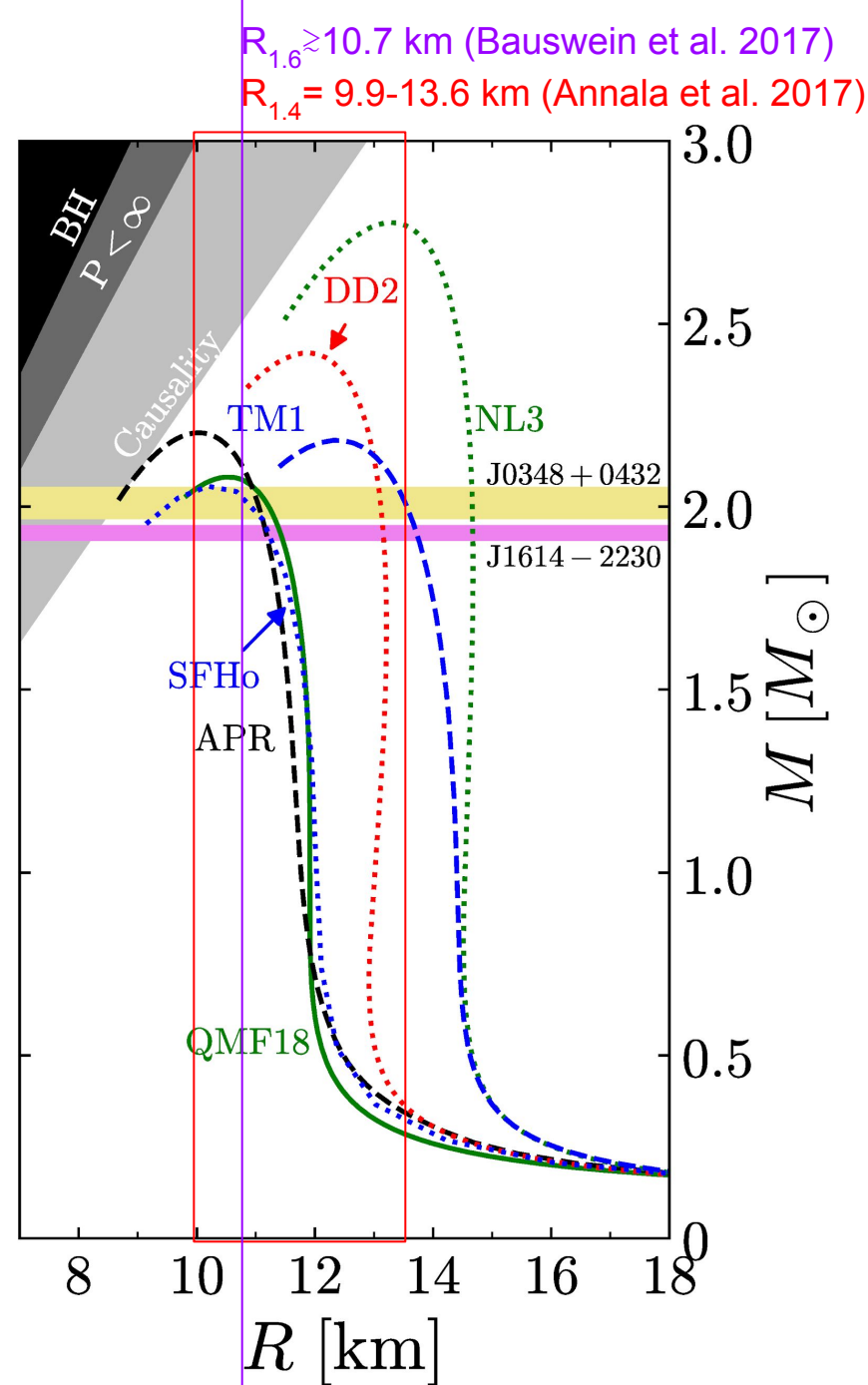
► Causality: $c \gtrsim v_s$ or $R \gtrsim 2.9GM/c^2$

► Nucleon (m_N, r_N)

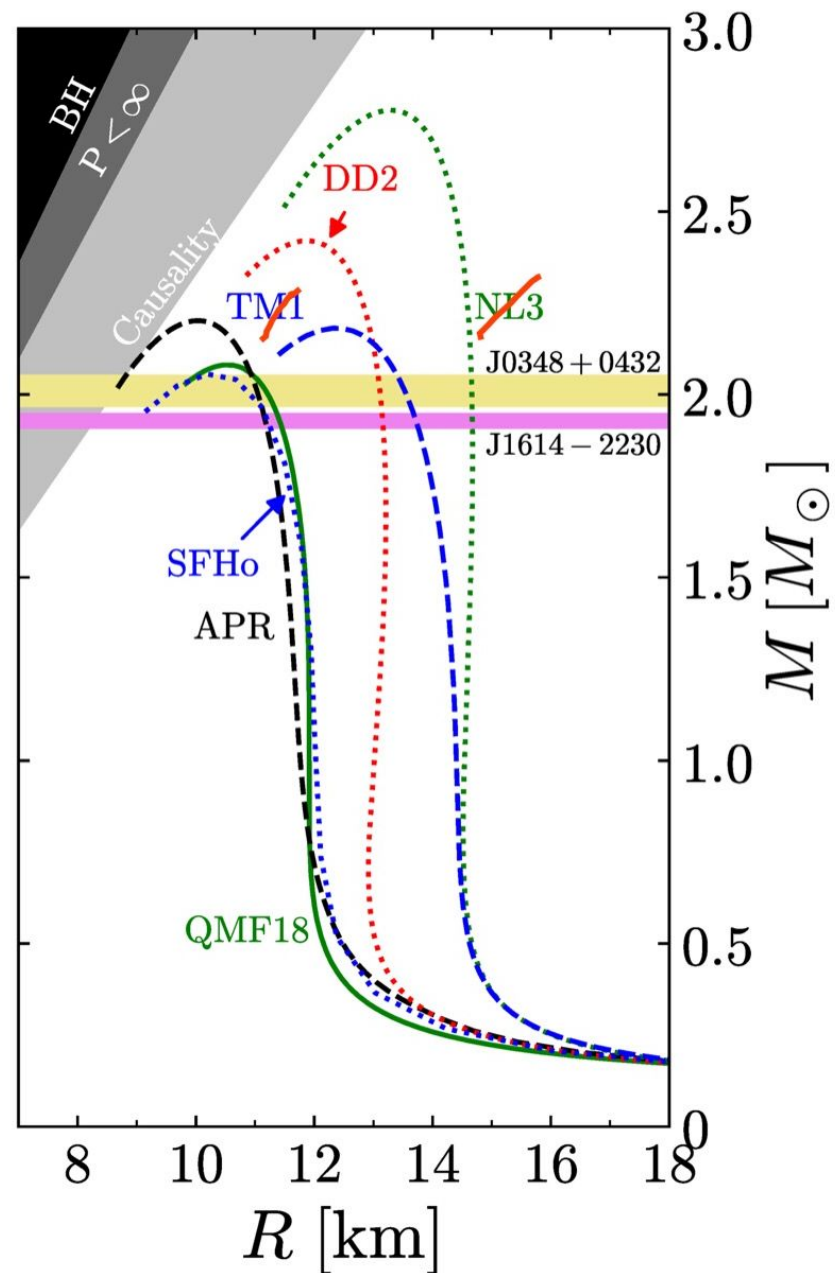
► Nuclear saturation ($\rho_0, E/A, K, E_{\text{sym}}, L, M_N^*$)

► Heavy pulsar mass measurements around 2 solar mass

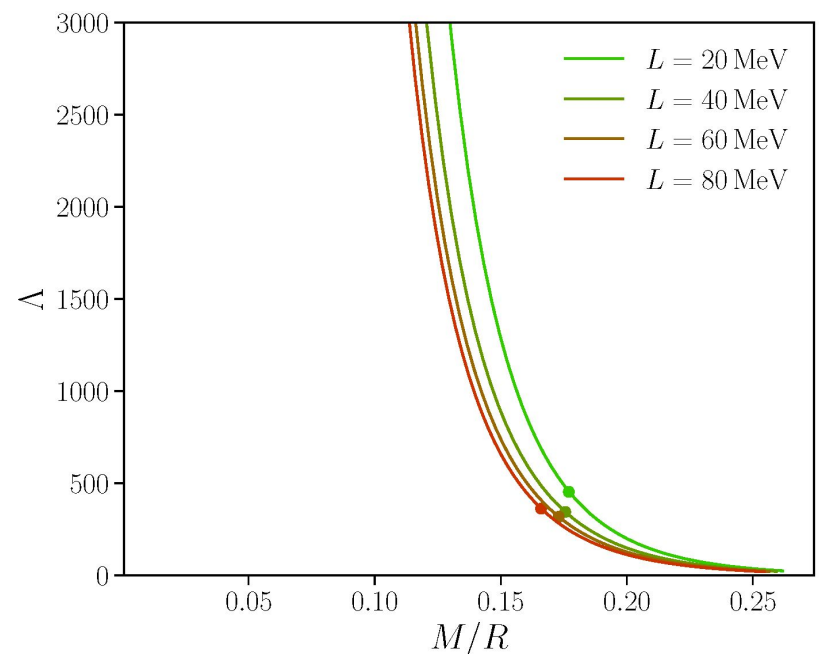
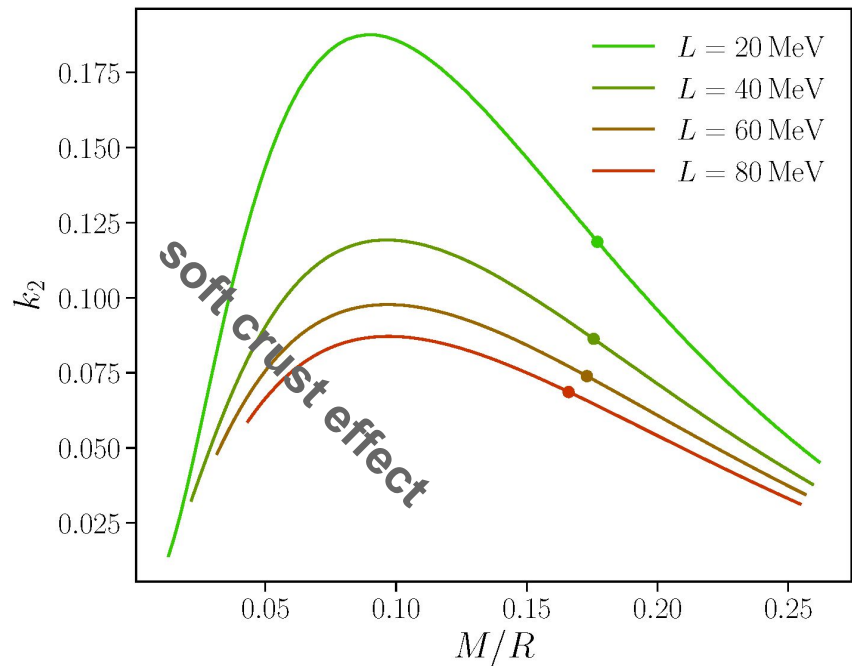
► Clean/robust GW constraint of tidal deformability



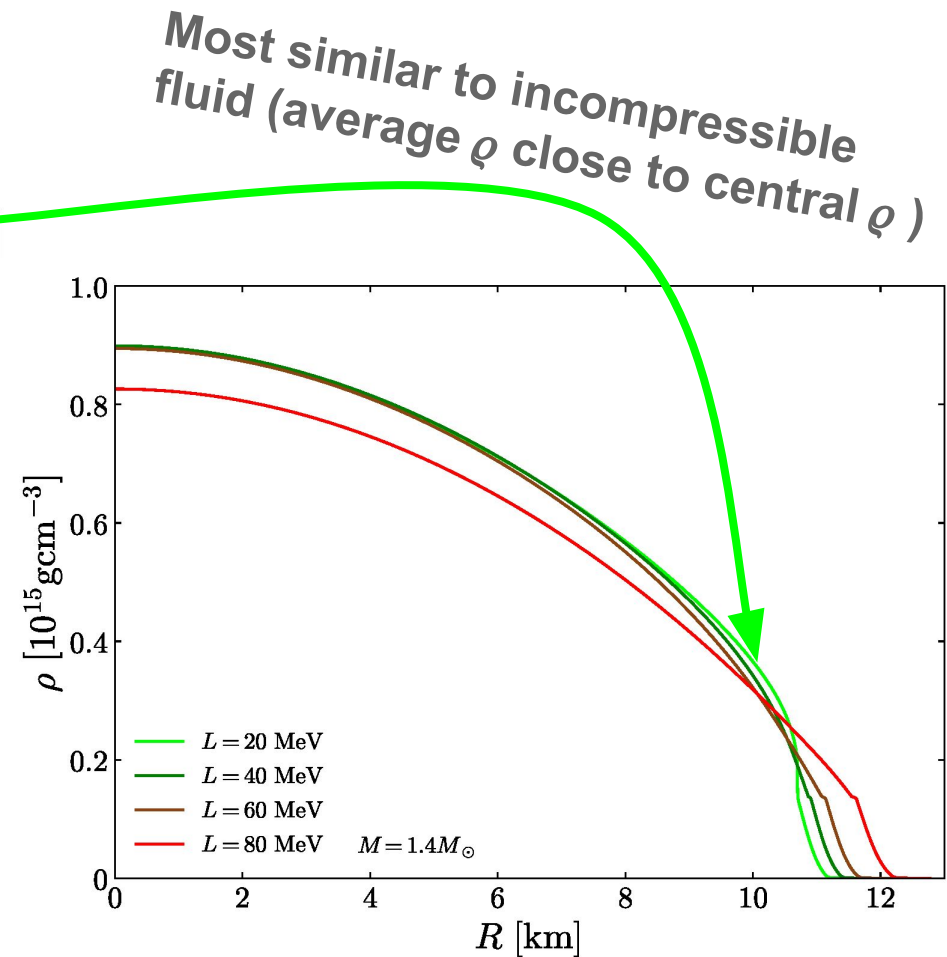
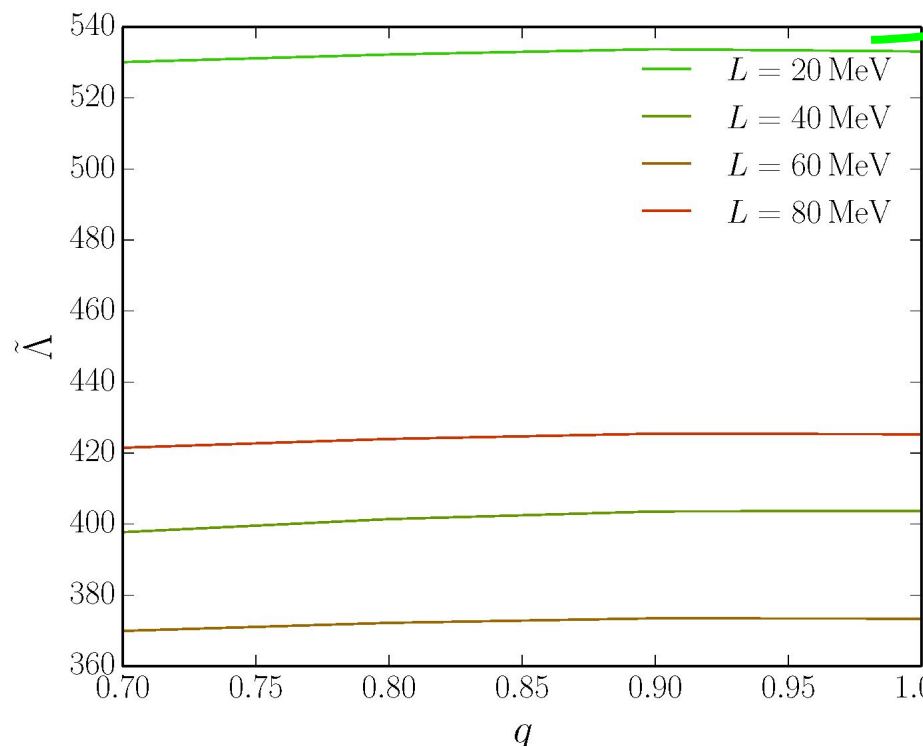
- ▶ “QMF18” from the quark level
- ▶ GR: $R > 2GM/c^2$
- ▶ $P < \infty$: $R > (9/4)GM/c^2$
- ▶ Causality: $c \gtrsim v_s$ or $R \gtrsim 2.9GM/c^2$
- ▶ Nucleon (m_N, r_N)
- ▶ Nuclear saturation ($\rho_0, E/A, K, E_{\text{sym}}, L, M_N^*$)
- ▶ Heavy pulsar mass measurements around 2 solar mass
- ▶ Clean/robust GW constraint of tidal deformability



- ▶ **NO** L -vs- Λ correlation found, despite good L -vs- R correlation.
- ▶ Tidal deformability Λ : describes the amount of induced mass quadrupole moment when reacting to a certain external tidal field.
- ▶ Tidal 2nd Love number k_2 : measures how easily the bulk of the matter in a star is deformed by an external tidal field.
- ▶ Larger L leads to smaller k_2
- ▶ **NOT** monotonic dependence of Λ .

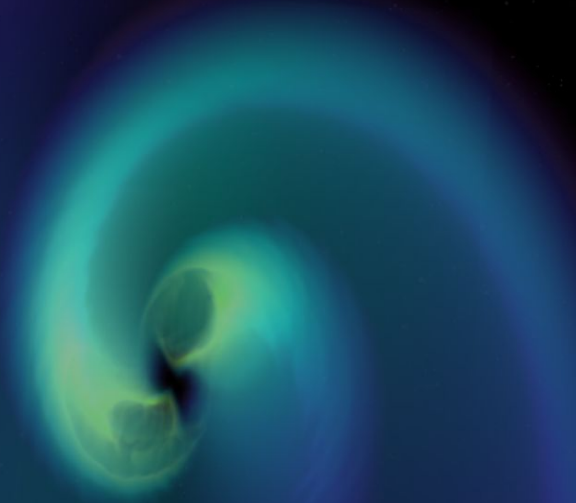


- ▶ To better understand the nonmonotonic behaviour:
- ▶ Maybe dangerous to probe R/L via Λ ; Maybe K_{sym} (L.-W. Chen from iHIC last week)



$$\tilde{\Lambda} = \frac{16(m_1 + 12m_2)m_1^4\Lambda_1 + (m_2 + 12m_1)m_2^4\Lambda_2}{13(m_1 + m_2)^5}$$

FIRST COSMIC EVENT OBSERVED IN GRAVITATIONAL WAVES AND LIGHT



In this talk

- Intro of NS
- NS EOS from GW170817
- New NS EOS “QMF18” proposed

► Collaborators (with compliments):

PKU: E.-P. Zhou & R.-X. Xu

BNU: H. Gao & Z.-J. Cao

NKU: J.-N. Hu & H. Shen

ZJUT: M.-B. Wan

IMP: X.-L. Shang & J.-M. Dong

SDU: N.-B. Zhang & B. Qi

XAO: X. Zhou & J.-B. Wang

XMU: T. Liu & F. Huang

UNLV: B. Zhang

Aizu/RIKEN: H. Sagawa

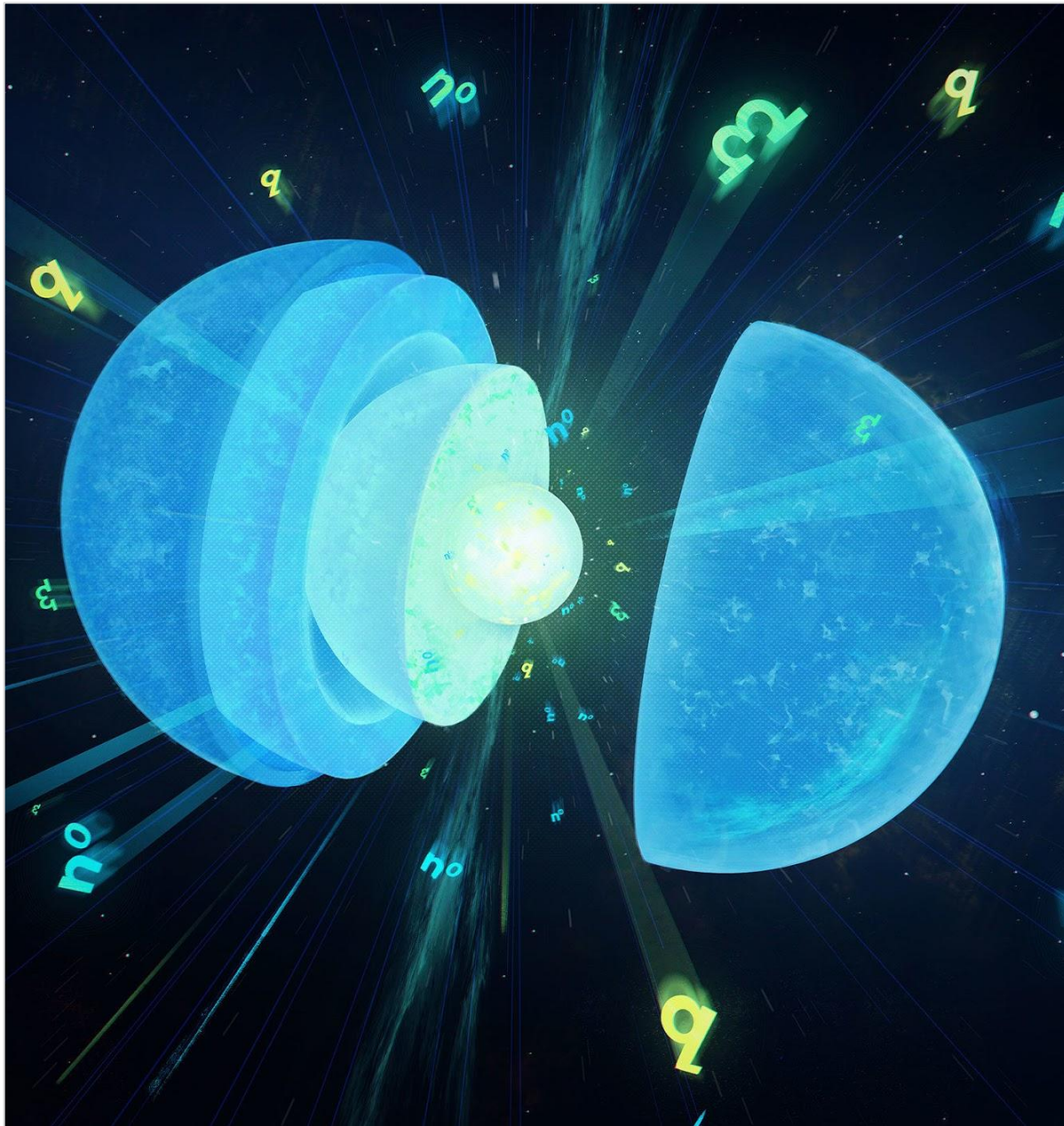


Zhen-Yu Zhu
PhD the 4th year;
To visit L. Rezzolla's group via CSC



Zhi-Qiang Liao
Graduate the 1st year

Also several undergraduate students.



Multi-messenger, multi-scale future

- ▶ Nuclear theory, Atomic theory, GR
- ▶ Stellar scale simulation
- ▶ Origin of the heavy element in the galaxy
- ▶ Nuclear experiment
- ▶ GW experiment
- ▶ Astronomical survey

Xiamen-CUSTIPEN Workshop

**on the EOS of Dense Neutron-Rich Matter
in the Era of Gravitational Wave Astronomy
January 3 to 7, 2019**



Organizing Committee

Lie-Wen Chen (Shanghai Jiao Tong University, China)
Pawel Danielewicz (Michigan State University, USA)
Tao-Tao Fang (Xiamen University, China)
Ang Li (**Co-Chair**, Xiamen University, China)
Bao-An Li (**Co-Chair**, Texas A&M University-Commerce,
USA)
Jorge Piekarewicz (Florida State University, USA)
Fu-Rong Xu (Peking University, China)
Ren-Xin Xu (Peking University, China)
Bing Zhang (University of Nevada, USA)

Confirmed speakers

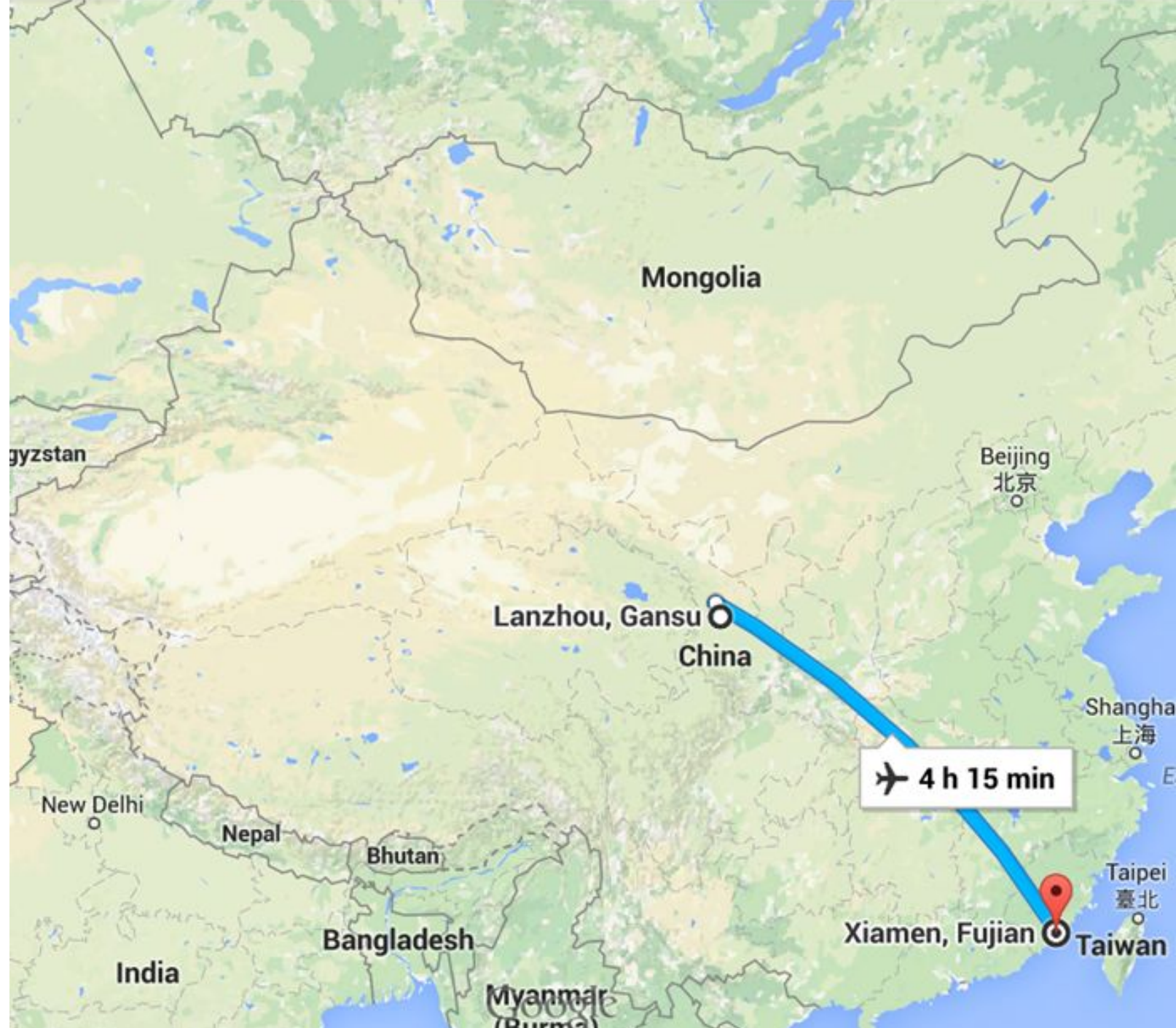
Betty Tsang
Pawel Danielewicz
Bill Lynch
Jorge Piekarewicz
Chuck Horowitz
James Lattimer
Jeremy Holt
Anna L. Watts
Nils Andersson
Ben Tal Margalit
Paul Lasky
Wynn Ho Until 4/10/18

Xiamen-CUSTIPEN Workshop

**on the EOS of Dense Neutron-Rich Matter
in the Era of Gravitational Wave Astronomy
January 3 to 7, 2019**



- EOS of Neutron-Rich Matter from Nuclear Theories and Terrestrial Experiments
- Properties of Neutron Stars from Theories and Observations
- Impacts of Nuclear EOS on the Evolution Dynamics and Products of Compact Binaries
- Imprints of Nuclear EOS on Gravitational Waves from Various Sources
- Nature of Dense Matter and Synthesis of Heavy Elements in the Cosmos
- Isospin Dependence of Strong Interactions and Correlations in Dense Matter



Mongolia

Beijing
北京

Lanzhou, Gansu
China

Shanghai
上海

✈ 4 h 15 min

New Delhi

Nepal

Bhutan

Bangladesh

India

Myanmar
(Burma)

Xiamen, Fujian
Taipei
臺北

Taiwan

Thank you.

Backup

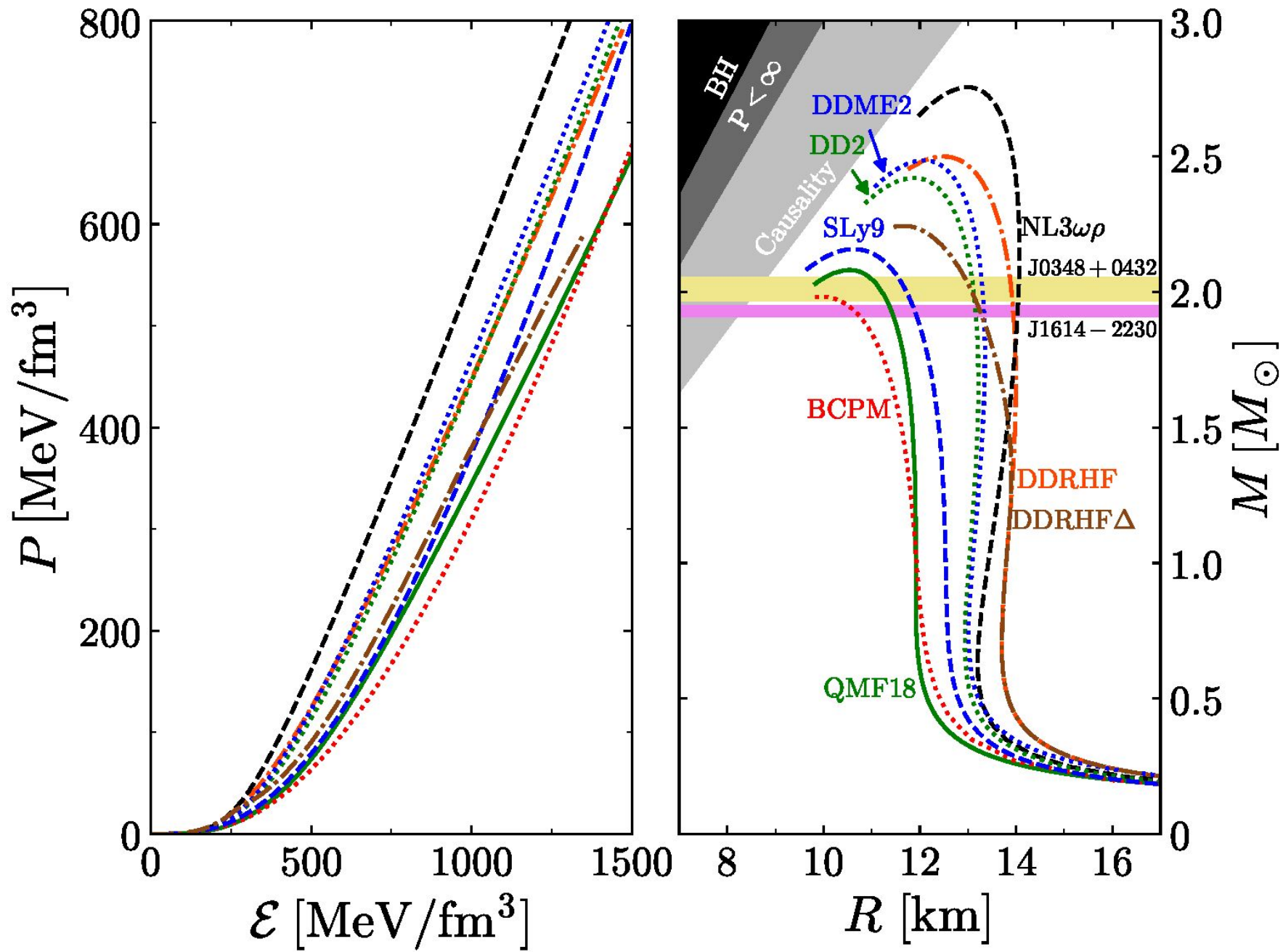
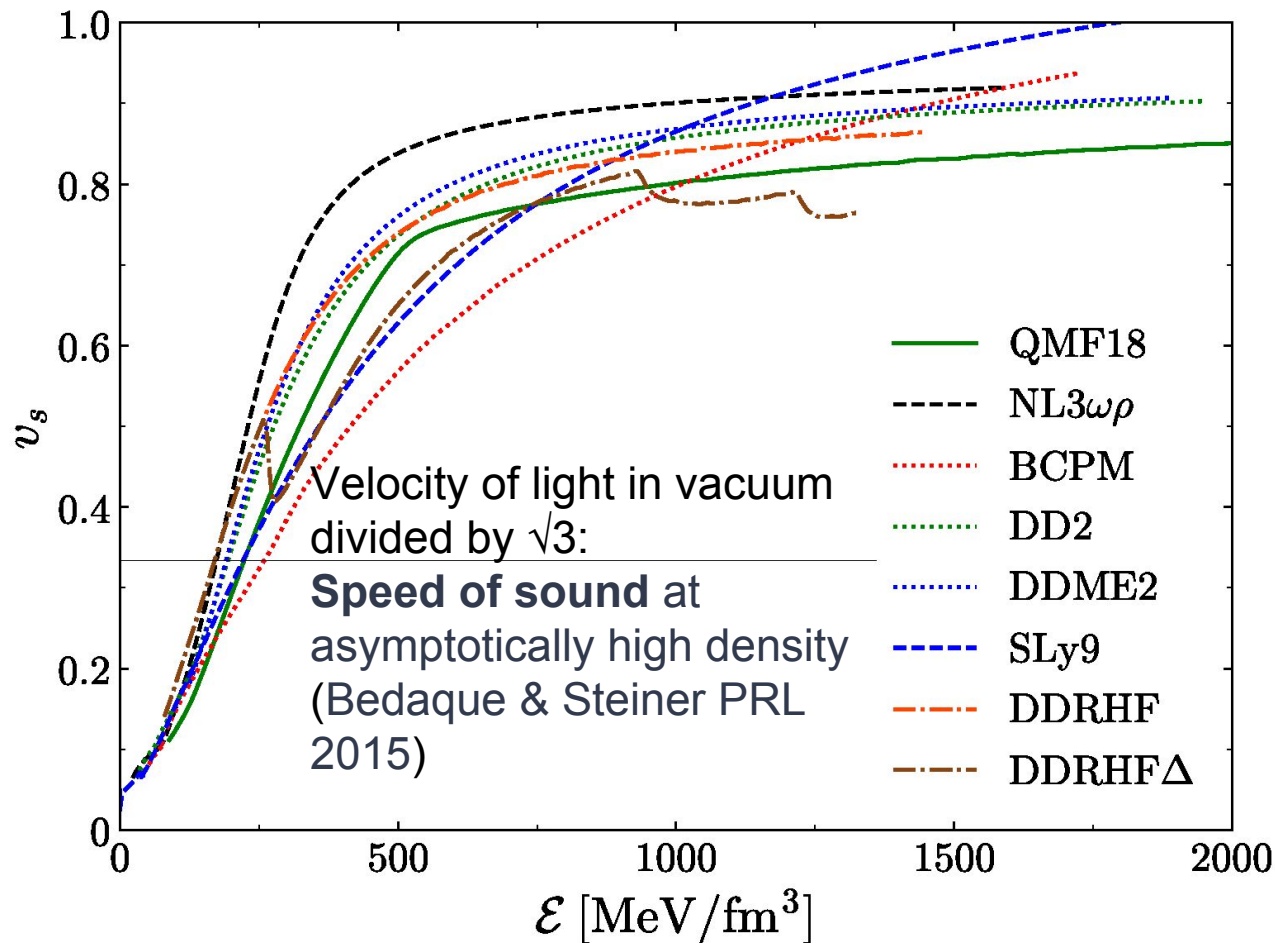


Table 4. Radius, compactness and tidal deformability for a $1.4 M_{\odot}$ star are provided for various advanced NS EOSs, together with their maximum static gravitational mass M_{TOV} and the symmetry energy slope L .

	QMF18	DDRHF	DDRHF Δ	NL3 $\omega\rho$	DDME2	DD2	Sly9	BCPM
$M_{\text{TOV}} [M_{\odot}]$	2.08	2.50	2.24	2.75	2.48	2.42	2.16	1.98
L [MeV]	40	82.99	82.99	55.5	51.2	55.0	54.9	52.96
$R(1.4)$ [km]	11.77	13.74	13.67	13.75	13.21	13.16	12.46	11.72
$M/R(1.4)$	0.1756	0.1505	0.1512	0.1503	0.1566	0.1571	0.1660	0.1765
$\Lambda(1.4)$	344	865	828	925	681	674	446	294

9.9-13.6 km

120-800/1400
(Annala et al.)



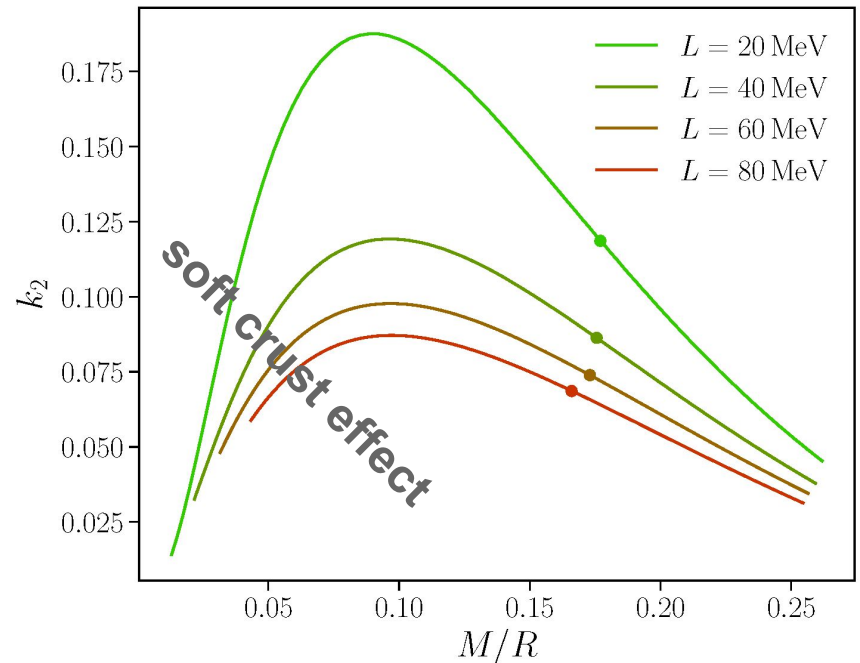
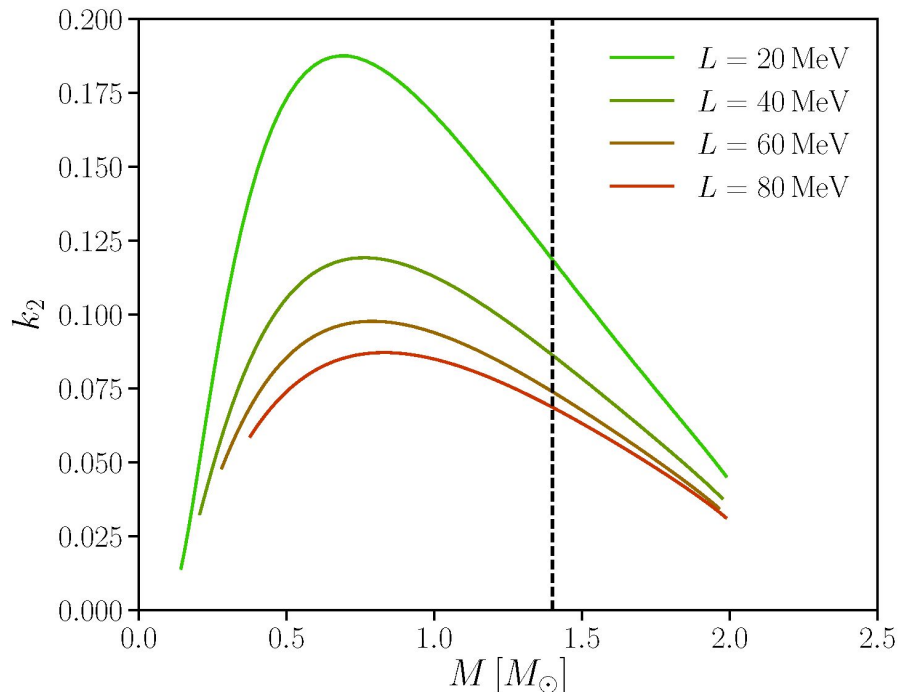
Details in
 Zhu, Zhou & **AL**
 1802.05510

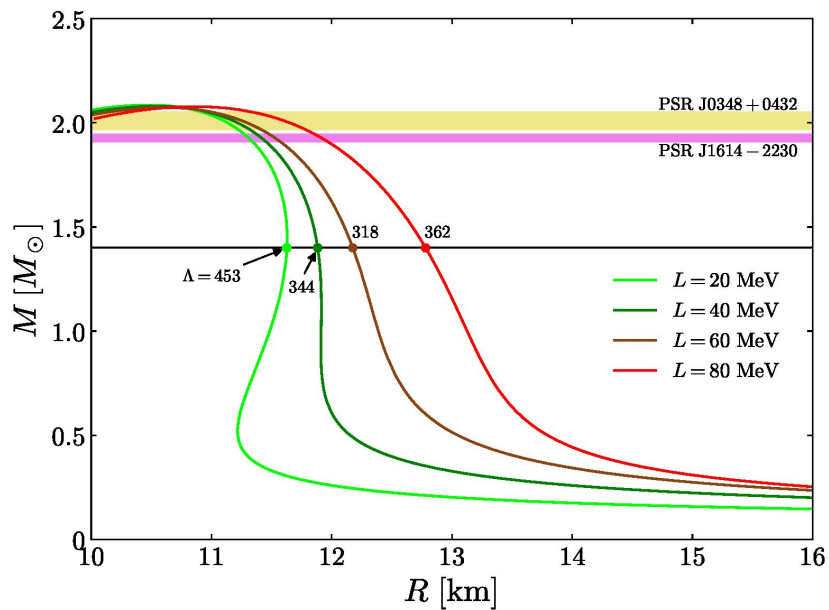
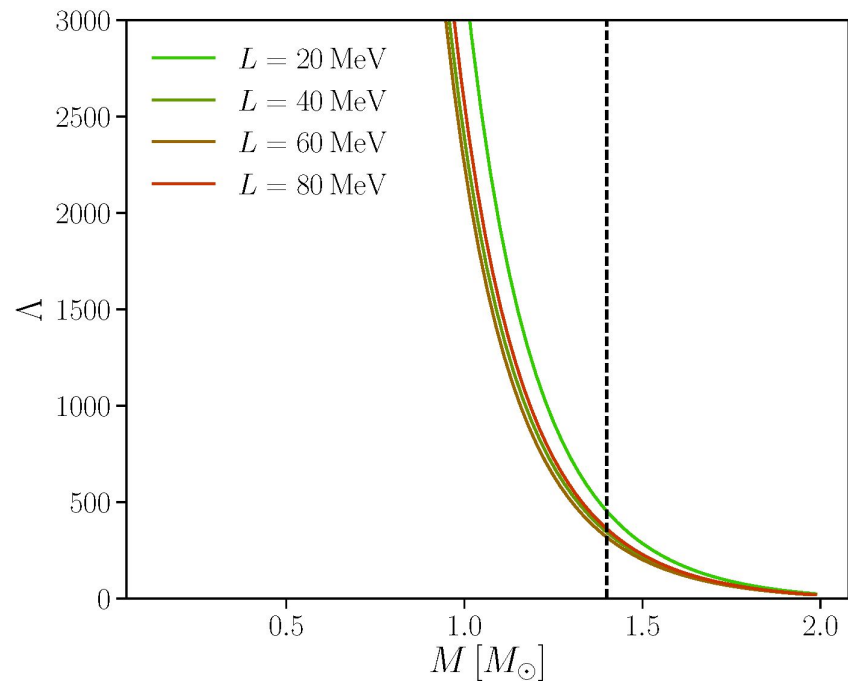
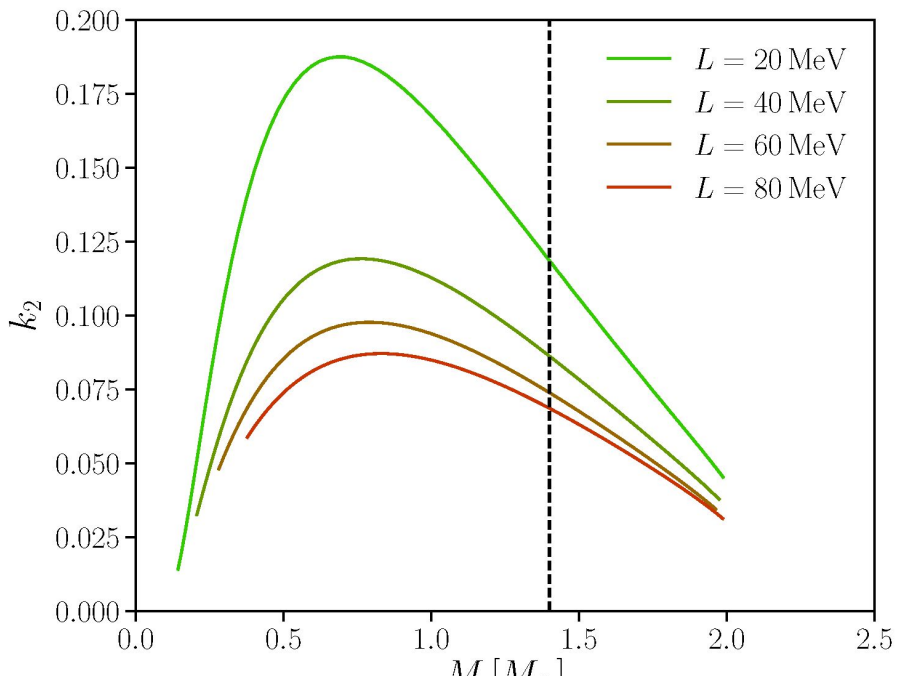
► Tidal deformability: $\Lambda = \frac{2}{3}k_2(M/R)^{-5}$

describes the amount of induced mass quadrupole moment when reacting to a certain external tidal field.

► Tidal 2nd Love number k_2 : $Q_{ij} = -k_2 \frac{2R^5}{3G} E_{ij}$
measures how easily the bulk of the matter in a star is deformed by an external tidal field.

► Larger L leads to smaller k_2 , for a star with certain amount of mass/compactness.





$$\Lambda = \frac{2}{3} k_2 (M/R)^{-5}$$

- Λ is normalized with a factor of R^5 , from k_2
- Differences in radius scatter the dependence on L .

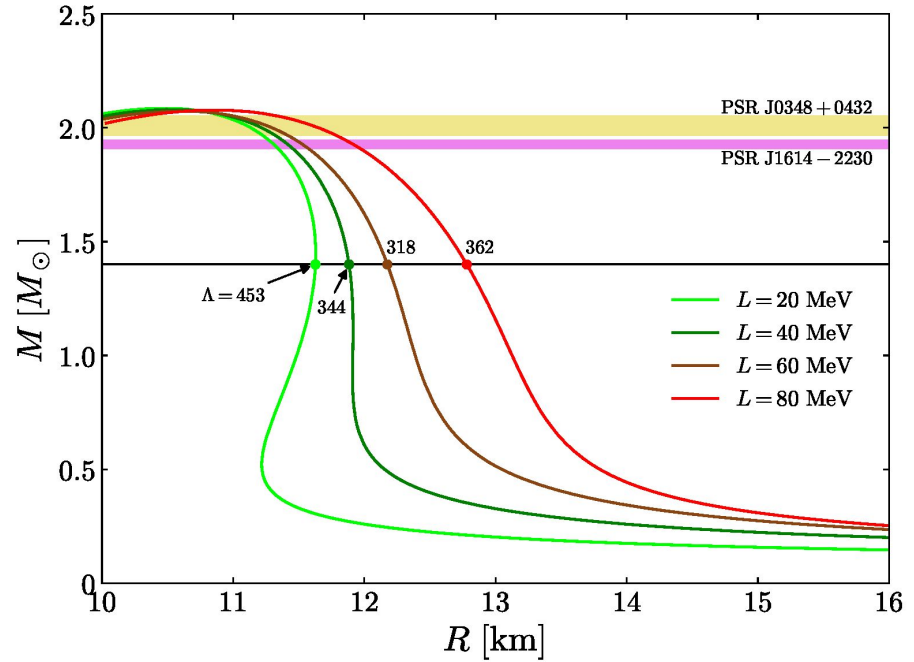
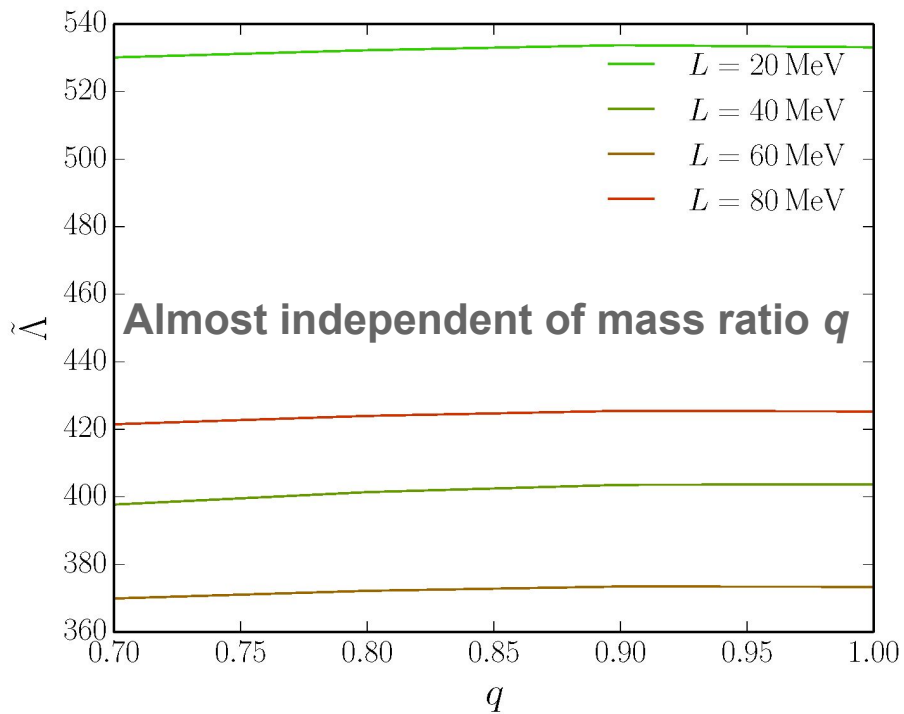
► Employing very well-constrained chirp mass of GW170817;

$$\mathcal{M} = (m_1 m_2)^{3/5} (m_1 + m_2)^{-1/5} = 1.188_{-0.002}^{+0.004} M_{\odot}$$

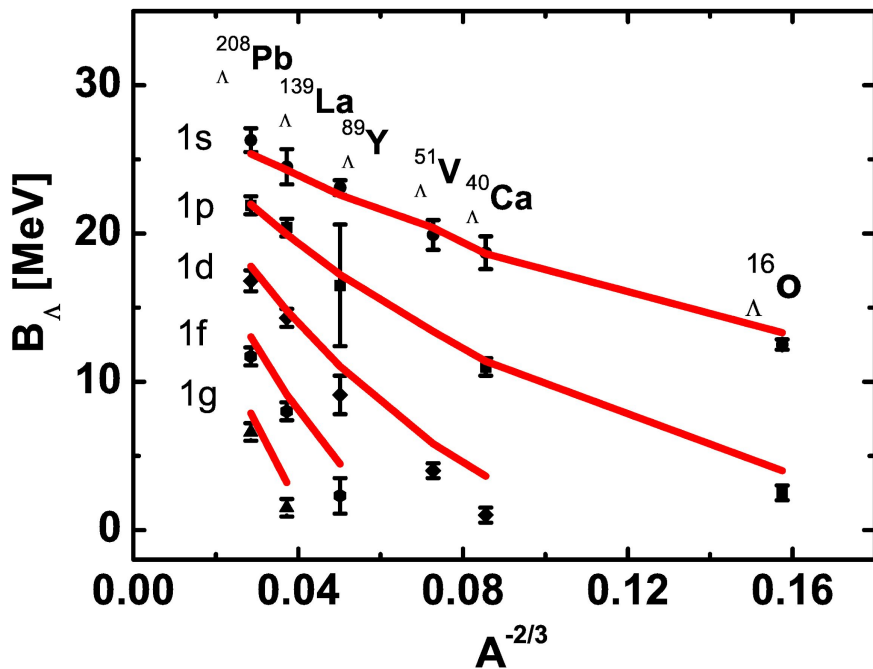
► Combined dimensionless tidal deformability (**Directly measured!**)

$$\tilde{\Lambda} = \frac{16}{13} \frac{(m_1 + 12m_2)m_1^4 \Lambda_1 + (m_2 + 12m_1)m_2^4 \Lambda_2}{(m_1 + m_2)^5}$$

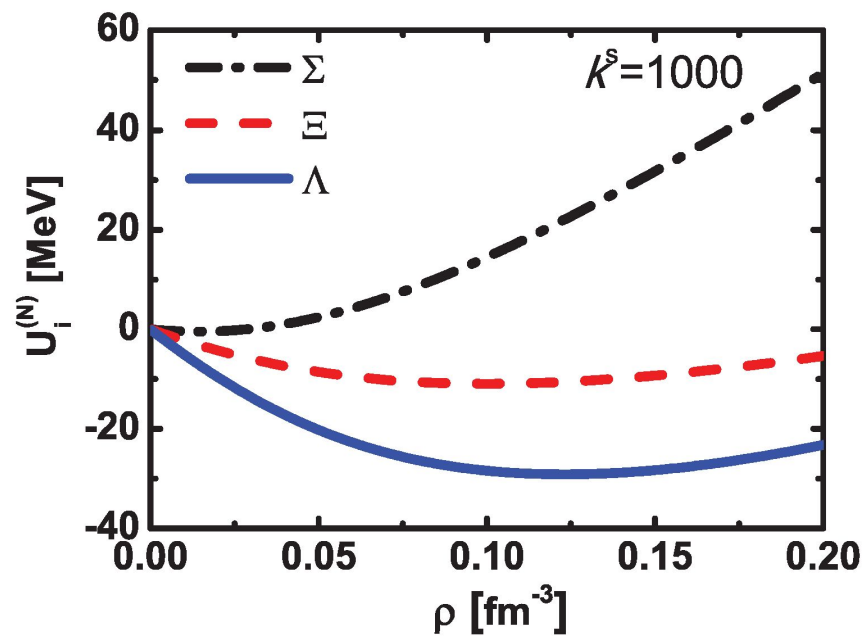
► Violation of monotonic dependence: Maybe dangerous to probe R/L via Λ .

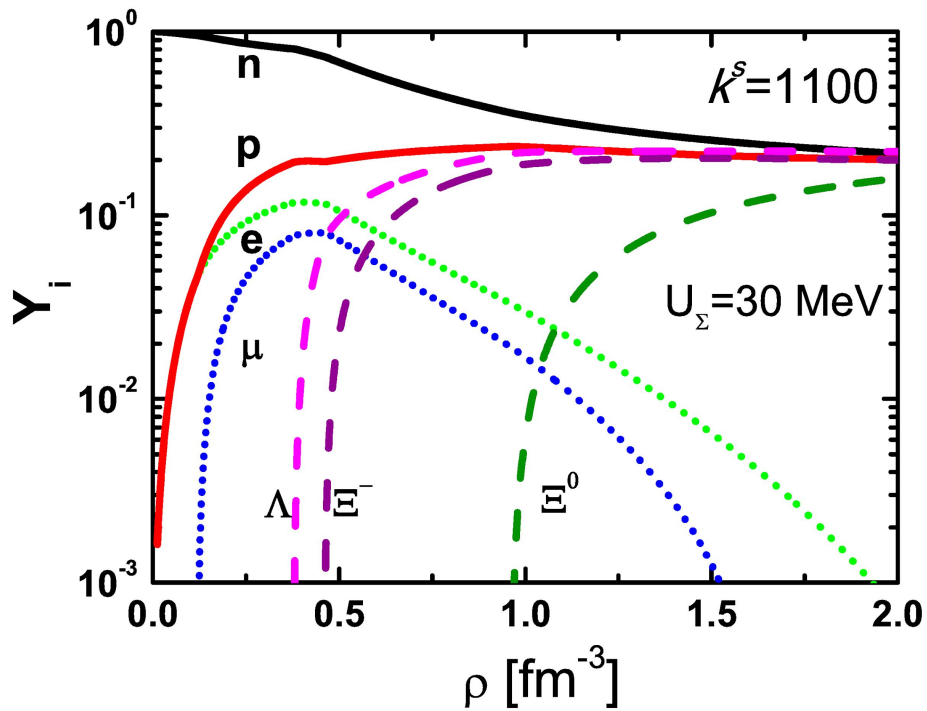


single Λ hypernuclei data
at mass number A

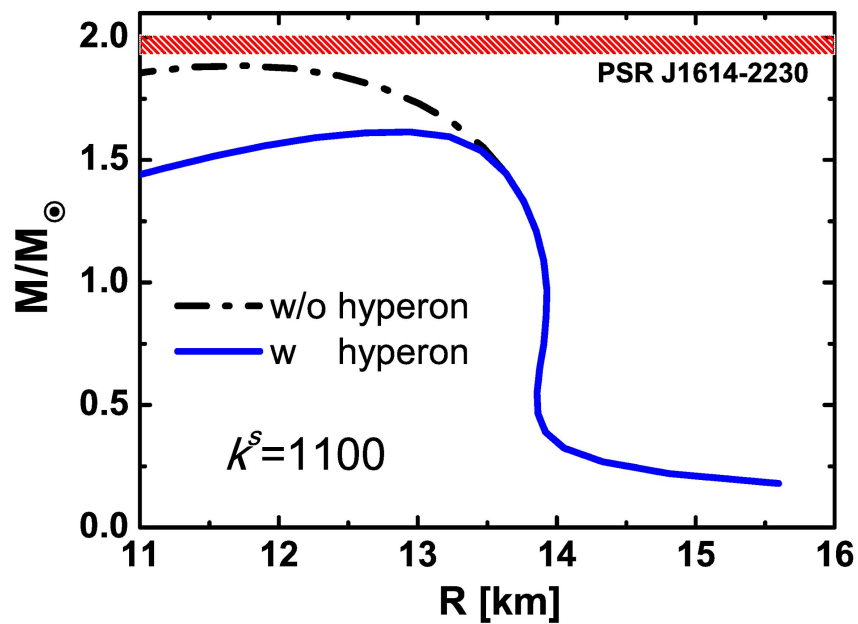


Single hyperon potentials
in nuclear medium at density ρ

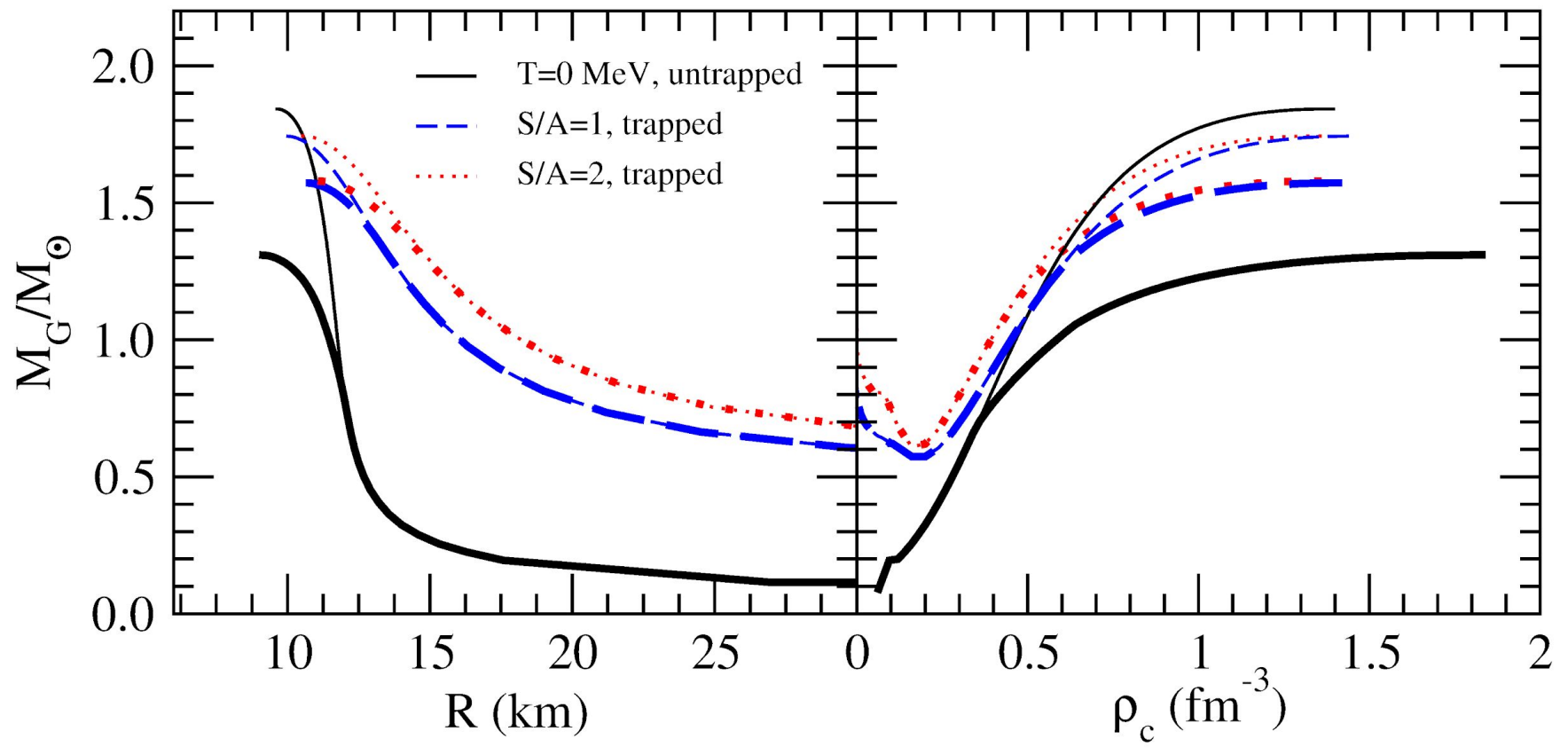




Hyperon star
with nuclear hyperon potentials



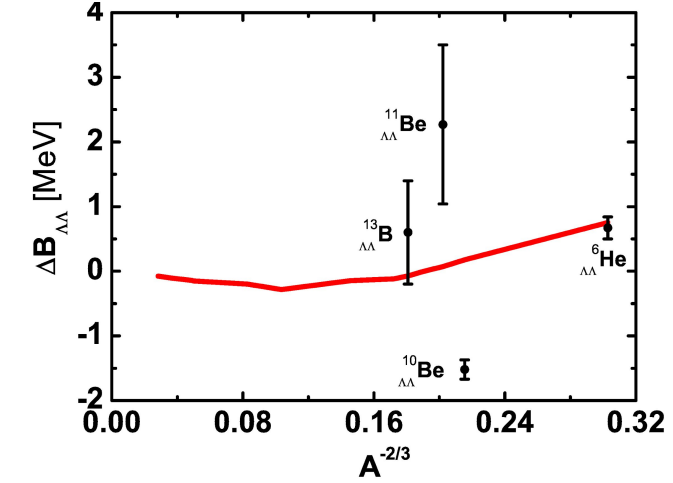
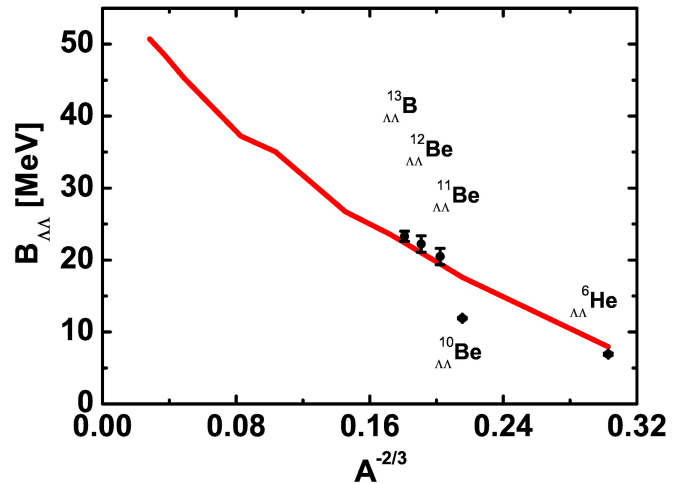
Hyperon star
with nuclear hyperon potentials
At finite temperature



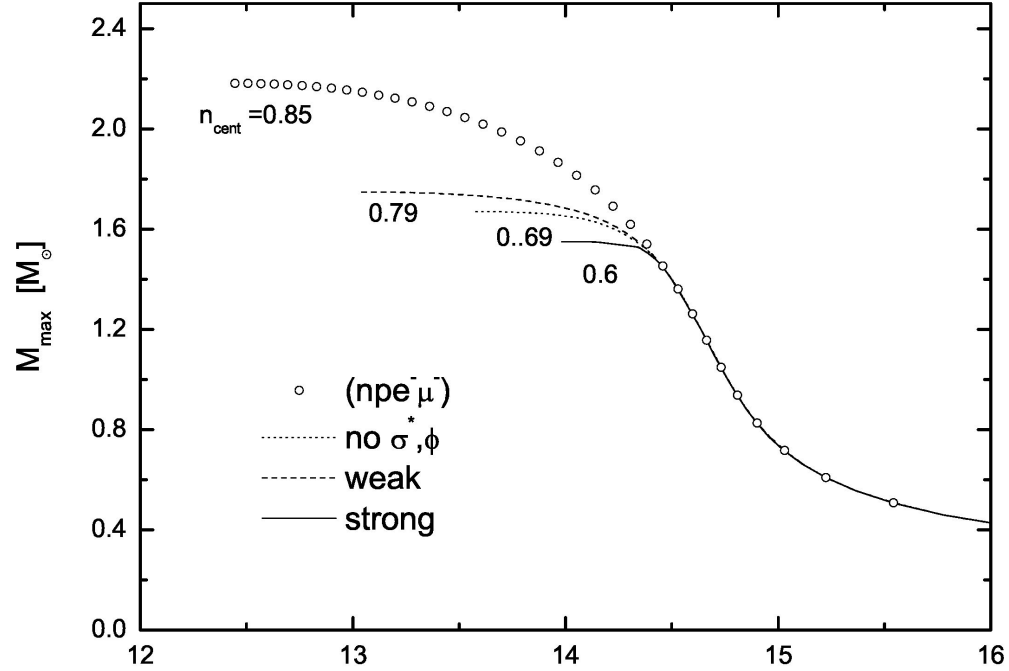
Double Λ hypernuclei data:
 $\Lambda\Lambda$ binding energy and bond energy

$$B_{\Lambda\Lambda}(^A_{\Lambda\Lambda}Z) = B(^A_{\Lambda\Lambda}Z) - B(^{A-2}Z),$$

$$\Delta B_{\Lambda\Lambda}(^A_{\Lambda\Lambda}Z) = B_{\Lambda\Lambda}(^A_{\Lambda\Lambda}Z) - 2B_{\Lambda}(^A_{\Lambda}Z).$$



Hyperon star
with nuclear hyperon potentials
And hyperon-hyperon interaction

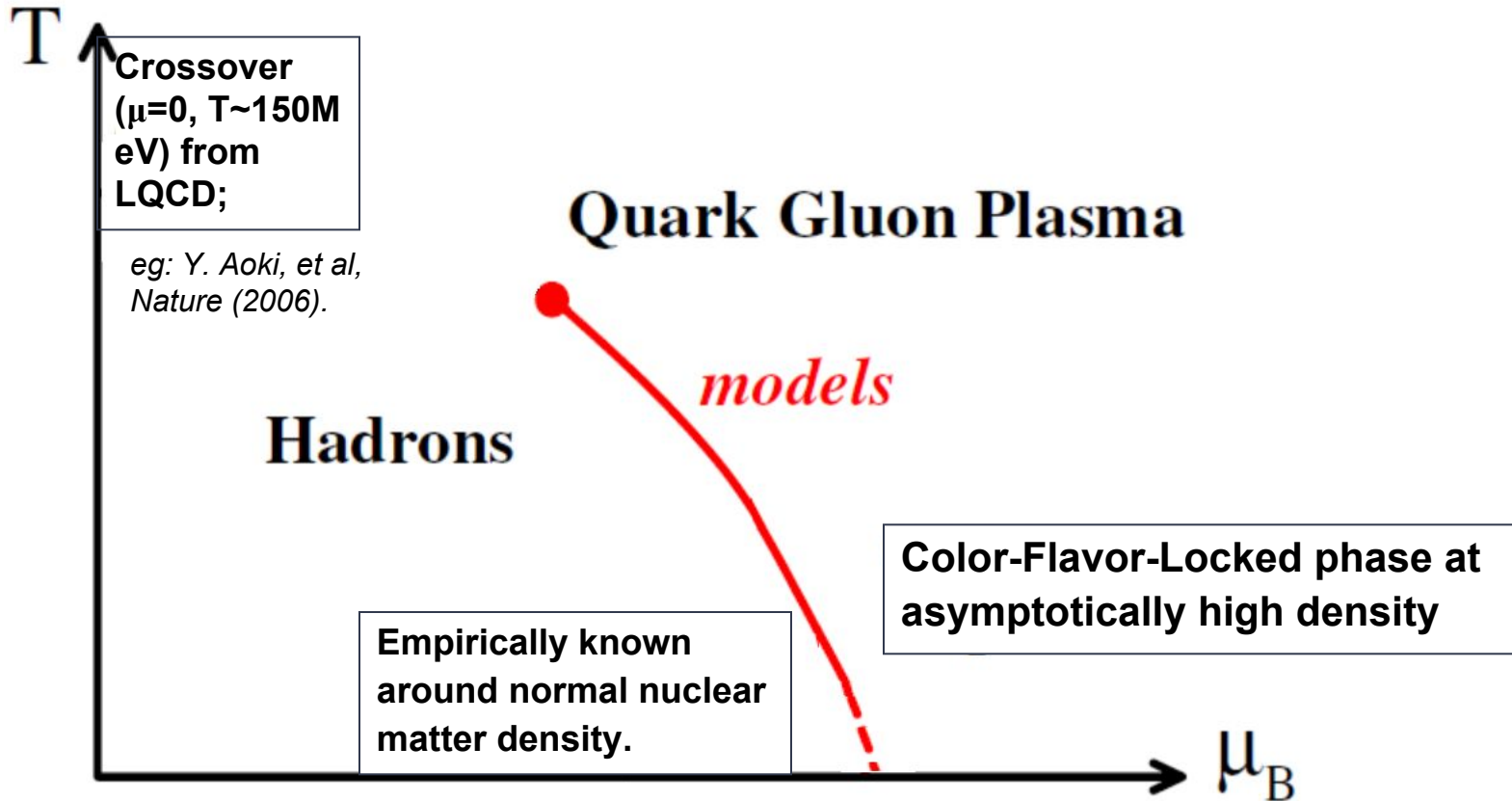


Hyperon puzzle?!

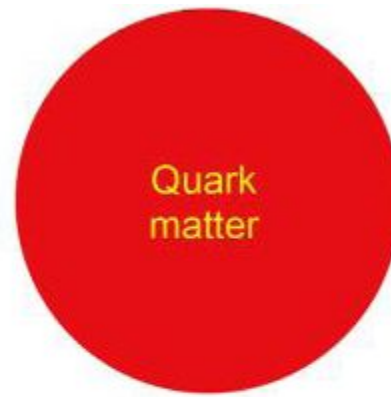
NS EoS model

2. QCD phase uncertainty:

Strangeness phase transition?!



QS EoS model



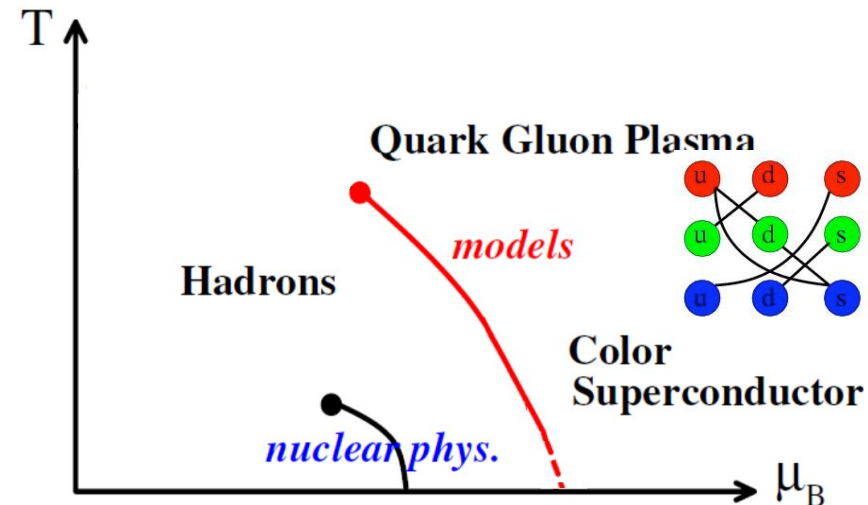
Quark star:
quarks de-confined
self-bound on surface

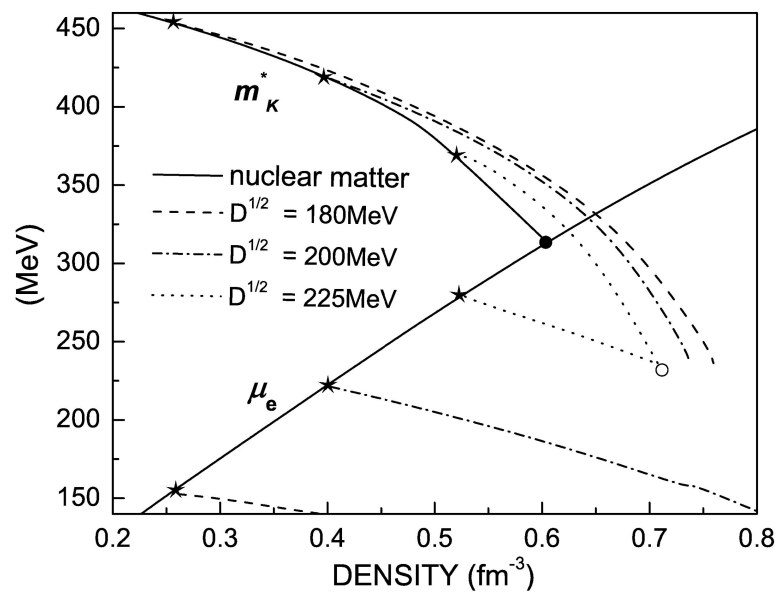
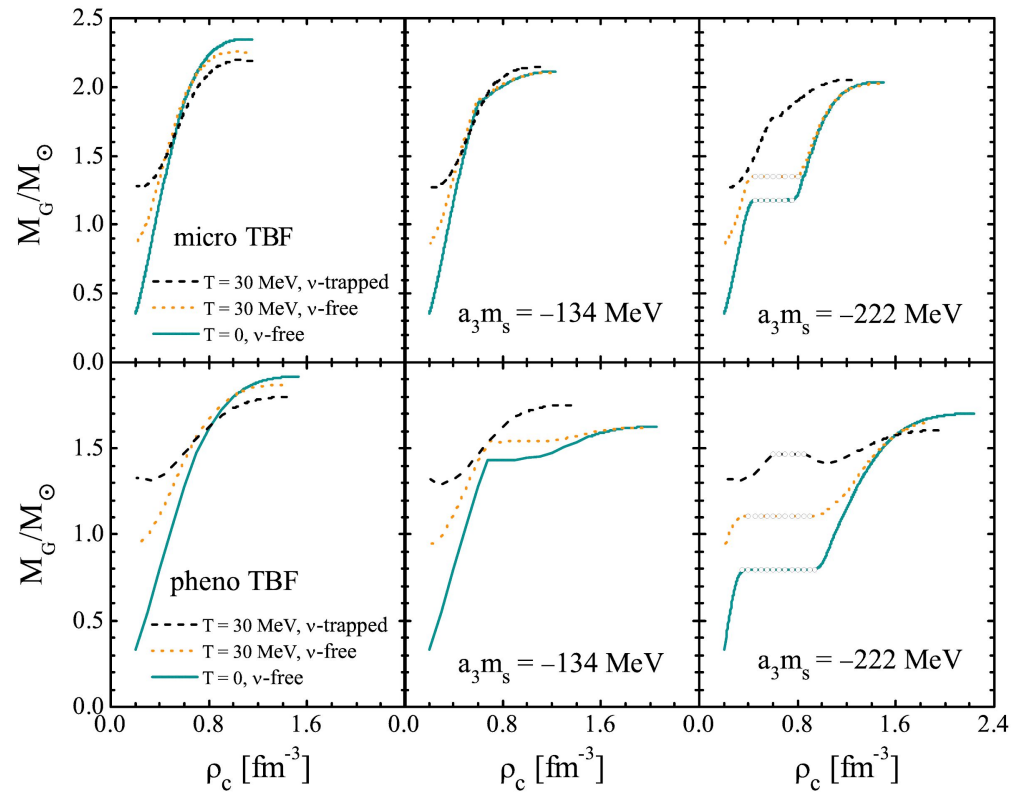
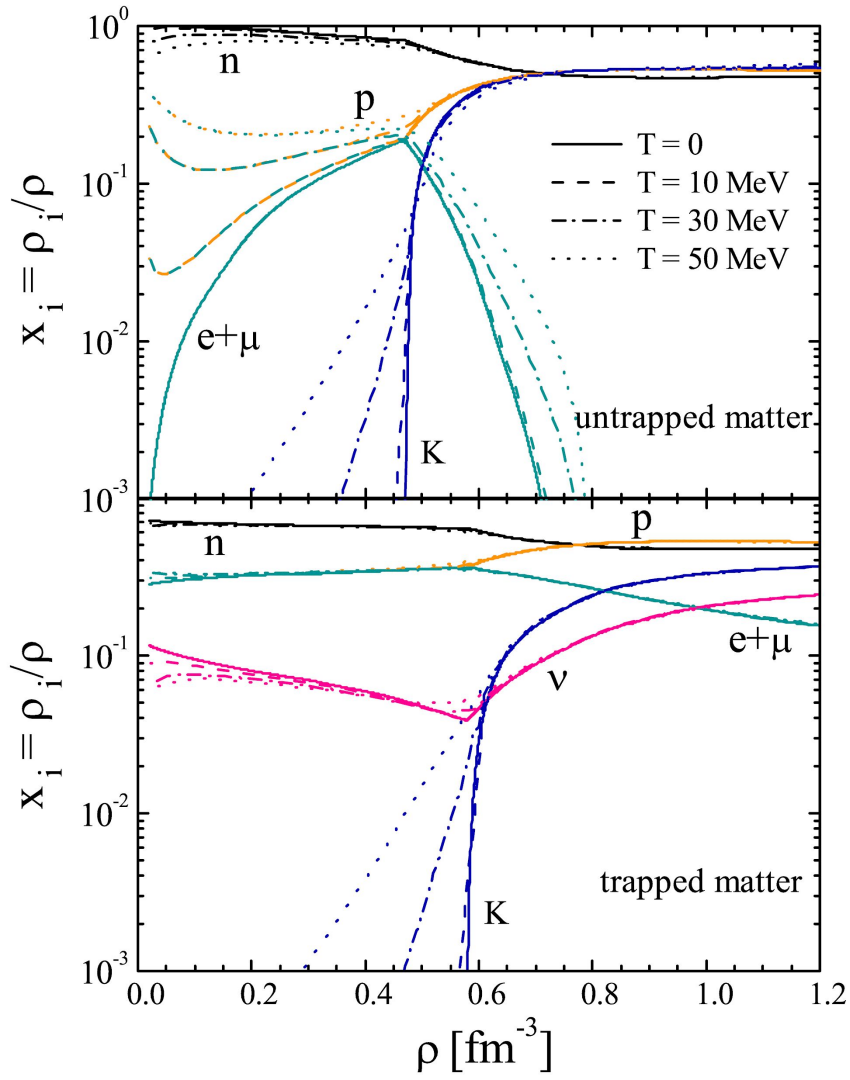


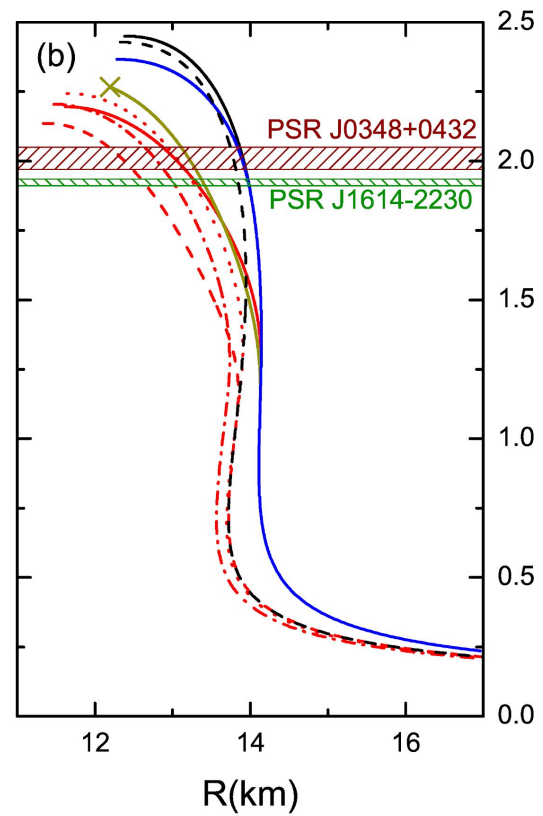
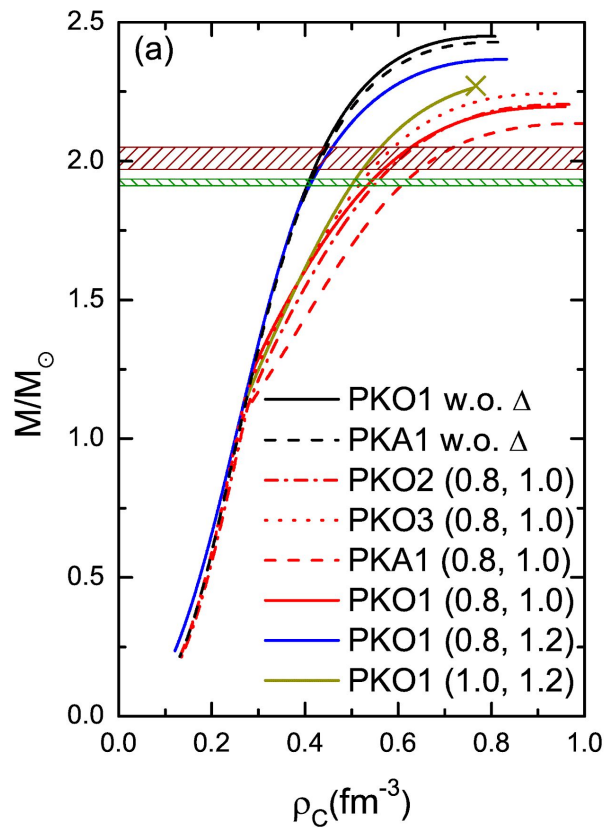
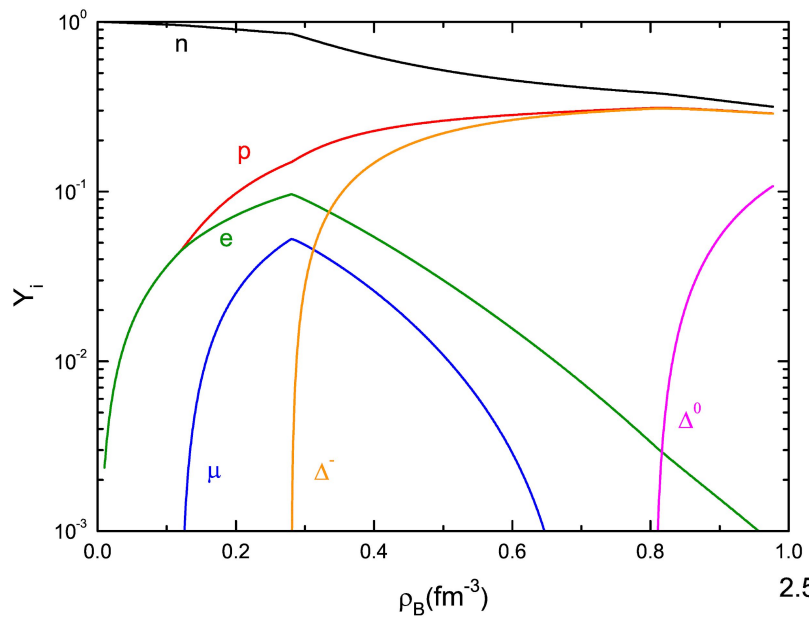
Quark-cluster star:
quarks localized
self-bound on surface

- QCD perturbation theory
- Dyson-Schwinger model
- Nambu–Jona-Lasinio (NJL) model
- Polyakov-loop extended NJL model
- Confined-density-dependent-mass (CDDM) model
- MIT bag model
- ...

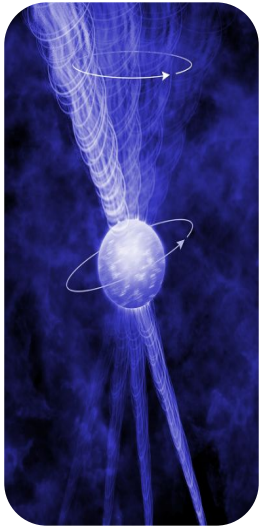
Still, quark superfluid...







Rotating star



- **NS/QS**
structures are
unique to the
underlying
EoS.

□ Static

$$\frac{dP(r)}{dr} = -\frac{GM(r)\varepsilon(r)}{r^2} \frac{\left[1 + \frac{P(r)}{\varepsilon(r)}\right] \left[1 + \frac{4\pi r^3 P(r)}{M(r)}\right]}{1 - \frac{2GM(r)}{r}}, \quad (1)$$

$$\frac{dM(r)}{dr} = 4\pi r^2 \varepsilon(r), \quad (2)$$

□ Slow rotation $\Omega \ll \Omega_{\max} \approx \sqrt{GM/R^3}$

Spherical-symmetry metric + Axis-symmetry perturbation

Vela
pulsar @
AL, Dong, Wang, Xu,
2016 *ApJS*,
1512.00340

□ Fast rotation

Relativistic stars in full GR from *rns* code

(www/gravity.phys.uwm.edu/rns),

Komatsu H, Eriguchi Y and Hachisu I 1989 *Mon. Not. R. Astron. Soc.* **237** 355

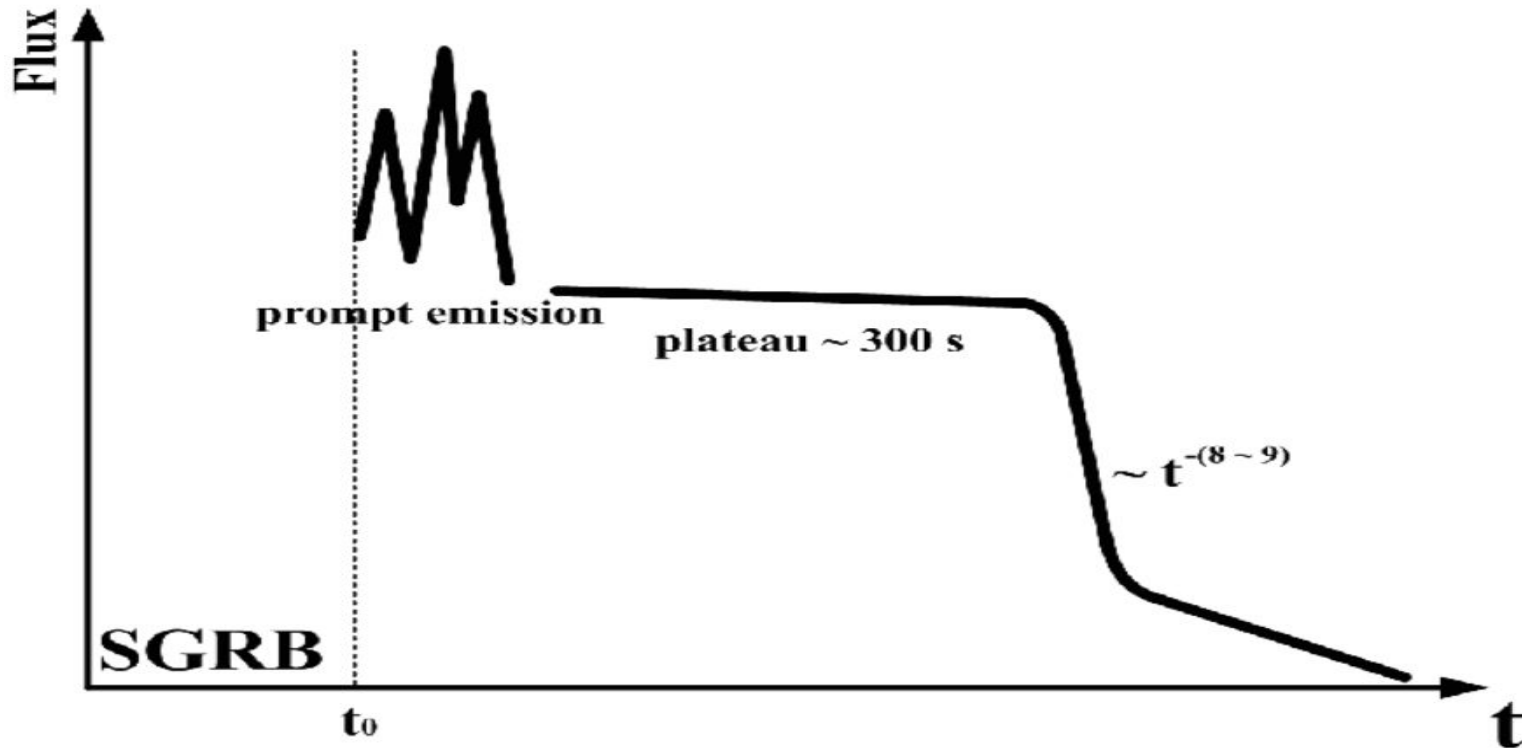
Cook G B, Shapiro S L and Teukolsky S A 1994 *ApJ* **422** 227

Stergioulas N and Friedman J L 1995 *ApJ* **444** 306

Post-merger
millisecond star @

AL, Zhang, Zhang, Gao,
Qi, Liu, 2016 *PRD*,
1606.02934

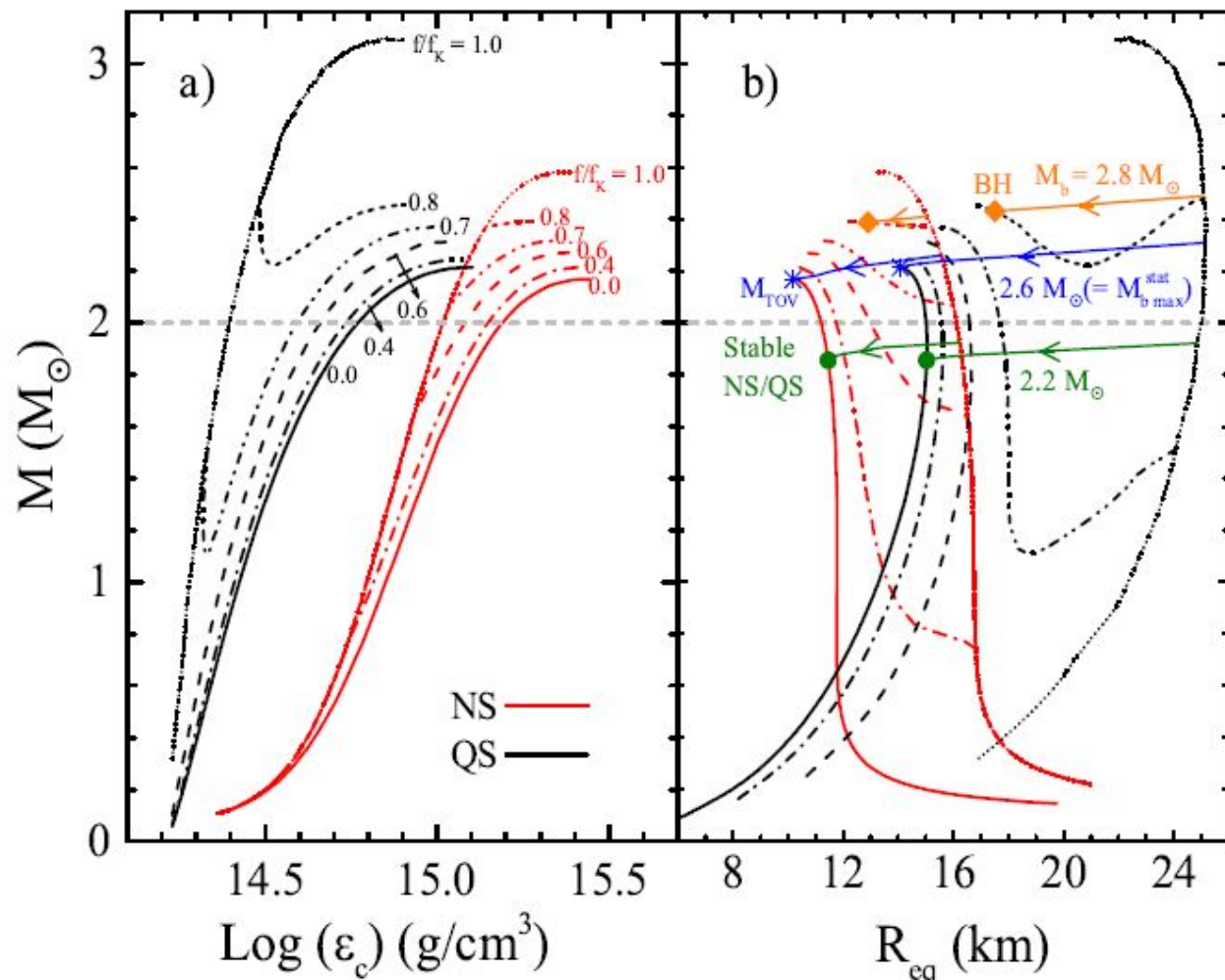
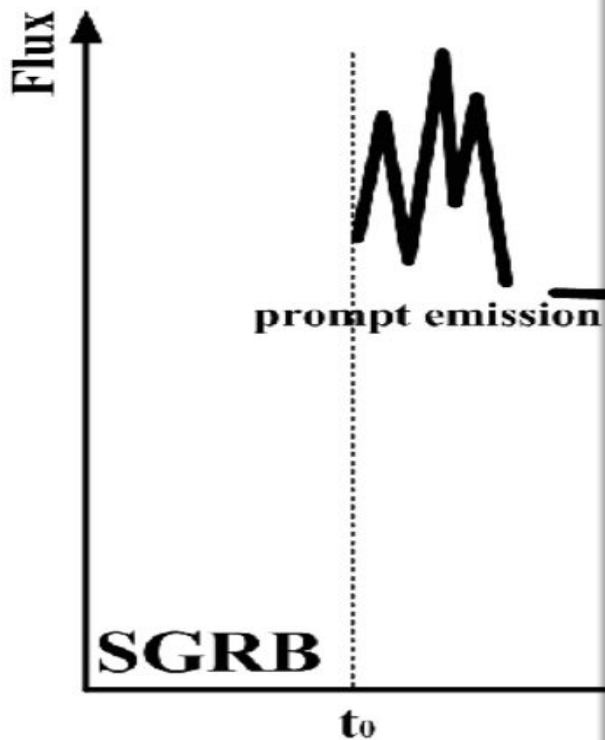
Supramassive star as central engine



Supramassive star as central engine

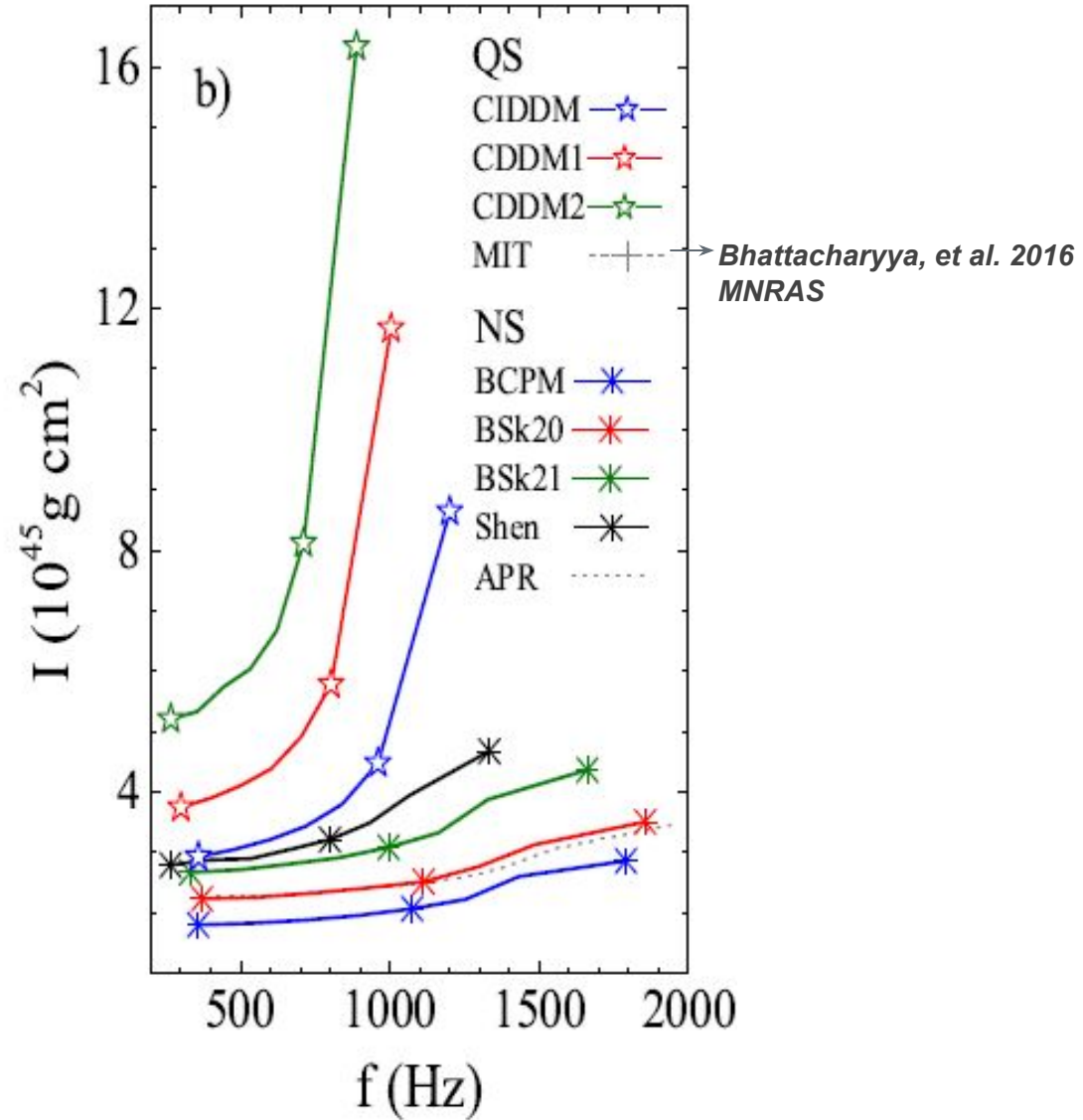
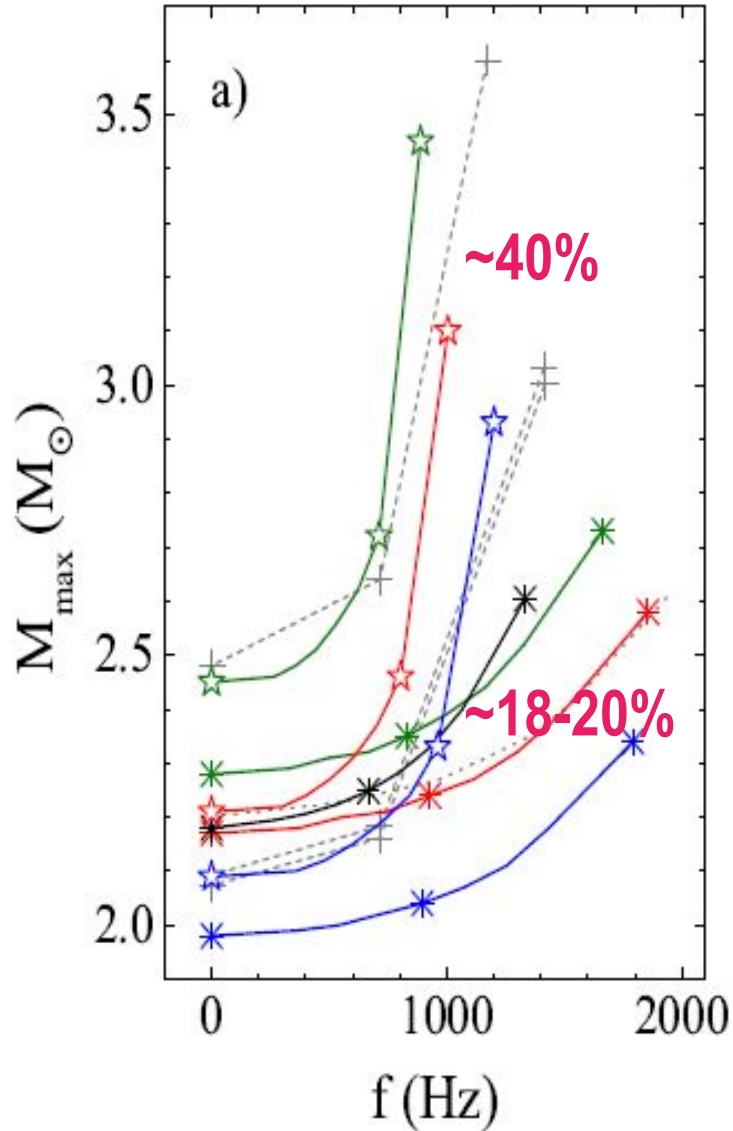


Spin-down induced collapse



Data prepared

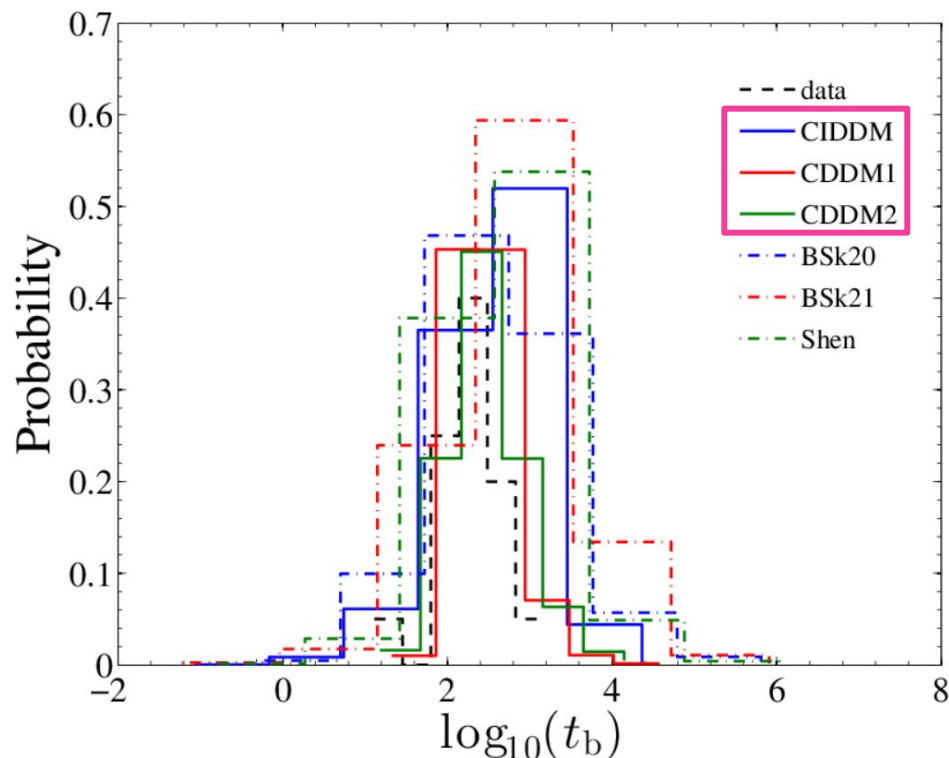
AL, Zhang, Zhang, Gao, Qi, Liu, 2016 PRD, 1606.02934



MC simulation

AL, Zhang, Zhang, Gao, Qi, Liu, 2016 PRD, 1606.02934

- ❑ Reproducing simultaneously all 3 observed distributions (t_b , L_b , E_{total}); (Fig.) time simulation
- ❑ Including both EM and GW;
- ❑ Constraining star parameter (ε , P_i , B_p);
- ❑ QS instead of NS.



	ε	P_i (ms)	B_p (G)	η	$P_{\text{best}}(t_b)$
BSk20	0.002	0.70 – 0.75 (0.75)	$N(\mu_{Bp} = 10^{14.8-15.4}, \sigma_{Bp} \leq 0.2)$ [$N(\mu_{Bp} = 10^{14.9}, \sigma_{Bp} = 0.2)$]	0.5 – 1 (0.9)	0.20
BSk21	0.002	0.60 – 0.80 (0.70)	$N(\mu_{Bp} = 10^{14.7-15.1}, \sigma_{Bp} \leq 0.2)$ [$N(\mu_{Bp} = 10^{14.8}, \sigma_{Bp} = 0.2)$]	0.7 – 1 (0.9)	0.29
Shen	0.002 – 0.003 (0.002)	0.70 – 0.90 (0.70)	$N(\mu_{Bp} = 10^{14.6-15.0}, \sigma_{Bp} \leq 0.2)$ [$N(\mu_{Bp} = 10^{14.6}, \sigma_{Bp} = 0.2)$]	0.5 – 1 (0.9)	0.41
CIDDM	0.001	0.70 – 1.05 (0.95)	$N(\mu_{Bp} = 10^{14.8-15.4}, \sigma_{Bp} \leq 0.2)$ [$N(\mu_{Bp} = 10^{15.0}, \sigma_{Bp} = 0.2)$]	0.5 – 1 (0.5)	0.44
CDDM1	0.002 – 0.003 (0.003)	1.00 – 1.40 (1.0)	$N(\mu_{Bp} = 10^{14.7-15.1}, \sigma_{Bp} \leq 0.3)$ [$N(\mu_{Bp} = 10^{14.7}, \sigma_{Bp} = 0.2)$]	0.5 – 1 (1)	0.65
CDDM2	0.004 – 0.007 (0.005)	1.10 – 1.70 (1.3)	$N(\mu_{Bp} = 10^{14.8-15.4}, \sigma_{Bp} \leq 0.4)$ [$N(\mu_{Bp} = 10^{14.9}, \sigma_{Bp} = 0.4)$]	0.5 – 1 (1)	0.84

Millisecond Strongly magnetized

Efficiency related to the conversion of the dipole spin-down luminosity to the observed X-ray luminosity.

Internal x-ray plateau in short GRBs: Signature of supramassive fast-rotating quark stars?

Ang Li,^{1,2,*} Bing Zhang,^{2,3,4,†} Nai-Bo Zhang,⁵ He Gao,⁶ Bin Qi,⁵ and Tong Liu^{1,2}

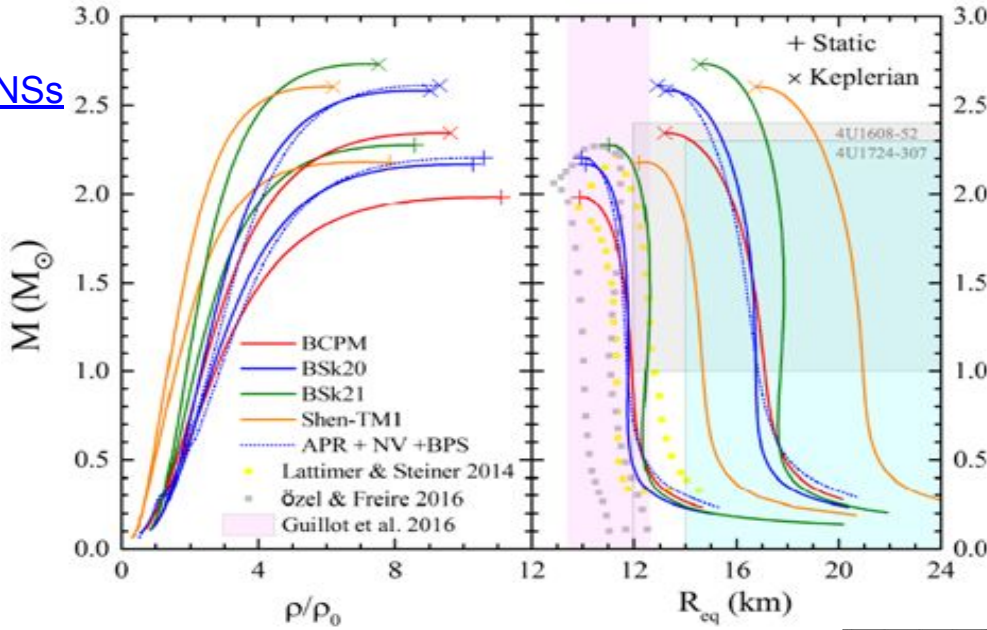
Summary.— To recap, we have carried out the following investigations: 1) Selecting unified NS EoSs that satisfy up-to-date experimental constraints from both nuclear physics and astrophysics, based on modern nuclear many-body theories; 2) Finding typical parameter sets for QS EoSs in developed CDDM model, under same constraints of the NS case

the fast-rotating
 oviding conve-
 s; 4) Checking
 ved fraction of
 on observation
 ating observed
 ple and reveal-
 cs. We finally

reach the conclusion that the post-merger products of NS-NS mergers are probably supramassive QSs rather than NSs. NS-NS mergers are a plausible location for quark de-confinement and the formation of QSs.

1. Post-merger products of NS-NS mergers are probably supramassive QSs rather than supramassive NSs;
2. NS-NS mergers are a plausible location for quark de-confinement and the formation of QSs.

2 X-ray bursts:
Rapidly spinning NSs
 (1610.08770)

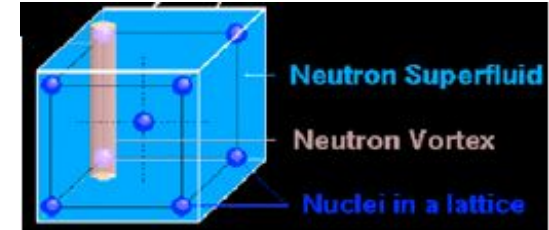


Glitch model:

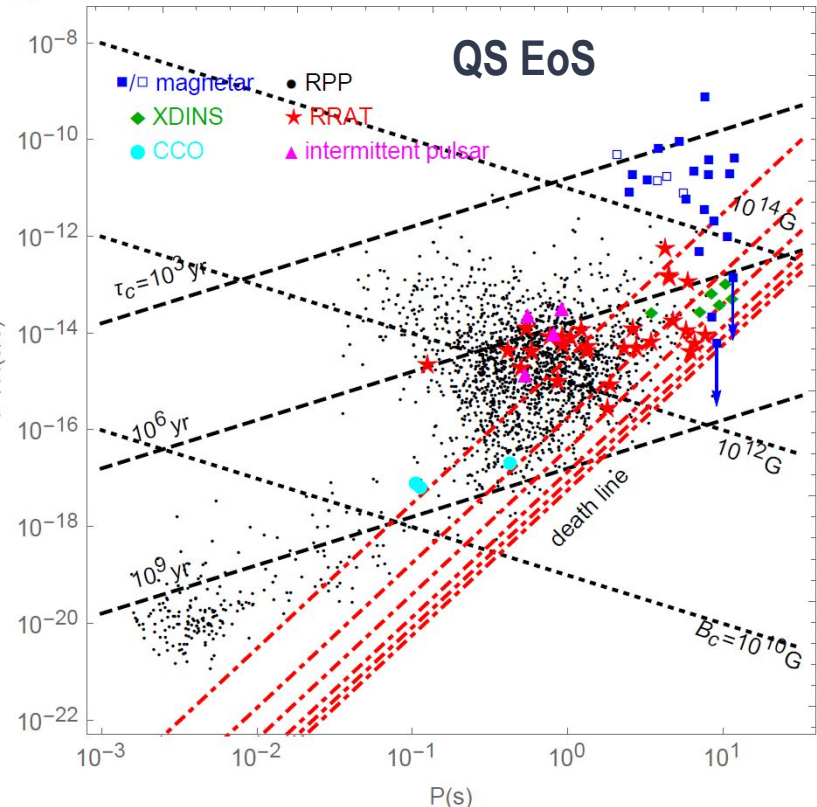
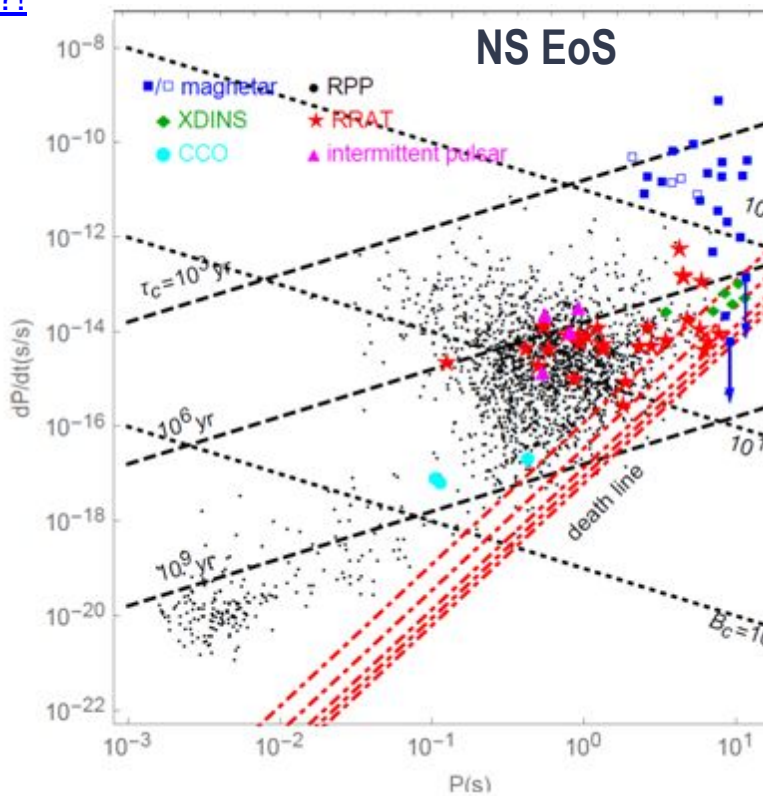
Hartree-Fock-Bogoliubov (HFB)

+
 Quasi-particle

Random-Phase-Approximation (QRPA)



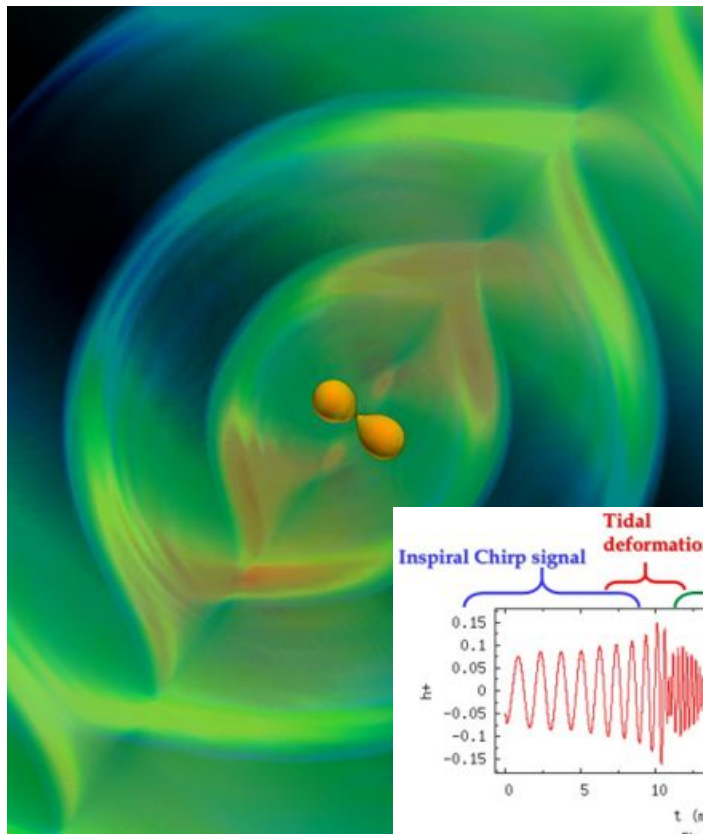
CCO: small QS?!



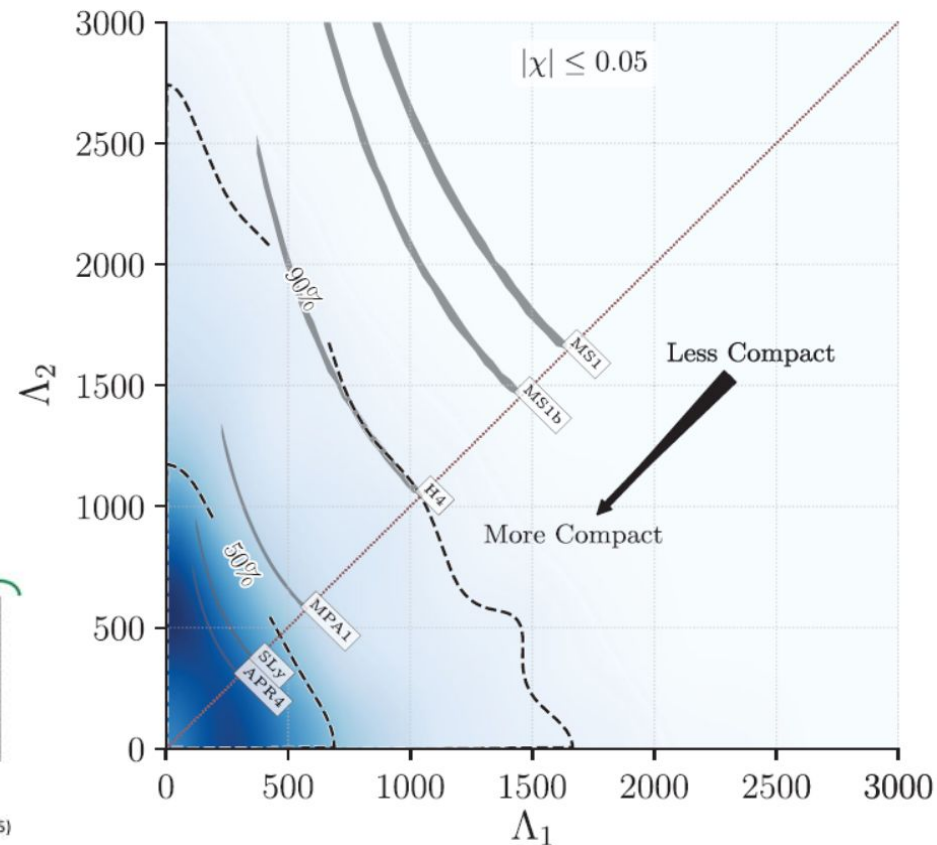
Low-spin priors ($|\chi| \leq 0.05$)

High-spin priors ($|\chi| \leq 0.89$)

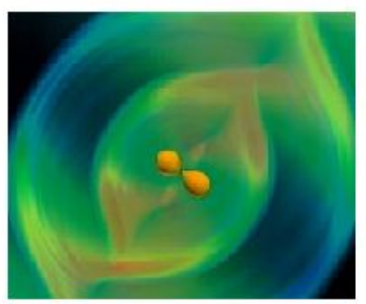
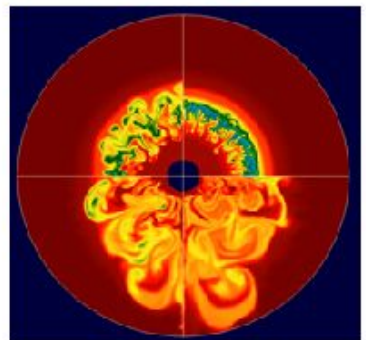
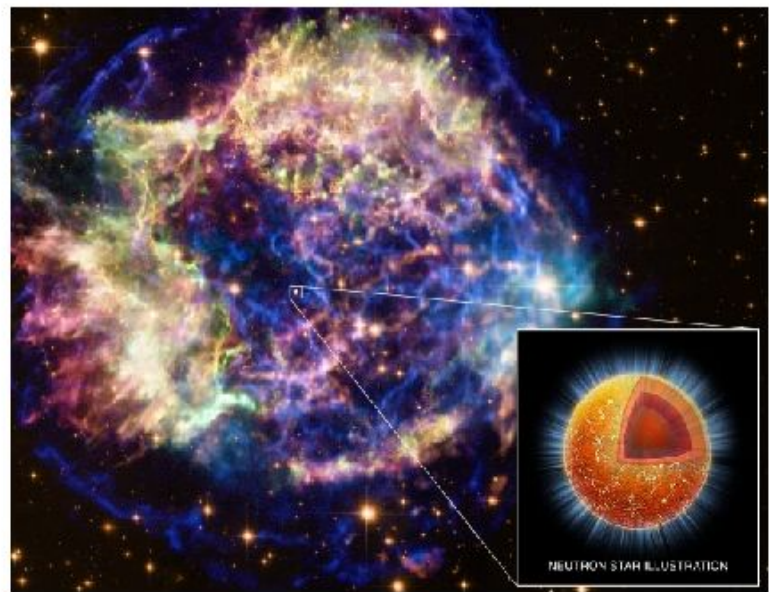
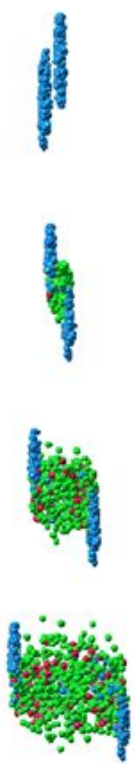
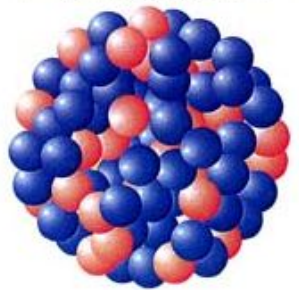
Primary mass m_1	1.36–1.60 M_\odot	1.36–2.26 M_\odot
Secondary mass m_2	1.17–1.36 M_\odot	0.86–1.36 M_\odot
Chirp mass \mathcal{M}	$1.188^{+0.004}_{-0.002} M_\odot$	$1.188^{+0.004}_{-0.002} M_\odot$
Mass ratio m_2/m_1	0.7–1.0	0.4–1.0
Total mass m_{tot}	$2.74^{+0.04}_{-0.01} M_\odot$	$2.82^{+0.47}_{-0.09} M_\odot$
Radiated energy E_{rad}	$> 0.025 M_\odot c^2$	$> 0.025 M_\odot c^2$
Luminosity distance D_L	40^{+8}_{-14} Mpc	40^{+8}_{-14} Mpc
Viewing angle Θ	$\leq 55^\circ$	$\leq 56^\circ$
Using NGC 4993 location	$\leq 28^\circ$	$\leq 28^\circ$
Combined dimensionless tidal deformability $\tilde{\Lambda}$	≤ 800	≤ 700
Dimensionless tidal deformability $\Lambda(1.4M_\odot)$	≤ 800	≤ 1400

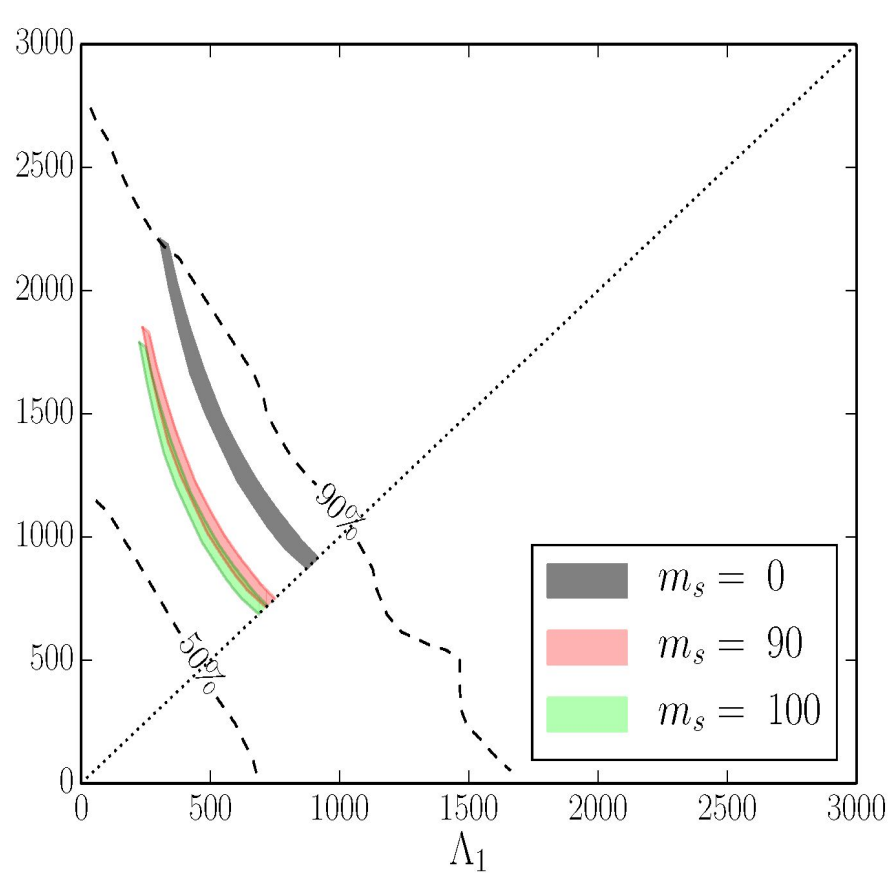
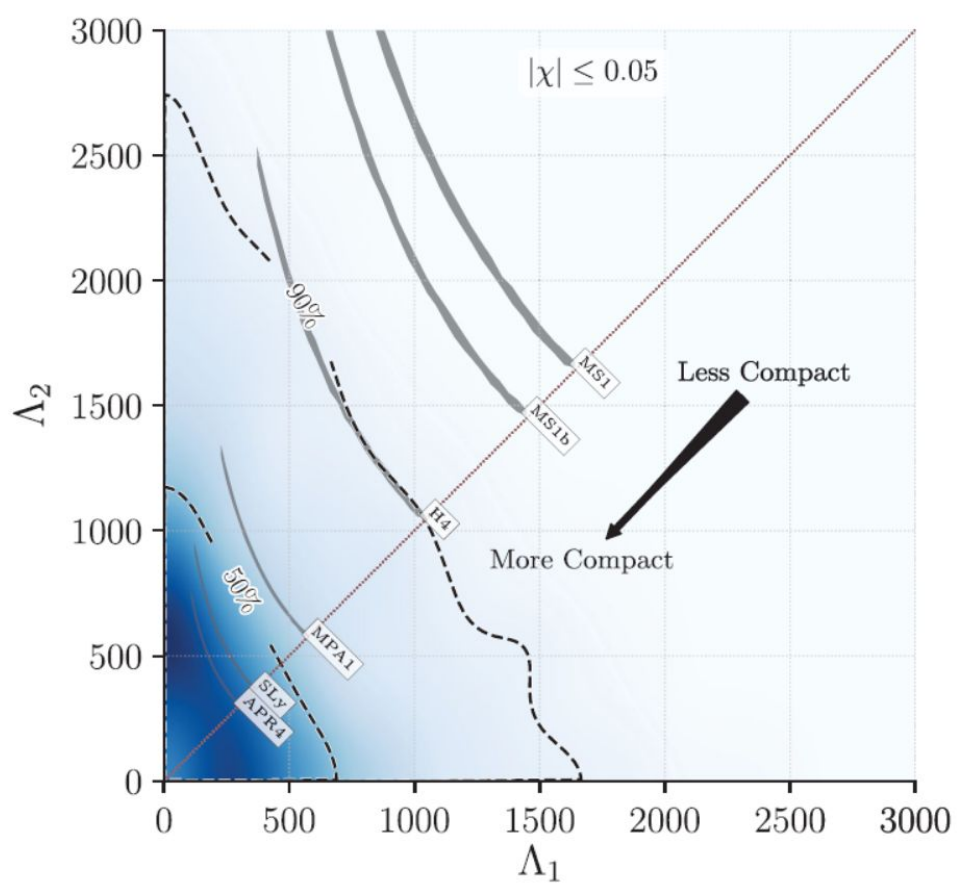


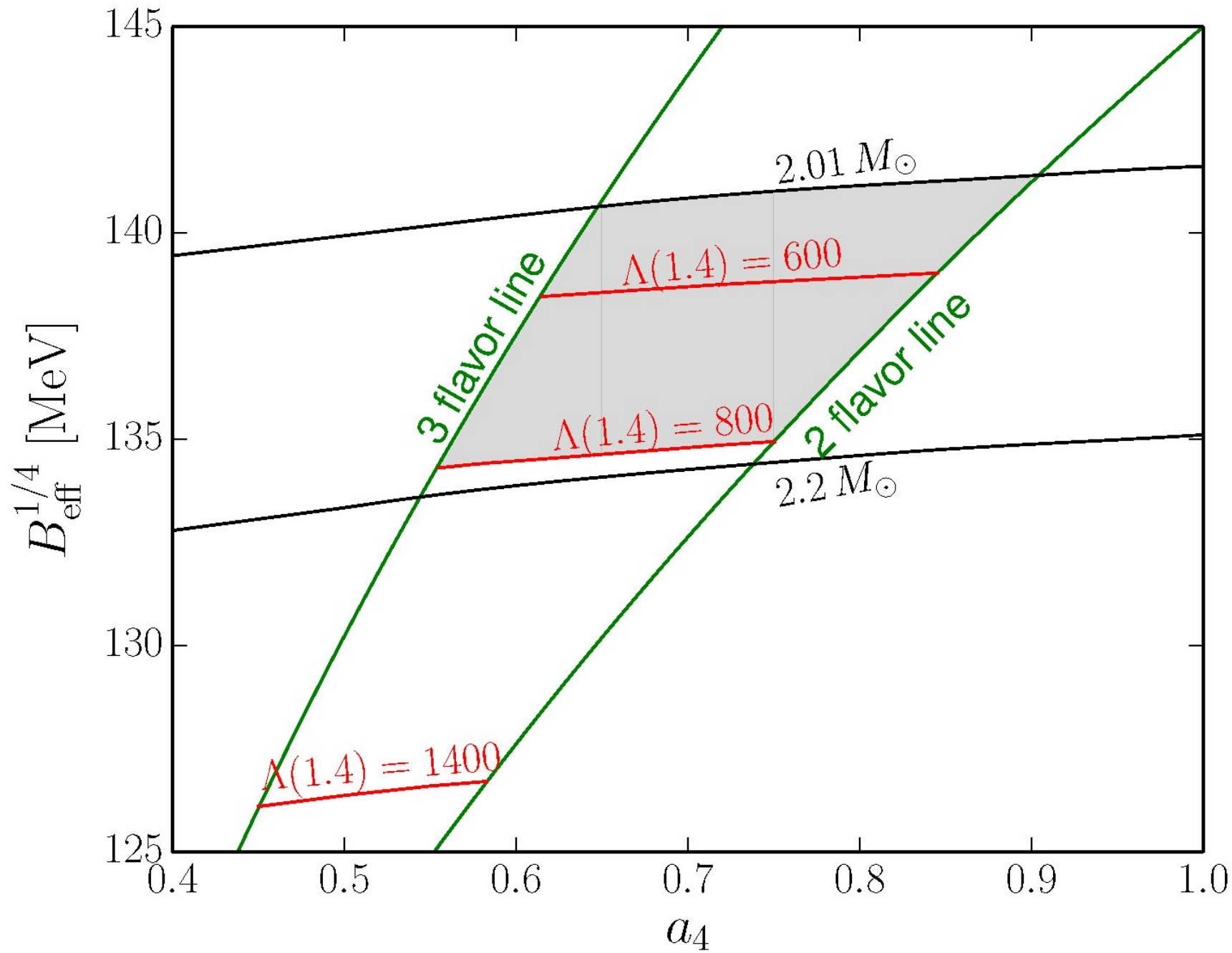
First suggested by Shibata (2005)



← 0.0000000000014 cm →







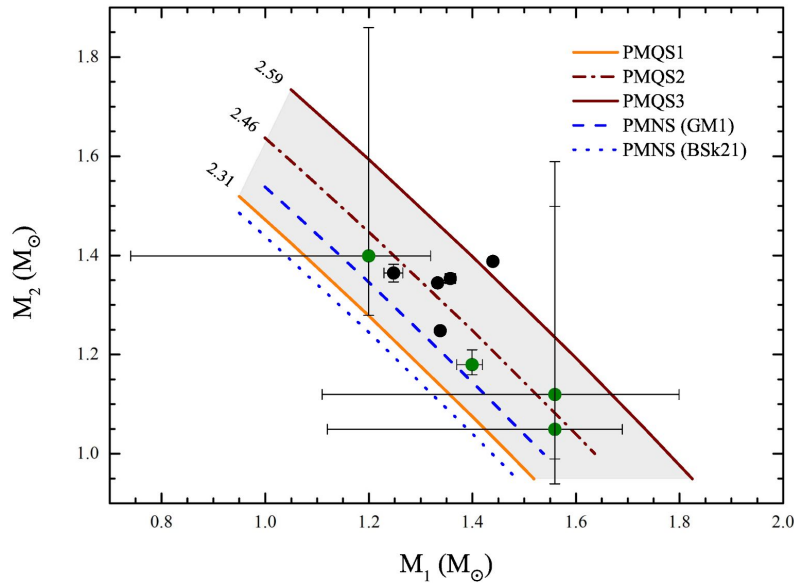
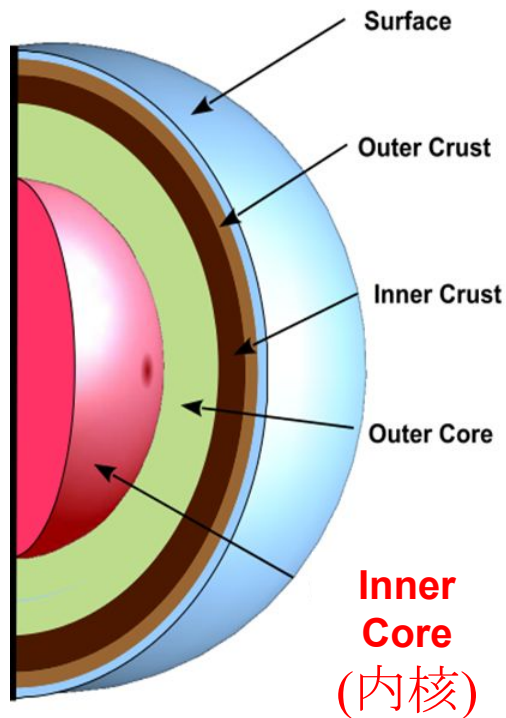


Figure 5. Measured gravitational mass for NSs in binary NSs (Kiziltan et al. 2013), along with lines indicating M_{TOV} for three new PMQS EoSs and two representative NS EoSs (GM1, BSk21).

Double Neutron Star Systems			
Pulsar	Mass (M_{\odot})	68% Central Limits	Refs. ^a
Double neutron star binaries			
J0737–3039			1
Pulsar A	1.3381	± 0.0007	
Pulsar B	1.2489	± 0.0007	
Total	2.58708	± 0.00016	
J1518+4904			2
Pulsar	1.56	$+0.13 / - 0.44$	
Companion	1.05	$+0.45 / - 0.11$	
Total	2.61	± 0.070	
B1534+12			3
Pulsar	1.3332	± 0.0010	
Companion	1.3452	± 0.0010	
Total	2.678428	± 0.000018	
J1756–2251			4
Pulsar	1.40	$+0.02 / - 0.03$	
Companion	1.18	$+0.03 / - 0.02$	
Total	2.574	± 0.003	
J1811–1736			5, 6
Pulsar	1.56	$+0.24 / - 0.45$	
Companion	1.12	$+0.47 / - 0.13$	
Total	2.57	± 0.10	
J1829+2456			7
Pulsar	1.20	$+0.12 / - 0.46$	
Companion	1.40	$+0.46 / - 0.12$	
Total	2.59	± 0.02	
J1906+0746			8, 9
Pulsar	1.248	± 0.018	
Companion	1.365	± 0.018	
Total	2.61	± 0.02	
B1913+16			10, 11
Pulsar	1.4398	± 0.0002	
Companion	1.3886	± 0.0002	
Total	2.828378	± 0.000007	
B2127+11C			12, *
Pulsar	1.358	± 0.010	
Companion	1.354	± 0.010	
Total	2.71279	± 0.00013	

Notes.

^a **References:** (1) Kramer et al. 2006; (2) Thorsett & Chakrabarty 1999; (3) Stairs et al. 2002; (4) Faulkner et al. 2005; (5) Stairs 2006; (6) Corongiu et al. 2007; (7) Champion et al. 2005; (8) Kasian 2008; (9) Lorimer et al. 2006b; (10) Weisberg et al. 2010; (11) Taylor 1992; (12) Jacoby et al. 2006; (*) in globular cluster.



Dark matter-mixed

- ▶ Li*, Liu, Gubler, Xu, 2015 AP
- ▶ Li*, Huang, Xu, 2012 AP

▶ Nucleons

- ▶ Zhu, Li*, 2018 PRC
- ▶ Li*, Dong, Wang, Xu, 2016 ApJS
- ▶ Li*, Zhang, Zhang, Gao, Qi, Liu, 2016 PRD
- ▶ Li*, Hu, Shang, Zuo, 2016 PRC
- ▶ Li*, Liu, 2013 A&A

▶ Excited nucleons (Δ -isobars)

- ▶ Zhu, Li*, Hu, Sagawa, 2016 PRC

▶ Kaon condensation

- ▶ Li*, Zhou, Burgio, Schulze, 2010 PRC
- ▶ Li*, Burgio, Lombardo, Zuo, 2006 PRC
- ▶ Zuo*, Li, Li, Lombardo, 2004 PRC

▶ Free quarks \rightarrow Hybrid star (混杂星)

- ▶ Li*, Peng, Zuo, 2015 PRC
- ▶ Peng*, Li, Lombardo, 2008 PRC

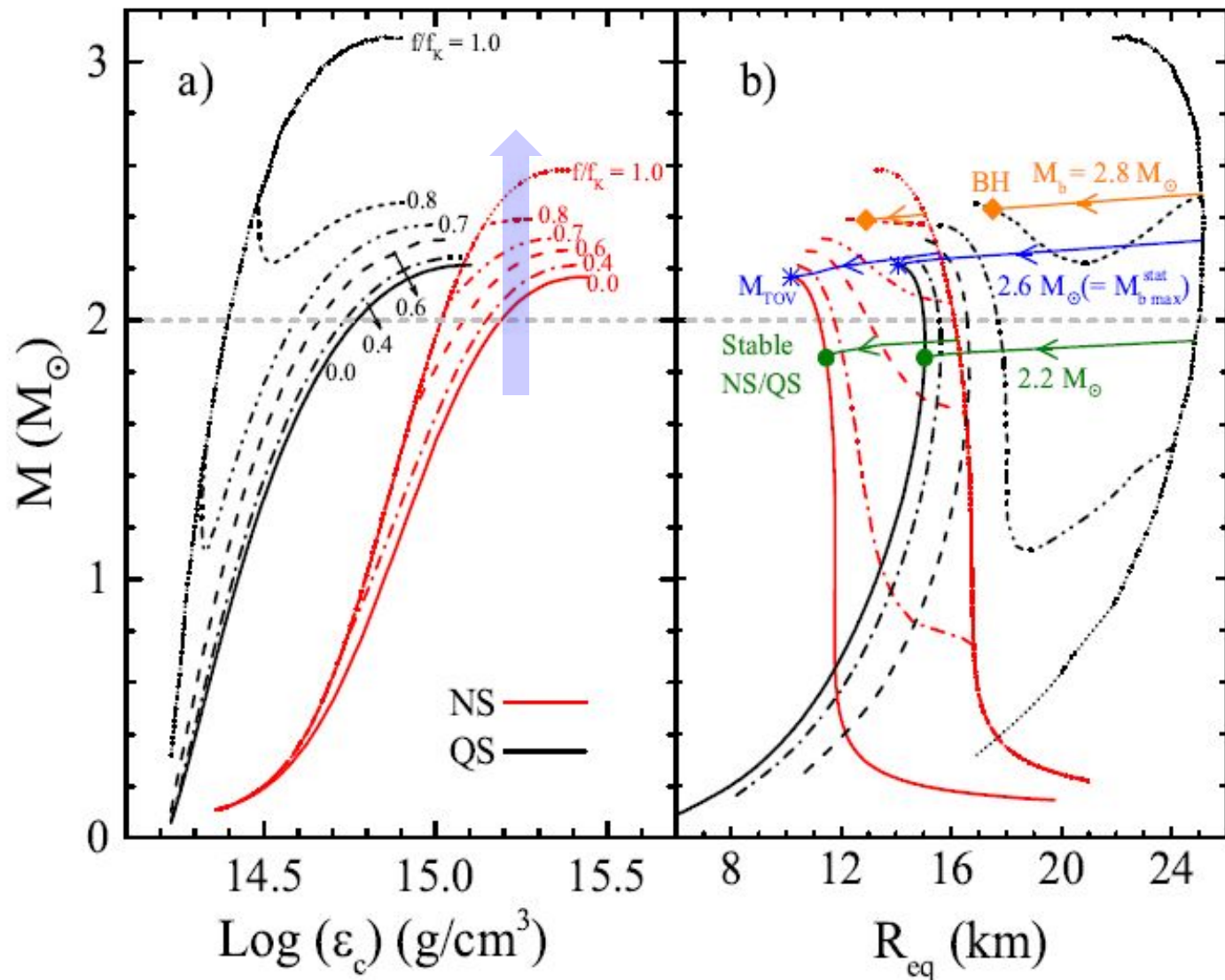
▶ Hyperons ($\Lambda^0, \Sigma^{0,\pm}, \Xi^{0,-}$) \rightarrow Hyperon star (超子星)

- ▶ Li*, Hiyama, Zhou, Sagawa, 2013 PRC
- ▶ Hu, Li*, Toki, Zuo, 2014 PRC
- ▶ Burgio*, Schulze, Li, 2011 PRC

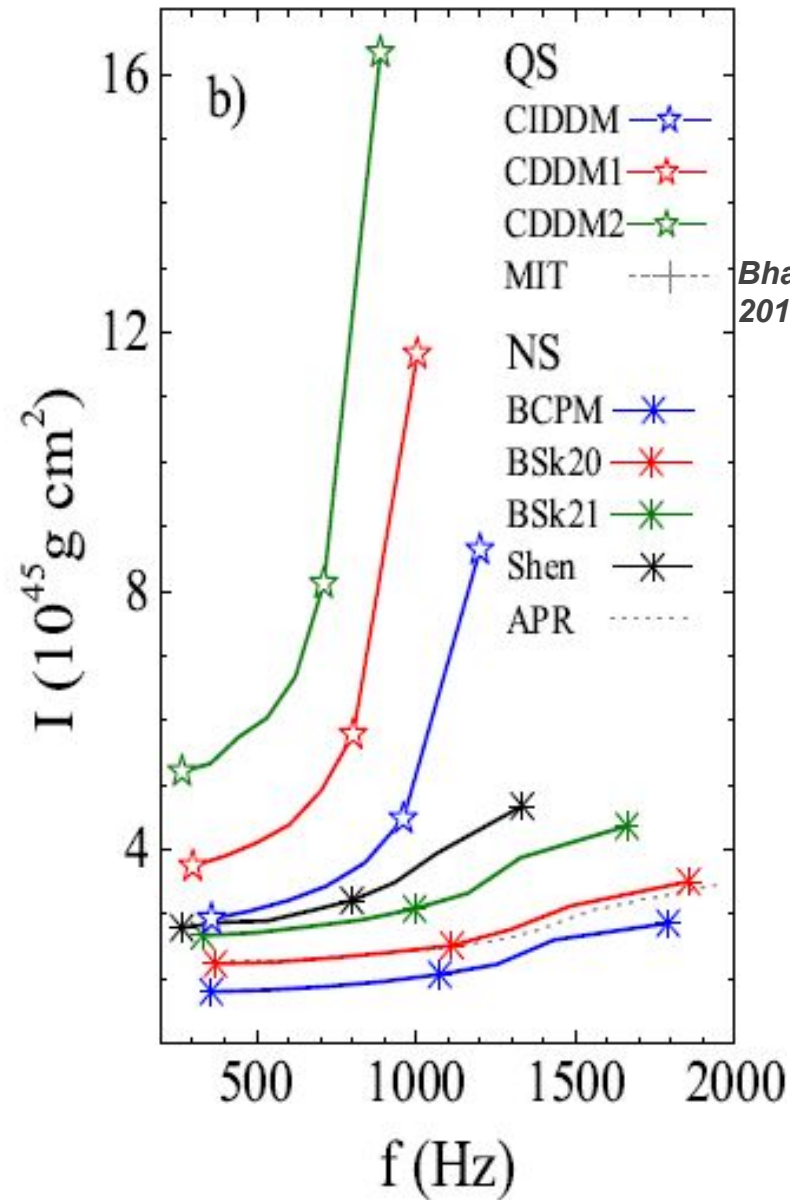
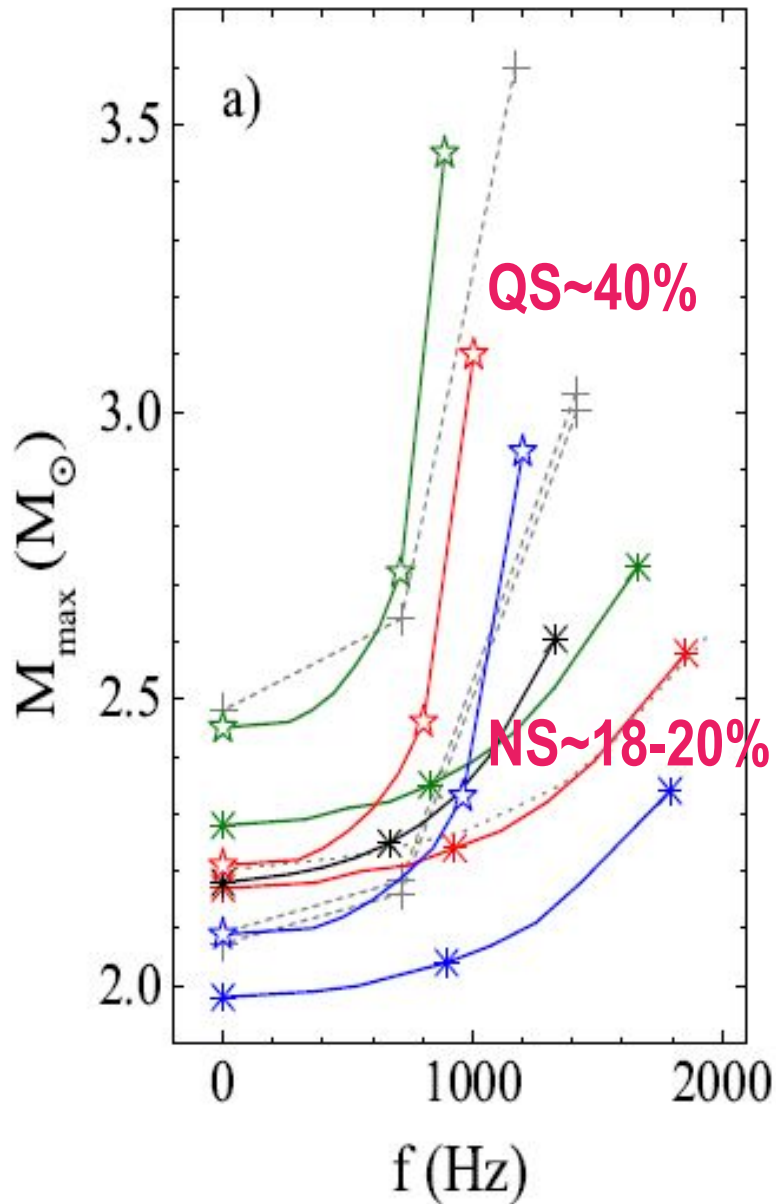
Supramassive star as central engine



Spin-down induced collapse



Mass and Moment of inertia vs. frequency



Bhattacharyya, S., et al.
2016 MNRAS

Internal x-ray plateau in short GRBs: Signature of supramassive fast-rotating quark stars?

Ang Li,^{1,2,*} Bing Zhang,^{2,3,4,†} Nai-Bo Zhang,⁵ He Gao,⁶ Bin Qi,⁵ and Tong Liu^{1,2}

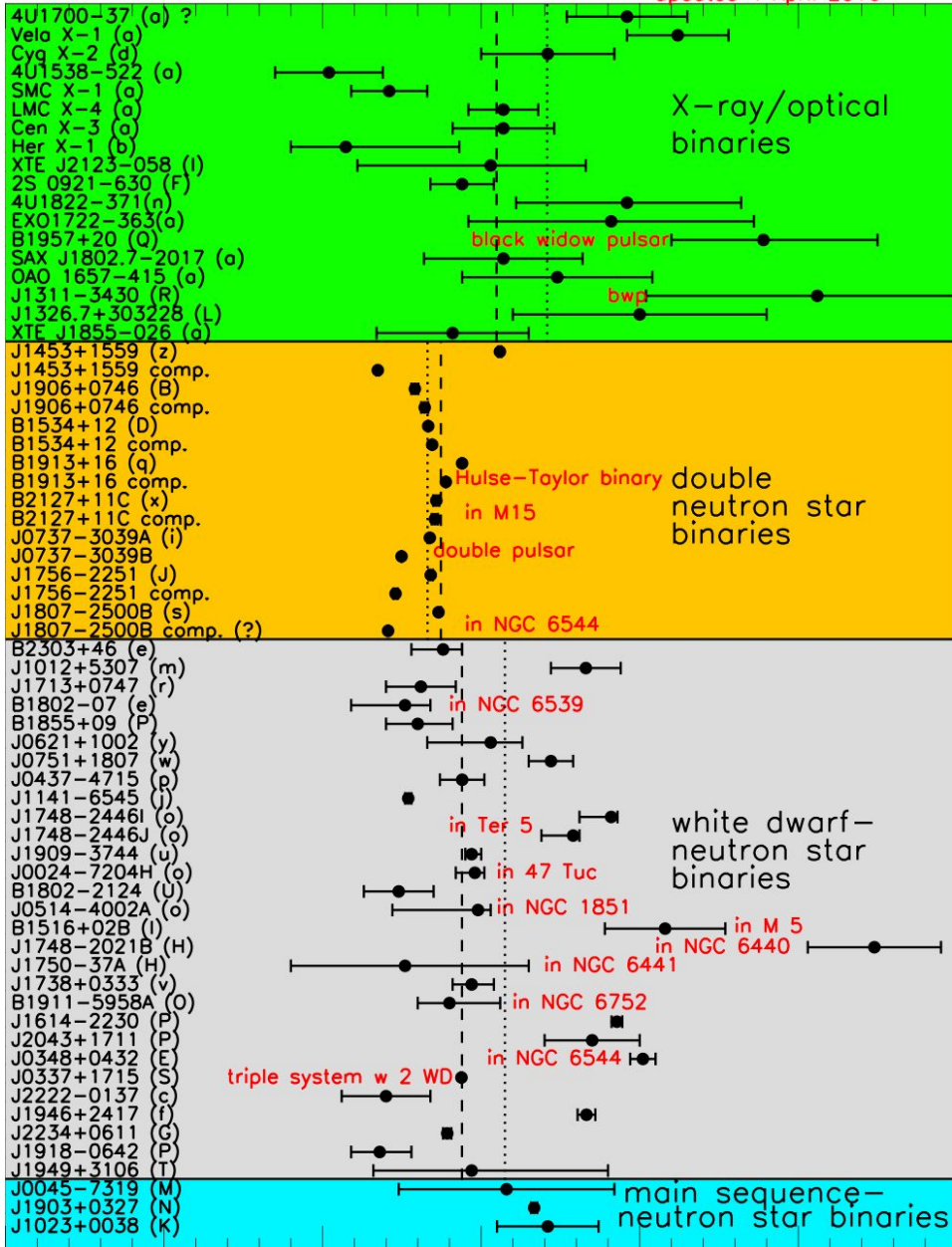
Summary.— To recap, we have carried out the following investigations: 1) Selecting unified NS EoSs that satisfy up-to-date experimental constraints from both nuclear physics and astrophysics, based on modern nuclear many-body theories; 2) Finding typical parameter sets for QS EoSs in developed CDDM model, under same constraints of the NS case

Summary

1. Post-merger products of NS-NS mergers are probably supramassive QSs rather than NSs;
2. NS-NS mergers are a plausible location for quark de-confinement and the formation of QSs.

properties of the SGRB internal plateaus sample and revealing the post-merger supramassive stars' physics. We finally reach the conclusion that the post-merger products of NS-NS mergers are probably supramassive QSs rather than NSs. NS-NS mergers are a plausible location for quark de-confinement and the formation of QSs.

updated 4 April 2016



PSR J0348-0432

<https://stellarcollapse.org/nsmasses>

0.0 0.5 1.0 1.5 2.0 2.5 3.0
Neutron star mass (M_{\odot})